Identification of Bioplastic Degradation Abilities and Associated Genes in *Burkholderia* With Synthetic Biology Tools

By

Zhong Ling Yap

A Thesis submitted to the Faculty of Graduate Studies of The University of Manitoba in partial fulfilment of the requirements of the degree of

DOCTOR OF PHILOSOPHY

Department of Microbiology
University of Manitoba
Winnipeg, Manitoba, Canada

Copyright © 2025 by Zhong Ling Yap

ABSTRACT

The *Burkholderia* genus exhibits a dual nature; while some species are opportunistic pathogens, others hold immense biotechnological potential due to their vast metabolic capacity. Harnessing the beneficial traits of *Burkholderia* while mitigating risks would require genetic tools to elucidate gene-to-function relationships and enable genetic manipulation. This thesis focuses on developing and utilizing genetic tools for *Burkholderia* and applying them to study bioplastic degradation, specifically medium-chain-length polyhydroxyalkanoates (mcl-PHA).

To address some of the limitations in existing genetic tools, a CRISPR-associated transposase system, RhaCAST, was developed as a targeted DNA insertion platform for *Burkholderia*. RhaCAST enables loss- and gain-of-function applications and allows for iterative genetic manipulations by excising and reusing selection markers. The system was applied to three species, *B. cenocepacia* K56-2, *B. multivorans* ATCC 17616, and *B. vietnamiensis* LMG 16232, demonstrating its versatility across different *Burkholderia* strains. RhaCAST increases the genetic toolkit available for studying non-model bacteria.

Building on this genetic tool development, the extracellular mcl-PHA degradation capacities of various *Burkholderia* strains were explored. Screening revealed that strains such as *B. gladioli*, *B. multivorans*, and *B. vietnamiensis* could degrade mcl-PHA, highlighting the genus's diverse metabolic potential. In order to elucidate the genetic basis of this activity, transposon mutagenesis coupled with Tn-seq analysis was performed on *B. vietnamiensis* LMG 16232. This analysis identified genetic elements involved in mcl-PHA degradation, including lipase and chaperone genes, type II secretion system components, and regulatory elements such as transcriptional activators and repressors of PHA synthesis. Further validation of mutants generated with RhaCAST confirmed the involvement of these genes in the extracellular mcl-PHA degradation activity, highlighting the role of lipases as enzymes with substrate ambiguity.

Overall, this thesis demonstrates how the development of genetic tools can drive functional genomics studies in non-model bacteria such as *Burkholderia*. RhaCAST's versatility extends beyond bioplastic degradation, allowing its use in various biotechnological fields, including metabolic engineering and pathogenicity studies. The insights gained into extracellular mcl-PHA degradation mechanisms provide opportunities for enzyme engineering and industrial applications in bioplastic waste management, paving the way for sustainable biotechnology innovation.

ACKNOWLEDGEMENTS

Firstly, I would like to thank my supervisor, Dr. Silvia Cardona, for her mentorship and guidance. Your passion and dedication to research have set an example of what I aspire to achieve in the future.

I would also like to express my gratitude to my committee members, Dr. David Levin, Dr. Richard Sparling, and Dr. Gerd Prehna. Your valuable input, feedback, and support have been crucial to this journey.

I am thankful to my collaborators, Dr. Warren Blunt, Gabriel Garcia, and Dr. Dario Fernandez Do Porto, for sharing your expertise and for expanding my boundaries.

I am also grateful to Ryan Darragh, Mohammad Safkloua, and Sarah Iqbal, who have helped me to grow as a mentor and for your contribution to this research. I want to extend my thanks to everyone in the Cardona lab, both past and present, for your support throughout this journey. Dr. Tasia Lightly, Dr. Andrew Hogan, Dr. Anna Motnenko, Dr. Zisanur Rahman, Dustin Maydaniuk, Becca Lohmann, Zayra Batun, Jules Novomisky Nechcoff, Dr. Katherine Romero, and Miranda Palumbo. I have learned so much from each of you, and I am grateful for all the brainstorming sessions and your support.

I would also like to thank everyone in the Department of Microbiology for providing a supportive learning and working environment. It has been an amazing experience working in this department.

Additionally, I would also like to thank the funding sources that supported this work: Research Manitoba, NSERC, University of Manitoba Faculty of Science, Faculty of Graduate Studies, and the Department of Microbiology.

Finally, I would like to thank my family: my parents, Goon Ying and Chiew Har, and my siblings, Han Xin and Zhong Pei. Your unconditional love and support have been invaluable to me.

TABLE OF CONTENTS

ABSTRACT....ii

ACKNOWLEDGEMENTS....iv

TABLE OF CONTENTS....v

PERMISSIONS....x

AUTHOR CONTRIBUTIONS....xi

LIST OF TABLES....xii

LIST OF FIGURES....xiii

LIST OF ABBREVIATIONS....xvi

1. CHAPTER 1: LITERATURE REVIEW....1

1.1 History and taxonomy of the *Burkholderia* genus....1

1.2 Biotechnological potential of *Burkholderia* species....2

1.3 The concern of using *Burkholderia* biotechnologically....5

1.4 The challenges of manipulating *Burkholderia* and possible solutions....6

1.4.1 Limited selection marker....6

1.4.2 Not naturally competent: DNA uptake, host defence mechanisms, and restriction-modification....7

1.4.3 High GC content....9

1.5 *Burkholderia* genetic tool arsenal....11

1.5.1 Gene insertion: Site-specific integration....13

1.5.2 Single copy insertion: Mini-Tn7 insertion....14

1.5.3 Clean/Unmarked deletion....15

1.5.4 Allelic replacement-based gene deletion or replacement 16
1.5.5 Deletion of the third chromosome 18
1.5.6 Recombineering 19
1.5.7 Transposon mutagenesis to uncover novel gene functions in *Burkholderia* 20
1.5.8 CRISPR-based genetic tools 23
1.5.9 Plasmid-based gene expression tools 25
1.5.10 Reporter systems 27
1.6 Uncovering *Burkholderia* catabolic potential in degrading bioplastic 28
1.7 Rationale of the Thesis Research 31
1.8 Hypotheses and Objectives 32
2. CHAPTER 2: A CRISPR-CAS ASSOCIATED TRANSPOSON SYSTEM FOR GENOME EDITING IN *BURKHOLDERIA CEPACIA* COMPLEX SPECIES 33
2.1 Abstract 33
2.2 Importance 33
2.3 Introduction 34
2.4 Materials and Methods 36
2.4.1 Strains, Selective Antibiotics, and Growth Conditions 36
2.4.2 Construction of the RhaCAST system 41
2.4.3 Cloning of crRNAs into pRhaCAST 42
2.4.4 Construction of pDonorTp-fugfp 42
2.4.5 Tetra-parental mating 43
2.4.6 Removal of antibiotic resistance cassette using Flp-FRT recombination 43

2.4.7 Phenotypic characterization of phenylacetic acid auxotroph mutant 43

2.4.8 Flagellum staining.....44

2.4.9 Nile red staining and detection of PHA granules.....44

2.4.10 FuGFP detection 45

2.4.11 Plate-based motility assay.....45

2.4.12 Genome sequencing and data analysis.....45

2.5 Results 46

2.5.1 Construction of the RhaCAST system for use in Bcc strains 46

2.5.2 Use and validation of the RhaCAST system for insertional mutagenesis in *B. cenocepacia* K56-2 49

2.5.3 Further application of the RhaCAST system to target *fliF* and *phbC* in *B. cenocepacia* K56-2 50

2.5.4 RhaCAST-mediated gain-of-function, recycling of resistance marker for subsequent mutagenesis, and plasmid curing 55

2.5.5 Optimized RhaCAST for *B. multivorans* ATCC 17616 58

2.5.6 Long-read sequencing confirms on-site insertional mutagenesis and detects the frequency of whole plasmid integration 61

2.6 Discussion 63

2.7 Plasmid and data availability.....65

3. CHAPTER 3: IDENTIFYING BIOPLASTIC DEGRADATION GENES IN BURKHOLDERIA EMPLOYING TN-SEQ AND CRISPR-CAS.....66

3.1 Abstract 66

3.2 Introduction 66

3.3 Materials and Methods 70

3.3.1 Strains, Selective Antibiotics, and Growth Conditions 70

3.3.2 Genomic and plasmid extraction 74

3.3.3 Substrate and media preparation 74

3.3.4 Screening for mcl-PHA and tributyrin degradation 75

3.3.5 Transposon mutagenesis, Tn-seq library preparation and genome mapping 75

3.3.6 Determination of the PHO content beneath inoculated culture 77

3.3.7 *In silico* analysis 77

3.3.8 Construction of *B. vietnamiensis* LMG 16232 insertional mutants 78

3.4 Results 78

3.4.1 Diversity of extracellular mcl-PHA degradation activity in *Burkholderia* strains 78

3.4.2 Genetic basis of *B. vietnamiensis* LMG 16232 extracellular mcl-PHA degradation activity 82

3.4.3 Characteristic of mcl-PHA degrading enzyme in *B. vietnamiensis* LMG 16232 predicted via *in silico* analysis 90

3.4.4 Validation of genetic elements responsible for mcl-PHA degradation identified from transposon mutagenesis 94

3.5 Discussion 100

4. CHAPTER 4: DISCUSSION AND CONCLUSION 106

5. CHAPTER 5: REFERENCES 111

6. CHAPTER 6: APPENDIX 146

6.1 Related to Chapter 2 146

6.1.1 Supplemental Figures 146

6.2 Related to Chapter 3 159

6.2.1 Supplemental Figures 159

6.3 Complete Genome Sequence of *Burkholderia vietnamiensis* LMG16232 165

6.3.1 Abstract 165

6.3.2 Announcement 165

6.3.3 Data availability statement 166

6.3.4 References for appendix 167

PERMISSIONS

Several tables, figures, and passages of text in this thesis have been taken directly and/or adapted from publications that I have authored.

Chapter 2 is reprinted largely as it appears in: Yap, Z.L., Rahman, A.S.M.Z., Hogan, A.M., Levin, D.B., and Cardona, S.T. 2024. A CRISPR-Cas-associated transposon system for genome editing in *Burkholderia cepacia* complex species. Appl Environ Microbiol 90(7): e0069924. doi:10.1128/aem.00699-24

Copyright © American Society for Microbiology (ASM), [Applied and Environmental Microbiology, 90(7): e0069924. doi:10.1128/aem.00699-24]. Authors retain the right to reuse the full article in their dissertation or thesis per the ASM Journals policy.

Chapter 3: Yap, Z.L., Safkloua, M., Darragh, R., Hogan, A.M., Motnenko, A., Blunt, W., Sparling, R., Levin, D.B., Cardona, S.T. Identifying Bioplastic Degradation Genes in *Burkholderia* Employing Tn-seq and CRISPR-Cas. Manuscript in preparation.

This manuscript has been formatted for submission to fit the requirements of a "sandwich" style thesis as per the Faculty of Graduate Studies, but has not yet been submitted to a journal.

Appendix 6.3 is reprinted largely as it appears in: Yap, Z.L., Motnenko, A., and Cardona, S. 2023. Complete Genome Sequence of *Burkholderia vietnamiensis* LMG16232. Microbiol Resour Announc 12(8): e0032823. doi:10.1128/mra.00328-23.

Copyright © American Society for Microbiology (ASM), [Microbiol Resour Announc 12(8): e0032823. doi:10.1128/mra.00328-23]. Authors retain the right to reuse the full article in their dissertation or thesis per the ASM Journals policy.

AUTHOR CONTRIBUTIONS

Multiple authors have contributed to the work presented in Chapters 2, 3, and Appendix 6.3.

Chapter 2: S.T.C. and Z.L.Y. formulated the ideas and design of the project; Z.L.Y., A.S.M.Z.R., and A.M.H. designed and cloned the plasmids and mutants; Z.L.Y., A.S.M.Z.R., and A.M.H. performed phenotypic assays; Z.L.Y. and A.S.M.Z.R. processed and analyzed the data; Z.L.Y. wrote the manuscript and edited together with S.T.C., A.S.M.Z.R., A.M.H., and D.B.L.; S.T.C. and D.B.L. provided financial support and supervised the work.

Chapter 3: S.T.C. and Z.L.Y. formulated the ideas and design of the project; Z.L.Y and M.S. designed and cloned the plasmids and mutants; Z.L.Y., M.S., R.D., and W.B. performed phenotypic assays; Z.L.Y. and A.M.H. performed library prep for Tn-seq. Z.L.Y. wrote the manuscript and edited together with S.T.C., M.S., R.D., A.M.H., A.M., W.B., R.S. and D.B.L.; S.T.C, D.B.L., R.S., and W.B. provided financial support and supervised the work.

Appendix 6.3: Z.L.Y. performed the experiments; Z.L.Y. and A.M. processed and analyzed the data; Z.L.Y. wrote the manuscript and edited together with A.M. and S.T.C.; S.T.C. provided financial support and supervised the work.

LIST OF TABLES

Table 1. 1 Summary of molecular biology tools developed or applied to *Burkholderia*.....11

Table 2. 1 Strains and plasmids used in Chapter 2. 36

Table 2. 2 Primers/templates used for cloning and verification in Chapter 2.....39

Table 2. 3 Summary of targeting *paaA* with RhaCAST system in *B. cenocepacia* K56-2. ...50

Table 2. 4 Summary of targeting *paaA* with RhaCAST system in *B. multivorans* ATCC 17616. 59

Table 2. 5 Long read sequencing summary of mutants created using RhaCAST system in *B. cenocepacia* K56-2 and *B. multivorans* ATCC17616. 62

Table 3. 1 List of bacterial strains and plasmids used in Chapter 3.....70

Table 3. 2 Primers/templates used in Chapter 3. 73

Table 3. 3 *Burkholderia* isolates that exhibit extracellular mcl-PHA degradation activity.....80

Table 3. 4 Transposon mutant of *B. vietnamiensis* LMG 16232 with abolished (Pool 1) or reduced (Pool 2) extracellular mcl-PHA activity.....87

LIST OF FIGURES

Figure 1. 1 Schematic illustration of using the *Burkholderia* genus biotechnologically, challenges in modifying the genome, and genetic arsenal available for *Burkholderia*. 3

Figure 1. 2 General chemical structure of polyhydroxyoctanoate (PHO). 29

Figure 2. 1 Schematics of RNA-guided DNA integration by ShCAST developed for *Burkholderia cenocepacia* complex (Bcc) (RhaCAST). 48

Figure 2. 2 Targeting *fliF* by shCAST in *B. cenocepacia* K56-2 abolishes swimming motility. 52

Figure 2. 3 Targeting *phbC* with shCAST abolishes poly-β-hydroxybutyrate granule accumulation in *B. cenocepacia* K56−2. 54

Figure 2. 4 RhaCAST-mediated gain of function and recycling of antibiotic resistance cassette. 57

Figure 2. 5 Targeting *fliF* by shCAST in *B. multivorans* ATCC 17616 abolished flagellum formation.....60

Figure 3. 1 Overview of transposon mutagenesis and Tn-seq workflow to identify genetic elements involved in the extracellular mcl-PHA degradation activity in *B. vietnamiensis* LMG 16232.....83

Figure 3. 2 Genetic Organization of the *B. vietnamiensis* LMG 16232 gene clusters that affect the extracellular mcl-PHA degradation upon interruption by transposon. 85

Figure 3. 3 Amino acid sequence alignment of putative lipase that is able to degrade extracellular mcl-PHA depolymerase of *B. vietnamiensis* LMG 16232 (protein ID: WHU94860.1) with other mcl-PHA depolymerase sequences.....94

Figure 3. 4 Targeting genes involved in mcl-PHA degradation in *B. vietnamiensis* LMG 16232 abolish the strain's ability to degrade mcl-PHA.....95

Figure 3. 5 Targeting the putative *lipase* gene (locus tag: P4G95_16805) in *B. vietnamiensis* LMG 16232 abolishes the ability to degrade mcl-PHA.....97
Figure 3. 6 Targeting genes involved in mcl-PHA degradation in *B. vietnamiensis* LMG 16232 affects the ability to degrade tributyrin. 99
Figure 3. 7 Proposed model of components involved in *B. vietnamiensis* LMG 16232 extracellular mcl-PHA degradation activity. 104
Figure S2. 1 PCR targeting *paaA* in *B. cenocepacia* K56-2 after RhaCAST conjugation. ...146
Figure S2. 2 PCR targeting *fliF* of *B. cenocepacia* K56-2 after RhaCAST conjugation. 147
Figure S2. 3 PCR targeting *phbC* of *B. cenocepacia* K56-2 after RhaCAST conjugation....148
Figure S2. 4 PCR targeting *paaA* and the left end (LE) of the cargo insertion in *B. multivorans* ATCC17616 after RhaCAST conjugation. 149
Figure S2. 5 PCR targeting *fliF* of *B. multivorans* ATCC17616 after RhaCAST conjugation. 150
Figure S2. 6 Alignment of nanopore sequencing of *B. cenocepacia* K56-2 transconjugants with genomic integration in *paaA* created using the RhaCAST system. 151
Figure S2. 7 Alignment of nanopore sequencing of *B. cenocepacia* K56-2 transconjugants with genomic integration in *fliF* created using the RhaCAST system.....152
Figure S2. 8 Alignment of nanopore sequencing of *B. cenocepacia* K56-2 transconjugants with genomic integration of transposon in *phbC* created using the RhaCAST system. 153
Figure S2. 9 Alignment of nanopore sequencing of *B. cenocepacia* K56-2 transconjugants with genomic integration of *fugfp* in genetically neutral locus created using RhaCAST system..154
Figure S2. 10 Sequence alignment of *B. cenocepacia* K56-2::CAST-*fugfp* genome showing the removal of TpR via FLP-FRT mediated recombination.....155

Figure S2. 11 Alignment of nanopore sequencing of *B. cenocepacia* K56-2::CAST-fugfp *fliF*::CAST-Tp created with RhaCAST system using *B. cenocepacia* K56-2::CAST-fugfp-Tp as background by targeting *fliF*. 156

Figure S2. 12 The alignment of nanopore sequencing of *B. multivorans* ATCC17616 transconjugants with genomic integration of transposon in *paaA* and *fliF* created using the RhaCAST system. 157

Figure S3. 1 The mcl-PHA degradation activity of *Burkholderia* strains. 159

Figure S3. 2 Alignment of nanopore sequencing of *B. vietnamiensis* LMG 16232 transconjugants with genomic integration in triacylglycerol lipase CDS (locus tag: P4G95_16805) created using the RhaCAST system. 160

Figure S3. 3 Alignment of nanopore sequencing of *B. vietnamiensis* LMG 16232 transconjugants with genomic integration in A24 family peptidase CDS (locus tag: P4G95_07805) created using the RhaCAST system. 161

Figure S3. 4 Alignment of nanopore sequencing of *B. vietnamiensis* LMG 16232 transconjugants with genomic integration in *otsB* (locus tag: P4G95_10885) created using the RhaCAST system. 162

Figure S3. 5 Alignment of nanopore sequencing of *B. vietnamiensis* LMG 16232 transconjugants with genomic integration in *gspE* (locus tag: P4G95_05530) created using the RhaCAST system. 163

Figure S3. 6 Alignment of nanopore sequencing of *B. vietnamiensis* LMG 16232 transconjugants with genomic integration in TetR/AcrR family transcriptional regulator CDS (locus tag: P4G95_00865) created using the RhaCAST system. 164

LIST OF ABBREVIATIONS

Bcc	*Burkholderia cepacia* complex
BCCM	Belgium Coordinated Collection of Microorganisms
BONCAT	Bio-Orthogonal Noncanonical Amino Acid Tagging
bp	Base pair
BWA	Burrows-Wheeler transform
CANWARD	Canadian Ward Surveillance Study
CARA	Canadian Antimicrobial Resistance Alliance
CAST	CRISPR-Associated Transposases
CBCCRRR	The Canadian *Burkholderia cepacia* complex research and referral repository
CDC	Centers for Disease Control and Prevention
CDS	Coding DNA Sequence
CF	Cystic Fibrosis
CFP	Cyan Fluorescent Protein
Cm	Chloramphenicol
Cre	Cyclization recombination
CRISPR	Clustered Regularly Interspaced Short Palindromic Repeats
CRISPRa	CRISPR-based transcriptional activation system
CRISPRi	CRISPR interference
crRNA	CRISPR RNA
dCas9	Catalytically dead Cas9
DEHP	Di-(2-ethylhexyl) phthalate
DIC	Differential Interference Contrast
DMSO	Dimethyl sulfoxide

EDTA	Ethylenediaminetetraacetic acid
ET12	Electrophoretic Type-12
Flp	Flippase
FRT	Flippase Recombination Target
fugfp	Free-Use Green Fluorescent Protein
GC-FID	Gas Chromatography with Flame Ionization Detection
gDNA	Genomic DNA
GFP	Green Fluorescent Protein
GSP	General Secretion Pathway
HCl	Hydrochloric acid
IDT	Integrated DNA Technologies
INTEGRATE	Insertion of Transposable Elements by Guide RNA-Assisted Targeting
Kan	Kanamycin
kDa	Kilodaltons
LB	Lysogeny broth
LE	Left End
LoxP	Locus of X(cross)-over in P1
mcl-PHA	Medium-chain-length polyhydroxyalkanoate
$MetRS^{NLL}$	Methionyl-tRNA synthetase
NAU-PMI	Northern Arizona University-Pathogen & Microbiome Institute
NCBI	National Center for Biotechnology Information
NEB	New England Biolabs
OD_{600}	Optical Density measured at 600 nm
ONT	Oxford Nanopore Technology

ori	Origin of replication
PAA	Phenylacetic acid
PAM	Protospacer Adjacent Motif
PBS	Phosphate Buffered Saline
PCL	Polycaprolactone
PCR	Polymerase Chain Reaction
PHA	Polyhydroxyalkanoate
PHB	Polyhydroxybutyrate
PHO	Polyhydroxyoctanoate
pI	Isoelectric point
PLA	Polylactic acid
PRJNA	Project Accession Number in NCBI
RE	Right End
REBASE	Restriction Enzyme Database
RFP	Red Fluorescent Protein
Rha	L-rhamnose
RhaCAST	A ShCAST-based genetic tool driven by a rhamnose-inducible promoter
scl-PHA	Short-chain-length polyhydroxyalkanoate
sgRNA	single guide RNA
ShCAST	CRISPR-associated transposases from *Scytonema hofmannii*
SRA	Sequence Read Archive
Tel	Tellurite
Tn-Seq	Transposon site sequencing
TOM	Toluene ortho-monooxygenase

Tp	Trimethoprim
UV	Ultraviolet
VchCAST	CRISPR-associated transposases from *Vibrio cholerae*
WT	Wild type
YFP	Yellow Fluorescent Protein

CHAPTER 1: LITERATURE REVIEW

1.1 History and taxonomy of the *Burkholderia* genus

The genus *Burkholderia* is a diverse group of Gram-negative aerobic bacteria belonging to the β-proteobacteria subdivision that are metabolically diverse and broadly distributed in diverse niches, both natural and man-made (Depoorter et al. 2016). *Burkholderia* was first described by William Burkholder, who identified it as a plant pathogen responsible for onion rot, initially naming it *Pseudomonas cepacia* (Burkholder 1950). In 1992, seven species classified under *Pseudomonas* were transferred to the newly established genus *Burkholderia,* which consisted of *Burkholderia cepacia*, *B. mallei*, *B. pseudomallei*, *B. caryophylli*, *B. gladioli*, *B. pickettii*, and *B. solanacearum* (Yabuuchi et al. 1992). Later on, two of the species, *B. solanacearum* and *B. pickettii,* were transferred to the genus *Ralstonia* (Yabuuchi et al. 1992).

In 1997, *B. cepacia* was divided into different genomovars, which represent groups of phenotypically similar isolates that were genetically distinct enough to be designated as new species, known as *Burkholderia cepacia complex* (Bcc) (Vandamme et al. 1997; Mahenthiralingam et al. 2005). More recently, the genus *Paraburkholderia* was established to accommodate environmental bacteria previously classified under *Burkholderia* following phylogenetic and genomic analyses that revealed distinct evolutionary lineages (Sawana et al. 2014). This division has sparked some controversy, arguing that the split oversimplifies the issue and is potentially dangerous, as members of *Paraburkholderia* also have the potential to cause infection (Eberl and Vandamme 2016).

The current classification of the *Burkholderia* and *Paraburkholderia* genera includes over 120 species, with a complete list available (http://www.bacterio.net/burkholderia.html). Generally, *Burkholderia* can be broadly divided into three main groups (Sawana et al. 2014).

The first group is the Bcc, which consists of more than 20 species, such as *Burkholderia cenocepacia* and *Burkholderia multivorans,* and is prevalent in cystic fibrosis patients. Some species within the Bcc have demonstrated anti-pesticidal properties. For example, *B. vietnamiensis* B418 can inhibit root-knot nematodes on watermelon by modifying the rhizosphere microbial community (Liu et al. 2022). In the past, members of the Bcc group have been commercially utilized as biopesticides despite their pathogenic potential (Sawana et al. 2014; Eberl and Vandamme 2016; Espinosa-Victoria et al. 2020). The second is the *B. pseudomallei* group, which includes the causative agent of tropical disease melioidosis, glanders, and potential bioterrorism agents (Larsen and Johnson 2009; Sawana et al. 2014; Espinosa-Victoria et al. 2020). The third group consists of plant-pathogenic *Burkholderia* species, which include *B. gladioli, B. plantarii*, and *B. glumae* (Sawana et al. 2014).

1.2 Biotechnological potential of *Burkholderia* species

Burkholderia species possess a multi-replicon genome and have one of the largest genome sizes observed among Gram-negative bacteria, typically ranging from 6 to 9 Mb (Mahenthiralingam et al. 2005). The huge genome encodes for *Burkholderia's* functional and metabolic versatility, enabling them to thrive in a variety of environments (Mahenthiralingam et al. 2005). Some of these features make them ideal for biotechnological applications in agriculture, bioremediation, and as cell factories for producing commercially valuable products (**Figure 1.1**). For instance, some species have the ability to synthesize a wide range of natural products, promote plant growth, provide plant protection, degrade pollutants, and produce enzymes with commercial interest (Mahenthiralingam et al. 2005; Eberl and Vandamme 2016; Depoorter et al. 2016; Morya et al. 2020).

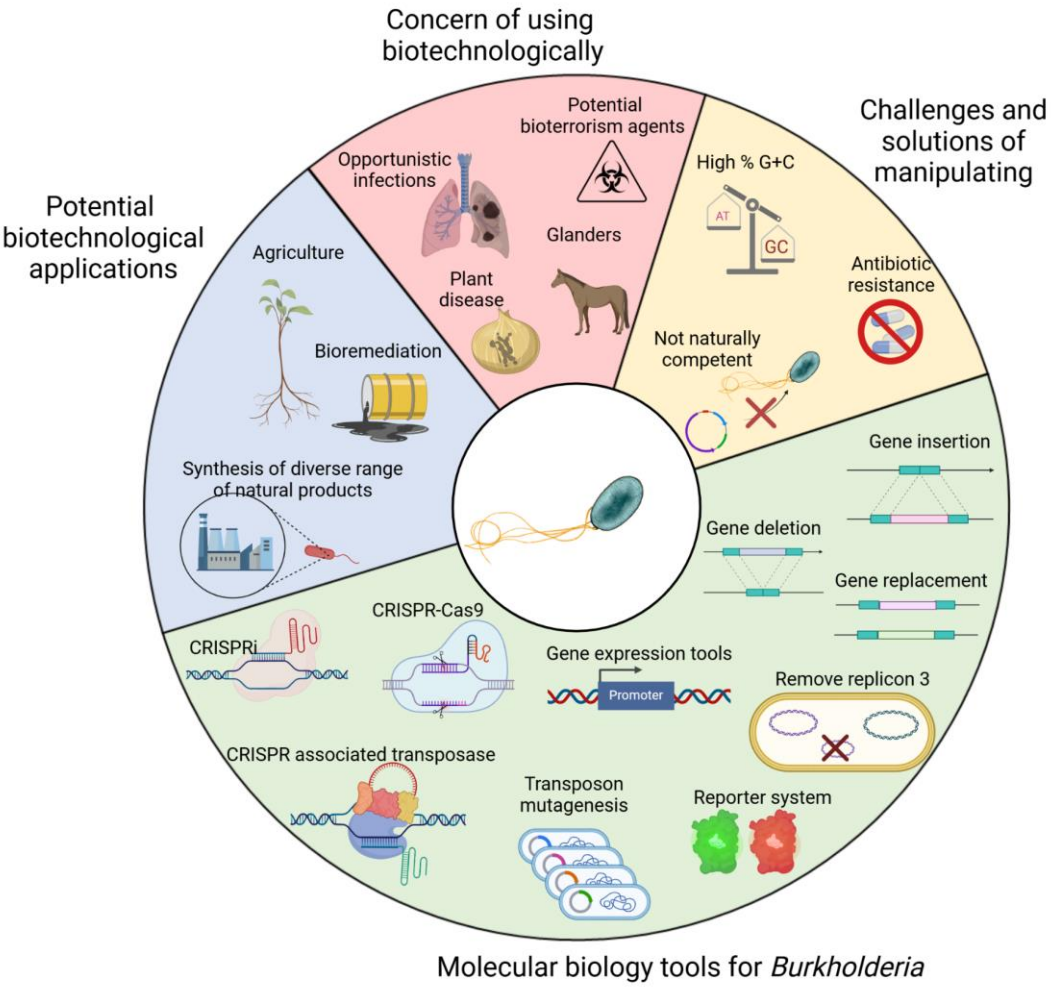


Figure 1. 1 Schematic illustration of using the *Burkholderia* genus biotechnologically, challenges in modifying the genome, and genetic arsenal available for *Burkholderia*.

Figure 1.1 was created with https://biorender.com/.

In agriculture, *Burkholderia*'s plant protective and growth-promoting properties offer notable benefits. These bacteria are well recognized for establishing symbiotic and mutualistic relationships with plants (Suárez-Moreno et al. 2012; Eberl and Vandamme 2016; Mannaa et al. 2018; Espinosa-Victoria et al. 2020). For example, *Burkholderia vietnamiensis* has nitrogen-fixing capacity (Santos et al. 2001), while *Burkholderia ambifaria* has been shown to

protect plants from damping-off disease by producing the antifungal compound cepacin (Mullins et al. 2019). Additionally, *Burkholderia rinojensis* exhibited activity against arthropod pests (Cordova-Kreylos et al. 2013). Meanwhile, *Burkholderia* sp. Nafp2/4-1b exhibits plant growth-promoting properties by producing pyoverdine siderophores, 1-Aminocyclopropane-1-Carboxylate Deaminase, and the phytohormone auxin (Hassen et al. 2018).

Burkholderia's biopesticidal ability has been linked partly to their ability to synthesize a diverse range of antimicrobial and toxic secondary metabolites (Parke and Gurian-Sherman 2001; Vial et al. 2007). The vast amount of natural products produced by *Burkholderia* species have ample therapeutic and biotechnological applications (Depoorter et al. 2016; Kunakom and Eustáquio 2019; Klaus et al. 2020). Examples of antimicrobial compounds include pyrrolnitrin, cepacin, enacyloxin, caryoynencin, lagriene, gladiolin, tropolone, thailandamides, bactobolins, and burkholdines (Kunakom and Eustáquio 2019). Additionally, certain species are capable of producing anti-tumour and anti-cancer compounds, such as FK228, spiruchostatin C, and thailandstatin A (Kunakom and Eustáquio 2019).

The production of enzymes and products with commercial, bioremediation, and pharmaceutical interest has also been found. For example, the lipase of *B. glumae* is currently used in the detergent industry (Frenken et al. 1993a; Rosenau and Jaeger 2000; Boekema et al. 2007), and lipases of *B. cepacia* can catalyze important pharmaceutical substrates (Tasnádi et al. 2009). Rhamnolipid, which can be found in *Burkholderia thailandensis* (Dubeau et al. 2009), *B. glumae* (Costa et al. 2011), and *B. plantarri* (Hörmann et al. 2010), is a biosurfactant with potential uses in enhanced oil recovery, environmental bioremediation, food processing, and pharmaceuticals. Besides that, *Burkholderia* can break down a wide range of aromatic compounds, including phenol, toluene, aniline, di-(2-ethylhexyl) phthalate (DEHP), p-cumate,

p-cymene, insecticides, and nonanthropogenic aromatic compounds (Morya et al. 2020). All these features make them a promising host for bioremediation and bioconversion.

1.3 The concern of using *Burkholderia* biotechnologically

Despite the features that justify the use of *Burkholderia* species biotechnologically, some bottlenecks hinder their utilization to total capacity (Parke and Gurian-Sherman 2001). This genus can act as both a "friend and foe" as certain species can cause opportunistic infections in humans (Eberl and Vandamme 2016). For example, within the pathogenic Bcc group, environmental isolates of biotechnological interest are prevalent (Cauduro et al. 2021). In the 1990s, several strains of Bcc were registered for use as biocontrol agents, including Deny®, Blue Circle®, and Intercept®. However, following a risk assessment of *Burkholderia* biopesticides, these products were withdrawn from the market, and a moratorium was placed on the registration of products containing Bcc species (Parke and Gurian-Sherman 2001). Non-Bcc strains can also cause human infections, such as *Burkholderia fungorum* and species from the *B. pseudomallei* group (Loong et al. 2016).

While genetic manipulation may help reduce the pathogenic risks, it is challenging to perform in *Burkholderia* for several reasons. Firstly, their genomes are large and have a multi-replicon structure (Morya et al. 2020). In addition, *Burkholderia* genomes have a high GC content and contain repetitive DNA elements, which make DNA-based applications, such as gene synthesis, PCR-based amplification, and genome sequencing, very challenging. Finally, the intrinsic antibiotic resistance of *Burkholderia* isolates (Rhodes and Schweizer 2016) renders many antibiotic-resistance genes used as genetic markers of mutagenesis ineffective. The subsequent section will discuss some barriers and solutions in developing molecular biology tools for *Burkholderia* and evaluate the genetic modification arsenal.

1.4 The challenges of manipulating *Burkholderia* and possible solutions

1.4.1 Limited selection marker

Burkholderia species generally have limited options for selection markers in genetic modification, and this is due to two primary reasons: (i) intrinsic resistance to many antibiotics, particularly among the Bcc species, and (ii) the limited selection markers that have been approved for use in *B. pseudomallei* and *B. mallei*. The common resistance markers used in the genetic manipulation of Bcc species are often limited to trimethoprim, chloramphenicol, and tetracycline (Shastri et al. 2017). In the case of *B. cenocepacia*, these markers can be selected for a single copy (Shastri et al. 2017). There are some aminoglycoside-sensitive strains, such as *B. cenocepacia* H111 or engineered strains, that can use aminoglycosides, including gentamicin and kanamycin, as selection agents (Shastri et al. 2017). A study has shown that gentamicin, kanamycin, and trimethoprim are good selection markers for *B. gladioli* ATCC33664, as this strain is susceptible to these antibiotics (Somprasong et al. 2010).

Other species that have difficulties in this area include the *B. pseudomallei* group, which consists of *B. pseudomallei* and *B. mallei*. These bacteria have been classified as Category B select agents by the Centers for Disease Control and Prevention (CDC) (https://www.selectagents.gov/sat/list.htm) due to their potential to pose serious threats to both human and animal health. Currently, the only selection markers approved for *B. pseudomallei* are kanamycin, gentamicin, zeocin, and polymyxin B. For *B. mallei*, approved selection markers include kanamycin, zeocin, and polymyxin B. However, both *B. pseudomallei* and *B. mallei* are naturally resistant to polymyxin B, which limits the use of this antibiotic for genetic manipulation. Additionally, *B. pseudomallei* exhibits natural resistance to gentamicin and other aminoglycosides. As a result, kanamycin and zeocin are the only antibiotics that have been used for genetic manipulation in the *B. pseudomallei* group (Schweizer and Peacock 2008). These challenges have been partially addressed by *in vivo* excision and recycling of these

precious selection markers via Flp and Cre site-specific recombinase systems (Choi et al. 2008). However, a drawback of this approach is that every Cre or Flp excision will leave behind a loxP or FRT site. In extremely rare events, this could cause unwanted recombination when the respective site-specific recombinases are reintroduced, which might result in deletions or inversions of chromosomal segments (Hoang et al. 1998; Choi et al. 2008). In addition to antibiotics, non-antibiotics have been developed as selection markers for *Burkholderia* by Barrett et al. (2008). One such marker is tellurite resistance (Tel^r), which has been applied in *B. thailandensis*, a member of the *B. pseudomallei* group that is a frequent surrogate for *B. pseudomallei* and *B. mallei* research (Howe et al. 1971; Barrett et al. 2008). The Tel^r marker can be recycled by generating an unmarked mutation by coupling Tel^r-FRT cassettes and FRT sequences (Barrett et al. 2008). Another engineered non-antibiotic selection marker is based on the *gat* gene, which encodes for glyphosate acetyltransferase. This enzyme confers resistance to the herbicide glyphosate in *B. pseudomallei* (Norris et al. 2009).

1.4.2 Not naturally competent: DNA uptake, host defence mechanisms, and restriction-modification

Natural competence is a mechanism driven by genes that allow some bacteria to uptake DNA from their environment. Transformation is usually more achievable in strains that are naturally competent, where the competence genes are expressed (Mell and Redfield 2014). Many of the genes that encode the DNA uptake apparatus are also present in the non-competent strains of *Burkholderia* (Blokesch 2016). However, in these strains, the competent genes are not continuously expressed but activated during specific growth phases or in response to specific environmental cues (Blokesch 2016). Similar patterns have been observed in other bacterial species, where inducers of DNA uptake include high cell density, antibiotic stress, DNA damage, intracellular growth, absence of preferred carbon sources, and general starvation (Blokesch 2016).

In the *Burkholderia* genus, only some species and strains are naturally competent. For example, natural competence has not been described in *B. mallei* or within the *B. cepacia* complex. Approximately 50% of *B. pseudomallei* are naturally transformable, including *B. pseudomallei* strain 1026b, which can uptake extracellular DNA, allowing easy genetic manipulation (Thongdee et al. 2008; Kang et al. 2011; Norris et al. 2017). However, gene modifications are more complex in prototype strains *B. pseudomallei* K96243 (Thongdee et al. 2008), *B. mallei* ATCC 23344, and *B. cenocepacia* K56-2, all of which are non-naturally competent (Norris et al. 2017).

Four fosmids, each containing 30 to 40 genes isolated from *B. pseudomallei* 1026b, were able to confer DNA transformation to non-naturally competent *Burkholderia* species, *B. pseudomallei* K96243, *B. mallei* ATCC 23344, and *B. cenocepacia* K56-2 (Norris et al. 2017). These species were able to uptake green fluorescent protein (*gfp*) DNA and grow using DNA as their sole carbon source. Mutation in five of these genes in *B. pseudomallei* 1026b resulted in a growth reduction on DNA and decreased *gfp* DNA uptake, indicating that these genes play a role in natural transformation (Norris et al. 2017). A subsequent study demonstrated that the *comE* and *crp* genes enable non-naturally competent *Burkholderia* species to catabolize DNA, uptake and express exogenous *gfp* DNA, and utilize the λ-red genetic engineering system. This system is a rapid chromosomal manipulation method, which will be discussed in a later section (Heacock-Kang et al. 2018).

Another factor that may influence the successful modification of *Burkholderia* is the native immune system of bacteria. One of the most important immune systems is the restriction-modification system. In order to evade this system, it is important to identify methylated motifs (Riley and Guss 2021). According to REBASE, a database that contains information on restriction-modification systems components, almost all *Burkholderia* spp. are predicted to have one or more methylation sites (Roberts et al. 2015). While not all

methyltransferases are associated with restriction enzymes, the methylated motifs indicate the potential maximum number of sites subject to restriction in each host (Riley and Guss 2021).

There are several ways to overcome the restriction-modification system, which include transforming DNA that lacks the identified motifs, mutating DNA so that it no longer contains the motif, methylating DNA of interest in a similar way as the target host (*Burkholderia*) before transformation, or *in vitro* methylation of the foreign DNA using commercially available enzymes or with cell-free extracts (Riley and Guss 2021). These methods have been shown to increase transformation efficiency in *Helicobacter pylori* (Donahue et al. 2000) and *Saccharopolyspora spinosa* (Matsushima and Baltz 1994). Despite numerous studies on the restriction-modification system in *Burkholderia*, to the best of my knowledge, none of these studies specifically address the restriction-modification barrier in the context of transforming exogenous DNA (Smith and Jeddeloh 2005; Hong et al. 2019; Vandenbussche et al. 2020; Mannweiler et al. 2021).

1.4.3 High GC content

Burkholderia genomes have high GC content and repetitive DNA elements, making DNA-based applications, such as gene synthesis, PCR-based amplification, and genome sequencing, challenging. Some of these issues have been addressed as the commercial enzymes have become more efficient, and specialized protocols have been developed for amplifying GC-rich regions. These include stepdown PCR, slowdown PCR, and PCR with multiple heat pulses during the extension phase (Frey et al. 2008; Orpana et al. 2012). Adding certain organic molecules to PCR reaction mixtures, such as DMSO, glycerol, and betaine, could also improve the amplification (Musso et al. 2006; Flores-Juárez et al. 2016). Chen *et al*. successfully knocked out a highly GC-rich gene (74.71% GC) from *Burkholderia pyrrocinia* JK-SH007 using a three-fragment mutagenesis cassette (Chen et al. 2021a). This was achieved by combining overlap extension with the touchdown PCR, overcoming the usual limitations

imposed by the size and GC content of target DNA (Chen et al. 2021a). While these techniques have improved the outcome when working with GC-rich genomes like *Burkholderia*, it is important to note that they may not be universally effective for all sequences.

The expression of heterologous genes in *Burkholderia* sometimes requires codon optimization. For instance, the native *cas9* or its engineered nuclease inactive counterpart *dCas9* (dead cas9) from *Streptococcus pyogenes* that has been expressed in *Escherichia coli, Bacillus subtilis, Staphylococcus aureus,* and *Acinetobacter baumannii* for Clustered Regularly Interspaced Short Palindromic Repeats (CRISPR)-based genetic tools. However, these genes were not expressed in *B. cenocepacia* K56-2 (Hogan et al. 2019). Codon optimization of the *dcas9* sequence was necessary for its expression in K56–2. A similar situation can be observed in species with high GC content, where codon optimization is also necessary, such as in *Pseudomonas aeruginosa* (Hogan et al. 2019). Codon optimization is also necessary for fluorescent tagging constructs in *Burkholderia* species. Commercially available fluorescent proteins are optimized for eukaryotic expression or for bacteria with low GC content (Norris et al. 2010). Thus, codon preference might be an issue during protein expression in *Burkholderia* spp. (Gustafsson et al. 2004; Norris et al. 2010). To address this, one optimization strategy for developing vectors for fluorescent labelling of *B. pseudomallei* and *B. thailandensis* involves changing the codons to those preferred by *B. pseudomallei* (Norris et al. 2010). Additionally, the application of bio-orthogonal noncanonical amino acid tagging (BONCAT) in *B. thailandensis* E264 involves introducing a plasmid with a codon-optimized methionyl-tRNA synthetase ($MetRS^{NLL}$) gene sequence of *E. coli*. This method requires the expression of *E. coli* $MetRS^{NLL}$ in *B. thailandensis* E264, enabling the labelling of newly synthesized proteins in *Burkholderia* spp. with orthogonal amino acid labelling (Franco et al. 2018). These examples highlight the role of codon optimization in efficient heterologous gene expression in *Burkholderia* species.

1.5 *Burkholderia* genetic tool arsenal

Despite these challenges, researchers can still address some of the issues and perform genetic manipulation on *Burkholderia.* Here, various genetic tools are available and demonstrated in this genus, which comprises gene deletion, replacement, insertion, plasmid-based expression, CRISPR-based system, reporter systems, and transposon mutagenesis will be discussed (see **Table 1.1**).

Table 1. 1 Summary of molecular biology tools developed or applied to *Burkholderia*.

Genetic tool arsenal	**Vectors**	**Species or strains of *Burkholderia* for which the tool was used**
Gene insertion		
Site-specific integration	pGPΩ series	*B. cenocepacia* (Flannagan et al. 2007), *B. ambifaria* (Mullins et al. 2019), *B. gladioli* (Jones et al. 2021), *B. multivorans* (Denman and Brown 2013)
	pKNOCK series	*B. ambifaria* (Chapalain et al. 2013), *B. pseudomallei* (Srinon et al. 2020), *B. gladioli* (Elshafie et al. 2019), *B. glumae* (Chen et al. 2015), *B. phytofirmans*, *B. phymatum* (Coutinho et al. 2013), *B. cenocepacia* (Castonguay-Vanier et al. 2010), *B. thailandensis* (Dubeau et al. 2009), *B. xenovorans* (Denef et al. 2006)
Single copy insertion	pUC18T-mini-Tn7T, pUC18R6K-mini-Tn7	*B. thailandensis* (Choi et al. 2005), *B. mallei*, *B. pseudomallei* (Choi et al. 2006), *B. gladioli* (Somprasong et al. 2010), *B. glumae* (Jang et al. 2014; Nam et al. 2021), *B. ubonensis*, *B. dolosa* (Schaefers et al. 2017 p.; Roux et al. 2018; Somprasong et al. 2020), *B. cenocepacia* (Heacock-Kang et al. 2018)
Gene deletion		
Clean/ Unmarked deletion	pGPI-SceI and pDAI-SceI	*B. cenocepacia* (K56-2 and J2315) (Flannagan et al. 2008), *B. ambifaria* (Masschelein et al. 2019), *B. multivorans* (Schmerk and Valvano 2013), *B. gladioli* (Jian and Challis 2018)
	pAA1-MB1 and pSceI	*B. cenocepacia* (PC184) (Abdu et al. 2018)
Allelic replacement-based gene deletion or replacement	pEX18 and pEX19	*B. cepacia* (Huber et al. 2001), *B. cenocepacia* (Malott et al. 2005), *B. glumae* (Iqbal et al. 2021), *B. lata* (Hendry et al. 2021), *B. multivorans* (Sato et al. 2017), *B. thailandensis* (Chandler et al. 2009), *B. mallei* (Burtnick et al. 2010), *B. pseudomallei* (Mima and Schweizer 2010)
	pEX18-derivaties and pBAKA	*B. thailandensis* (Barrett et al. 2008), *B. ambifaria* (Chapalain et al. 2017), *B. cenocepacia* (Fazli et al. 2013)

	pDONRPEX18 series and pDAI-SceI-pheS	*B. cenocepacia* (Fazli et al. 2015)
	pEXKm5 and pBADSce	*B. pseudomallei* (López et al. 2009), *B. ubonensis* (Somprasong et al. 2020), *B. multivorans* (Myers-Morales et al. 2019), *B. dolosa* (Perault and Cotter 2018), *B. cenocepacia* (Loeven et al. 2021), *B. thailandensis* (Garcia et al. 2013), *B. mallei* (Memišević et al. 2013)
	pDM4 or derivative	*B. pseudomallei* (Denef et al. 2006)
	pSHAFT	*B. cenocepacia* (Agnoli et al. 2006)
	pSHAFT derivatives	*B. cenocepacia*, *B. lata*, *B. thailandensis*, *B. vietnamiensis* (Shastri et al. 2017; Wallner et al. 2021)
Deletion of third chromosome	pMinic3	*B. ambifaria*, *B. anthina*, *B. cenocepacia*, *B. pyrrocinia*, *B. ubonensis*, *B. vietnamiensis* (Agnoli et al. 2012)
Recombineering		
λ Red recombination	pBBRRed	*B. cepacia* (Jia et al. 2010)
	pKD46 and pCR4Blunt-TOPO®	*B. gladioli* (Moebius et al. 2012)
	pKaKa series and pwFRT series	*B. thailandensis*, *B. pseudomallei*, *B. mallei*, *B. cenocepacia* (Kang et al. 2011; Heacock-Kang et al. 2018)
Redγ-BAS system	pBBR1-Rha-Redγ-BAS-km	*B. gladioli* (Chen et al. 2021b)
RecET system	pBBR1-Rha-Eth series	*B. glumae* and *B. plantarii* (Li et al. 2021)
Transposon mutagenesis (Tn5)	pUTmini-Tn5Tp	*B. cenocepacia* (Farmer and Thomas 2004)
	pLG99	*B. cenocepacia* (Higgins et al. 2017; Gualdi et al. 2022), *B. thailandensis* (Gallagher et al. 2013), *B. ubonensis* (Somprasong et al. 2020)
	EZ-Tn5<R6Kγori/KAN-2>Tnp	*B. seminalis* (Araújo et al. 2016), *B. plantarii*, *B. gladioli* (Yoshimura et al. 2020)
	pIT2	*B. thailandensis* (Gallagher et al. 2013; Mao et al. 2020)
	pRL27	*B. gladioli* (Ganesan et al. 2021)
	pUT-mini-Tn5Km2	*B. vietnamiensis* (O'Sullivan et al. 2007), *B. ambifaria* (Mahenthiralingam et al. 2011)
	pTGL166	*B. multivorans* (Malott et al. 2012)
	pTnMod-pKmOGm'	*B. thailandensis* (Park et al. 2020)
CRISPR-based genetic tools		
CRISPR interference	pAH-CTX1rah series and pSCB2-sgRNA	*B. cenocepacia*, *B. multivorans*, *B. thailandensis* (Hogan et al. 2019)
CRISPR associated transposase	pCasTn and pDonor	*B. thailandensis* (Trujillo Rodríguez et al. 2023)
CRISPR/Cas 9	pCasPA and pACRISPR	*B. multivorans* (Ferreira et al. 2024)
	pMLS7, pMLBAD	*B. cenocepacia* (Lefebre and Valvano 2002)

Plasmid-based expression tools	pSCPrhaB2, pSC201	*B. cenocepacia* (Cardona and Valvano 2005)
	pSCrhaB2plus, pSC201plus	*B. cenocepacia*, *B. thailandensis*, *B. multivorans*, *B. vietnamiensis* (Hogan et al. 2021 p.)
	pFTR5, pFCyGe2	*B. thailandensis* (Schuster and Reisch 2021)
	pHERD30T	*B. pseudomallei* (Qiu et al. 2008)
	pBTBX-5	*B. cepacia* (Prior et al. 2010)
Reporter system	mini-Tn7-gat/kan-cfp/gfp/rfp/yfp	*B. pseudomallei, B. thailandensis* (Norris et al. 2010)
	pmini-Tn7-gat-P1-gfp/rfp	*B. mallei, B. pseudomallei* (Su et al. 2014)
	pFRT1-gfp/lux-Telr	*B. thailandensis* (Kang et al. 2009)

1.5.1 Gene insertion: Site-specific integration

Gene insertion is a rapid and efficient method for interrupting genes and studying their function in *Burkholderia* species. A series of suicide plasmids (pGPΩ) has been developed by Flannagan et al. (2007) to inactivate genes in a targeted fashion. These plasmids include pGPΩTp, pGPΩTet, and pGPΩCm, which confer resistance to trimethoprim, tetracycline, and chloramphenicol, respectively. These plasmids are derived from the pGP704 backbone, which carries the Pir protein-dependent R6K origin of replication (Kolter et al. 1978). The gene targeted by the pGPΩ plasmid will result in a polar mutation due to the antibiotic resistance cassette flanked by the Ω fragment (Prentki and Krisch 1984). Initially developed for *B. cenocepacia*, these plasmids have been used in several other *Burkholderia* spp., including *B. ambifaria* (Mullins et al. 2019), *B. gladioli* (Jones et al. 2021), and *B. multivorans* (Denman and Brown 2013). Another series of broad host range suicidal integrative vectors, pKNOCK and its derivatives, have also been used for gene knock-out and targeted DNA insertion into chromosomes in *Burkholderia*. These vectors contain the γ-origin of replication of the R6K plasmid (Alexeyev 1999) and have been used in various *Burkholderia* species, including *B. ambifaria* (Chapalain et al. 2013), *B. pseudomallei* (Srinon et al. 2020), *B. gladioli* (Elshafie et al. 2019), *B. glumae* (Chen et al. 2015), *B. phytofirmans*, *B. phymatum* (Coutinho et al. 2013),

B. cenocepacia (Castonguay-Vanier et al. 2010), *B. thailandensis* (Dubeau et al. 2009), and *B. xenovorans* (Denef et al. 2006).

1.5.2 Single copy insertion: Mini-Tn7 insertion

Transposon Tn7-based mini-Tn7 is a versatile tool for integrating cloned genes, which can be used for gene complementation, expression, and analysis (Choi et al. 2005, 2006). Typically, mini-Tn*7* vectors are inserted into the chromosome at an *att*Tn*7* site downstream of the essential *glmS* gene. All *Burkholderia* spp. analyzed contained multiple *glmS* sites and, consequently, various *att*Tn*7* sites, except *B. glumae* (Choi et al. 2005, 2006). Choi et al. developed a Tn7-based broad-range bacterial cloning and expression system, demonstrating utility in *B. thailandensis* by transposing a mini-Tn*7*T-Gm-REP derivative containing the R6K origin of replication into its genome. In all of the transformants obtained, Tn*7* insertion occurred 25 bp downstream of either *glmS*1 or *glmS*2 but not at both sites (Choi et al. 2005). Subsequently, the same group developed the mini-Tn7 insertion for bacteria with multiple *glmS*-linked *att*Tn*7* sites in *B. mallei* (Choi et al. 2006). The mini-Tn*7* vectors used for *B. mallei* include pUC18T-mini-Tn7T, pUC18T-mini-Tn7T-Gm, pUC18T-mini-Tn*7*T-Gm-REP. In their study, 96% of the insertions occurred at the *glmS1 att*Tn*7* site, 8% at the *glmS2 att*Tn*7* site, and only 4% of the transformants had insertions at both sites. In *B. pseudomallei*, which contains three *glmS* genes, insertions predominantly occur downstream of *glmS2*. Similarly, in *B. gladioli*, all tested transformants exhibited a single mini-Tn7 insertion site. These findings suggest that one glmS-associated mini-Tn7 insertion site is preferentially used for site-specific mini-Tn7 insertions (Somprasong et al. 2010). The mini-Tn7 system has also been applied in other *Burkholderia* species, including *B. glumae* for green fluorescent protein fusion (Jang et al. 2014; Nam et al. 2021), *Burkholderia ubonensis* and *Burkholderia dolosa* for gene complementation (Schaefers et al. 2017; Roux et al. 2018;

Somprasong et al. 2020), as well as *B. pseudomallei* and *B. cenocepacia* for gene expression (Heacock-Kang et al. 2018).

1.5.3 Clean/Unmarked deletion

A clean deletion method developed by Flannagan et al. (2008) enables targeted, non-polar, unmarked deletions for *Burkholderia* species. This system utilizes the I-SceI homing endonuclease and involves two independent crossover events by homologous recombination. In this process, the upstream and downstream regions of the target gene are cloned into the suicide plasmid pGPI-SceI, which contains the I-SceI recognition site. This vector is then introduced into the cells, integrating into the genome via homologous recombination. The second crossover event occurs with the introduction of the plasmid pDAI-SceI, which expresses the I-SceI nuclease, into the strain that has undergone a single crossover. The expression of I-SceI homing endonucleases creates a double-stranded break at the I-SceI restriction site, stimulating another recombination within the host. This repair process results in either the restoration of the wild-type gene or the desired deletion. This method allows for multiple deletions within the same strain under consistent selection conditions. To effectively use this system, the genome of the strain must lack the I-SceI recognition site (Flannagan et al. 2008). Flannagan et al. successfully employed this method to delete an entire operon, specifically a 10.9 kb region encoding a Type III secretion system in *B. cenocepacia*. This system has been applied in several other species, including *B. ambifaria* (Masschelein et al. 2019), *B. multivorans* (Schmerk and Valvano 2013), and *B. gladioli* (Jian and Challis 2018). However, this method could not generate deletion mutants in certain *Burkholderia* strains, such as *B. ambifaria* AMMD (Masschelein et al. 2019) and *B. vietnamiensis* D0774 (Jassem 2012), and the reasoning is unknown.

The clean deletion system developed by Flannagan et al. has been mainly used in *B. cenocepacia* Electrophoretic Type-12 (ET12) lineage, including type strain J2315 and

genetically useful strain K56-2 (Mahenthiralingam et al. 2001; Coenye and LiPuma 2002; Buroni et al. 2009; Bazzini et al. 2011; Hanuszkiewicz et al. 2014; Abdu et al. 2018; Lightly et al. 2019; Vandenbussche et al. 2020). Abdu et al. (2018) expanded this system for use in other *Burkholderia* strains, including *B. cenocepacia* IIIB Midwest clones, the dominant *B. cenocepacia* epidemic clones in the USA (Coenye and LiPuma 2002). The modification involved replacing the *pir*-dependent R6K origin of replication with the pMB1 narrow-host-range origin of replication, yielding pAA1-MB1. Additionally, SceI-containing plasmids were constructed with various antibiotic-resistant markers (Abdu et al. 2018), who applied this modified clean deletion system in *B. cenocepacia* PC184 because it could not be manipulated using the original system of Flannagan et al. (2008) due to its high-level tetracycline resistance.

1.5.4 Allelic replacement-based gene deletion or replacement

Gene inactivation through allelic replacement using the Flp-*FRT* recombination system has also been applied in *Burkholderia* species (Barrett et al. 2008). In this approach, the wild-type gene is replaced by an antibiotic-resistance cassette through two recombination crossover events. Each crossover occurs on either side of the target gene, and no vector sequences remain integrated into the chromosome in the mutant (Shastri et al. 2017). The vectors, pEX18 and pEX19 are the commonly used vectors in *Burkholderia* for this method (Hoang et al. 1998). This system has been applied to various *Burkholderia* species, such as *B. cepacia* (Huber et al. 2001), *B. cenocepacia* (Malott et al. 2005), *B. glumae* (Iqbal et al. 2021), *B. lata* (Hendry et al. 2021), *B. multivorans* (Sato et al. 2017), *B. thailandensis* (Chandler et al. 2009), *B. mallei* (Burtnick et al. 2010), and *B. pseudomallei* (Mima and Schweizer 2010). Over time, additional derivatives of these vectors have been developed (Barrett et al. 2008; Fazli et al. 2015). For instance, Barrett et al. (2008) modified the allelic replacement vectors by replacing the counter-selection marker gene *sacB* with the mutant *pheS* gene from *B. pseudomallei*. One such vector, pBAKA, includes the asd_{Pa} gene as a non-antibiotic-selection marker. Among the developed

vectors, pBAKA was used to create mutants in *B. thailandensis*, pEX18Tet-*pheS* to generate mutants in *B. ambifaria* (Chapalain et al. 2017), and pEX18AP-*pheS* in *B. cenocepacia* (Fazli et al. 2013). Fazli et al. (2015) further modified the vectors from Barrett et al. (2008) to create a Gateway-compatible allelic exchange system incorporating the counter-selectable *pheS* gene and the I-SceI homing endonuclease, along with various resistance markers. The vectors created from this system include pDONRPEX18Tp-SceI-*pheS*, pDONRPEX18Gm-SceI-*pheS*, and pDONRPEX18Km-SceI-*pheS* (Fazli et al. 2015). They employed pENTRPEX18Tp-SceI-*pheS* to create gene replacements in *B. cenocepacia*, followed by gene deletion, which was achieved by introducing a double-stranded DNA break by I-SceI endonuclease expressed from pDAI-SceI-*pheS* (Fazli et al. 2015).

Another allelic exchange vector, pEXKm5, was developed by López et al. (2009) for generating unmarked, in-frame deletion mutations *B. pseudomallei*. This vector can be used alongside I-SceI and *sacB*-based methods to generate deletions. The I-SceI-based allele replacement system is completed using pBADSce, an arabinose-inducible I-SceI expression vector. This method has been applied to species such as *B. ubonensis* (Somprasong et al. 2020), *B. multivorans* (Myers-Morales et al. 2019), *B. dolosa* (Perault and Cotter 2018), *B. cenocepacia* (Loeven et al. 2021), *B. thailandensis* (Garcia et al. 2013), and *B. mallei* (Memišević et al. 2013). Additionally, Louge et al. (2009) developed an unmarked allele-replacement mutagenesis method, which uses efficient *sacB* counter-selection for *B. pseudomallei* to enable multiple deletions within single genes or larger multigenic loci. This system involves cloning the deleted allele into a suicide vector pDM4, which confers sucrose sensitivity and facilitates genomic integration and excision to yield either deletion mutants or revertants to wild-type (Logue et al. 2009).

Agnoli et al. (2006) and Shastri et al. (2017) have developed another allelic replacement system for *Burkholderia* spp., based on the suicidal vectors pSHAFT vector and its derivatives.

The original pSHAFT vector was derived from pUTmini-Tn*5*Cm (de Lorenzo et al. 1990), an R6K-based plasmid used to construct deletion mutants in *B. cenocepacia* (Agnoli et al. 2006). However, its utility was limited due to a limited number of unique restriction sites, partially due to the duplication of restriction sites around its large chloramphenicol resistance cassette, Cm^R. To address these limitations, the derivatives of pSHAFT- pSHAFT2, pSHAFT3, and pSHAFT-GFP were developed with reduced sizes of the Cm^R marker to increase the availability of unique restriction sites for use in the vectors. Additionally, these vectors provide increased expression of the antibiotic-resistance markers to facilitate single-copy selection and prevent polar effects by blocking transcriptional read-through into downstream genes. These vectors have demonstrated gene inactivation in *B. cenocepacia*, *B. lata, B. thailandensis,* and *B. vietnamiensis* (Shastri et al. 2017; Wallner et al. 2021).

1.5.5 Deletion of the third chromosome

The *Burkholderia* genome consists of a tripartite genome. During a transposon mutagenesis experiment, Agnoli et al. (2012) unexpectedly isolated mutants that had lost the third replicon (c3) and observed that these mutants exhibited attenuated virulence. To further investigate, they constructed a c3 mini-replicon and used it to cure the third chromosome via plasmid incompatibility. To construct the mini-replicon, they incorporated the pC3 origin of replication along with the *repA*, *parB*, and *parA* genes into a modified pEX18 backbone. This backbone contained a trimethoprim resistance gene as a selection marker and the *sacB* gene as a counter-selection marker during plasmid curing. The pMinic3 was introduced into *Burkholderia* strains and subsequently removed using sucrose counter-selection. The *Burkholderia* strains were then verified for the loss of both pMinic3 and the third chromosome. The pMinic3 plasmid proved to be a valuable tool for generating chromosome 3 null mutants in several Bcc strains, including *B. ambifaria, B. anthina, B. cenocepacia, B. pyrrocinia, B. ubonensis*, and *B. vietnamiensis* (Agnoli et al. 2012). The c3-null mutants have attenuated

virulence in several animal models, suggesting that this strategy could be employed to mitigate pathogenicity in *Burkholderia*.

1.5.6 Recombineering

Other than restriction site-based cloning and homologous recombination-based gene modification, the red recombinase system of lambda phage is a powerful genetic manipulation technique that is independent of restriction sites and has been successfully applied to several *Burkholderia* species. For instance, the λ Red recombination has been used for homologous lipase overexpression in *B. cepacia*. Jia et al. (2010) generated a 5 kb gene substitution with 500 bp homology and successfully created the desired mutant with an efficiency of 85%. The lipase activity of this mutant is approximately threefold higher than the wild type under the control of the T7 system. Notably, the authors reported that the ordinary suicide vector method failed to generate any transformants in their studies, indicating that the lambda red mutagenesis strategy is highly efficient and well-suited for complicated genome manipulation.

The λ red recombination system has also been applied in *B. gladioli* to investigate the *bon* gene cluster through gene replacement. The *bonA* gene was inactivated using PCR products containing flanking regions of 600–950 nucleotides homologous to the target sequence. Metabolic profiling of the Δ*bonA* mutant revealed that it does not produce bongkrekic acid (Moebius et al. 2012). Another study involved the knock-out of the gladiolin gene cluster in *B. gladioli* ATCC 10248 and compared the efficacy of three different versions of the red recombineering system: Redγβα, Redγ-Redαβ7029, and Redγ-BAS. Among these, Redγ-BAS proved to be the most efficient for manipulating *B. gladioli* ATCC 10248. Using this system, they replaced 1267 bp of the gladiolin gene cluster (*gbnD2*) with an apramycin resistance gene flanked by homology arms of varying length (50 bp, 75 bp, 100 bp), resulting in the complete abolition of gladiolin production. Using the same recombineering tool, they also replaced the native promoter with a potent exogenous promoter that expresses

constitutively to activate two silent non-ribosomal peptide synthetase gene clusters (*bgdd and hgdd*), enabling the production of novel lipopeptides (Chen et al. 2021b).

In naturally transformable *Burkholderia* species such as *B. thailandensis* and *B. pseudomallei,* the lambda red recombineering system has been used to knock-out and pull-out chromosomal DNA fragments. PCR fragments with flanking homology arms (40–45 bp) targeting specific regions were generated using primers with incorporated homology sequences. The one-step recombination was then achieved by incubating the PCR product with cells expressing lambda red proteins, followed by selection (Kang et al. 2011). This method was further extended to the non-competent *Burkholderia* species, including type strains *B. pseudomallei* K96243, *B. mallei* ATCC 23344, and *B. cenocepacia* K56-2 by integrating *comE* and *crp* genes into a Tn7 attachment-site (Heacock-Kang et al. 2018).

In addition to the lambda red recombinase system, another recombineering approach based on RecET proteins from Rec phage has been developed for *B. glumae* and *B. plantarii*. This system utilized three Rac bacteriophage RecET-like operons, $RecETh_{BDU8}$, $RecETh_{TJI49}$ and $RecETh1h2e_{YI23}$, which are obtained from *Burkholderia* and *Caballeronia* (Li et al. 2021). Li et al. demonstrated that a homology length of 125 bp exhibited the highest efficiency for $RecETh_{TJI49}$ and $RecETh1h2e_{YI23}$ in *B. glumae*. Using these recombineering systems, a functional promoter was inserted upstream of three cryptic non-ribosomal peptide synthetase biosynthetic gene clusters, activating these gene clusters and enabling the identification of new lipopeptides.

1.5.7 Transposon mutagenesis to uncover novel gene functions in *Burkholderia*

Transposon mutagenesis has been widely employed to identify essential genes in bacterial genomes by randomly inserting transposable elements, such as transposon (Hutchison et al. 1999). This technique has been applied to various *Burkholderia* species, including *B.*

pseudomallei, *B. thailandensis*, and three strains of *B. cenocepacia*, to elucidate their essential genes (Baugh et al. 2013; Moule et al. 2014; Wong et al. 2016; Higgins et al. 2017; Gislason et al. 2017). Additionally, transposon mutagenesis has been utilized to study conditional essential genes, which may serve as potential targets for antibiotics (Scoffone et al. 2021). In this section, examples of how transposon mutagenesis has been utilized as a tool to uncover gene functions in different *Burkholderia* species will be discussed. Generally, transposons are introduced into the cell to disrupt genes, where each cell carries a single insertion. Transposon mutants are then screened for phenotype changes, and the transposon-genome junctions are then sequenced and mapped to the genome, allowing for the identification of the transposon integration site (Scoffone et al. 2021).

For instance, using the mini-Tn5Tp transposon in *B. cenocepacia*, two mutants unable to produce pyochelin were isolated. The mutants have the transposons integrated into the *CysW* gene, which encodes for the sulphate/thiosulfate transporter. Further investigation revealed that the production of pyochelin in *B. cenocepacia* depends on the availability of sulphur and iron (Farmer and Thomas 2004). Moreover, genes involved in tolerance for gold and silver in *B. cenocepacia* H111 were identified using a Tn5 transposon mutant library (Higgins et al. 2017; Gualdi et al. 2022). They have identified 138 and 164 genes that facilitate the growth of *B. cenocepacia* H111 in the presence of silver and gold ions, respectively, primarily encoding transporters and membrane proteins (Gualdi et al. 2022).

Genes contributing to the suppression of orchid necrosis caused by *B. gladioli* were identified in *Burkholderia seminalis* using the commercial EZ-Tn5<R6Kγori/KAN-2>Tnp transposome kit from Epicentre Biotechnologies (Araújo et al. 2016). Transconjugants lacking the ability to suppress leaf necrosis were selected. The transposons were mapped to eight loci, including the *wcb* gene cluster, which is related to the synthesis of extracellular polysaccharides. This cluster is a crucial determinant in bacterial-host interactions in other systems. The other

seven loci are highly conserved among *Burkholderia* spp. (Araújo et al. 2016). Additionally, transposon mutagenesis was used to identify candidate insect colonization factors in a mutualistic *B. gladioli* symbiont of the beetle *Lagria villosa* (Ganesan et al. 2021). However, this study does not specify the factors involved in colonization (Ganesan et al. 2021).

In *B. vietnamiensis*, transposon mutants and pools created with mini-Tn5Km2 transposon have uncovered several genetic bases of various ecological and biologically useful functions (O'Sullivan et al. 2007). For phenol degradation, the toluene ortho-monooxygenase (TOM) catabolic pathway and several novel accessory genes were identified. Rhizosphere colonization by *B. vietnamiensis* was found to be influenced by several putative functions, including amino acid biosynthesis and general metabolism. Notably, the inactivation of a single virulence-associated autotransporter adhesin gene resulted in increased colonization (O'Sullivan et al. 2007).

Transposon mutagenesis using mini-Tn5-Km2 has been employed to identify the genetic basis responsible for the antibacterial activity of *B. ambifaria* AMMD (O'Sullivan et al. 2007; Mahenthiralingam et al. 2011). Some transconjugants exhibited a loss of antibacterial activity, and the insertion sites of the transposon were mapped to various regions of the *B. ambifaria* AMMD genome, which included a putative polyketide biosynthesis island. It was determined that enacyloxin is the compound responsible for the observed antibacterial activity (Mahenthiralingam et al. 2011).

Additionally, genes associated with polymyxin resistance in *B. multivorans* have been identified using transposon mutagenesis with Tn5-751S (Malott et al. 2012). A library of transposon mutants was screened for increased susceptibility to polymyxin B. In these transconjugants, the transposon was inserted into genes within a putative hopanoid biosynthesis cluster, which is presumed to be involved in membrane stability and barrier function. Further

analysis suggests that hopanoid biosynthesis is involved in multiple antimicrobial resistance mechanisms (Malott et al. 2012).

Similarly, genes involved in *B. ubonensis* meropenem resistance were identified using the Tn*5*-based transposon T23 to screen for increased susceptibility in meropenem (Somprasong et al. 2020). The transposon is inserted into a gene encoding for the outer membrane protein assembly factor BamC, as well as into genes encoding diverse cellular functions (Somprasong et al. 2020).

Transposon mutagenesis has been employed with fluorescent reporters to activate silent clusters in *B. thailandensis*. This process involved creating a mutant library to screen the desired phenotype via reporter gene expression. The transposon insertion into the *pyrF* gene, along with small molecule-mediated inhibition of PyrF, triggers the biosynthesis of malleilactone (Mao et al. 2020). In another study on *B. thailandensis,* Park et al. (2020) used phenotype-guided transposon mutagenesis to characterize a silent biosynthetic gene cluster using the mini-transposon TnMod-pKmOGm'. With this approach, this study linked the *org* operon to three novel cryptic metabolites, thailandene A, B, and C. Subsequently, the same group applied mass spectrometry-guided transposon mutagenesis to two other *Burkholderia* species, *B. plantarii* and *B. gladioli,* to unlock cryptic metabolites. This study revealed seven cryptic metabolites across three compound classes (Yoshimura et al. 2020).

1.5.8 CRISPR-based genetic tools

1.5.8.1 CRISPR interference

Clustered Regularly Interspaced Short Palindromic Repeats (CRISPR) and associated Cas system is a prokaryotic defence mechanism that has rapidly adapted into a powerful and versatile tool in molecular biology. CRISPR interference (CRISPRi) is a gene silencing method to silence gene expression based on catalytically inactive Cas9 protein (dCas9). When co-

expressed with guide RNA, it forms an RNA-protein complex that recognizes target DNA sequences and interferes with transcription elongation, RNA polymerase binding, or transcription factor binding (Qi et al. 2013). CRISPRi has been developed for *Burkholderia* species and has been demonstrated in *B. cenocepacia*, *B. multivorans*, and *B. thailandensis* (Hogan et al. 2019). This CRISPRi system is tunable, as the codon-optimized *dcas9* from *S. pyogenes* was placed under the control of a rhamnose-inducible promoter. The system has been used to target the *paaABCDE* operon, which regulates phenylacetic acid degradation. The targeting resulted in near-complete growth inhibition when phenylacetic acid was used as the sole carbon source, and the expression of *paaA* mRNA also decreased. This study further evaluated the CRISPRi system on a single-cell level by targeting *phbC*, which encodes an enzyme required for polyhydroxybutyrate (PHB) synthesis, and *fliF*, which encodes a transmembrane protein required for flagellar MS ring structure. Knockdown of *phbC* led to decreased PHB granule accumulation, while knockdown of *fliF* reduced bacterial motility. In contrast to CRISPRi-mediated knockdown, disruption of the *phbC* gene via insertional mutagenesis completely abolished PHA granule formation. Approximately 17% of CRISPRi mutants escaped the silenced phenotype, suggesting that this system exhibits a unimodal "all or none" effect at the single-cell level in *B. cenocepacia* K56-2 (Hogan et al. 2019).

1.5.8.2 CRISPR-associated transposase

The CRISPR-associated transposase (CAST) systems enable programmable targeting of transposons using co-expressed guide RNA, allowing for targeted gene disruption and integration of recombinant DNA (Strecker et al. 2019). Recently, Trujillo Rodríguez et al. (2023) developed a broad-host-range CAST system based on the CAST system from *Scytonema hofmannii* (Strecker et al. 2019), specifically for use in Proteobacteria. They applied this method to a species of *Burkholderia*, *B. thailandensis.* This method allows for both single and multiplex targeting of transposon insertion. However, 43% of the integration consisted of

the whole plasmid in *B. thailandensis*. While this event is undesirable, it did not prevent the disruption of the targeted genes. Rodríguez et al. (2023) successfully inserted an 11 kb operon into *Pseudomonas putida*, but they did not achieve the same results with *B. thailandensis.*

1.5.8.3 CRISPR-Cas9

A CRISPR-Cas9-based system has been developed for genetic manipulation in *B. multivorans* for unmarked gene deletion and targeted gene insertion (Ferreira et al. 2024). In contrast to the previously available allelic exchange system for *Burkholderia* that requires two-step homologous recombination, this CRISPR/Cas9-based system only requires a single-step allelic exchange. This system consists of two plasmids: pCasPA, which encodes for L-arabinose inducible Cas9 endonuclease and the λ-Red system proteins, and pACRISPR, which expresses the sgRNA and carries the repair template necessary for homology-directed repair. They demonstrated the efficacy of this system by deleting four genes (*rpfR*, *bceF*, *cepR*, and *bcsB*) in two strains of *B. multivorans* and inserting a *gfp* gene into the chromosome. However, it was found that pCasPA is unstable, resulting in significant plasmid loss even under selective pressure, which reduces the overall efficiency of the system. Additionally, curing the plasmid for this system could take a long time, as the curing of pACRISPR-Km requires multiple passages, especially for one of the strains, P0213-1, in which the SacB curing could not be used.

1.5.9 Plasmid-based gene expression tools

Gene expression tools are important for studying gene function and pathogenicity in *Burkholderia.* Several gene expression vectors have been developed and used in this genus. This section will discuss the development of vectors. Lefebre and Valvano (2002) pointed out that the P_{lac} and P_{tac} promoters, which are commonly employed for regulated gene expression in *E. coli*, are non-functional in several *Burkholderia* species. Consequently, various expression vectors have been created and refined in *Burkholderia* spp. For example, vectors

like pMLS7 and pMLBAD utilized either the constitutive promoter from the S7 ribosomal protein gene of *Burkholderia* spp. strain LB400 or the arabinose-inducible P_{BAD} promoter from *E. coli* (Lefebre and Valvano 2002). However, it was found that to achieve maximal expression with pMLBAD, a concentration of 2 to 3% or more arabinose is required, which can lead to osmotic stress. To mitigate this issue, researchers developed pSCPrhaB2, featuring the rhamnose-regulated P_{rhaB} promoter of *E. coli*, which requires only low rhamnose concentration (Cardona and Valvano 2005). A further modification was made by combining the bacteriophage T7 gene 10 stem-loop and engineered *rhaI* transcription factor-binding sites in the rhamnose-inducible expression system. This combination resulted in increased activity and a broader dynamic range (Hogan et al. 2021). The modified promoter was then added into pSCrhaB2 and pSC201, creating pSCrhaB2plus and pSC201plus. The vector pSCrhaB2plus has been used to study gene expression in *B. thailandensis*, *B. multivorans*, and *B. vietnamiensis,* while pSC201plus has been used to control the highly expressed essential genes from the *B. cenocepacia* chromosome (Hogan et al. 2021).

Some gene expression vectors developed for Proteobacteria have demonstrated their utility in *B. thailandensis* (Schuster and Reisch 2021). Three vectors containing different promoter-regulator pairs (AraC/P_{BADmin}, $CymR^{AM}$/P_{CymRC}, and TetR/P_{TetA}) demonstrated >50-fold induction of mRFP reporter in *B. thailandensis*. Schuster and Reisch (2021) reported that promoter-regulator pairs identified in the mRFP screening exhibit very low levels of leaky transcription, with nearly 200,000-fold difference in colony counts between the uninduced and induced samples. Additionally, the study constructed degenerate promoter libraries from pFTR5 in *B. thailandensis.* The library was developed using the TetR/P_{TetA} promoter-regulator pair, with the best variant achieving the greatest fold change of 105, compared to the original pFTR5 construct, which only had a fold change of 3 (Schuster and Reisch 2021).

Vectors have also been developed for the functional analysis of toxic and highly regulated genes in *B. pseudomallei* (Qiu et al. 2008). These vectors were derived from *Escherichia-Pseudomonas* shuttle vectors, where the *lac* promoter was replaced with the P_{BAD} promoter and the *araC* regulator. One of the vectors, pHERD30T, was shown to be effective in *B. pseudomallei* Bp50 by complementing the Δ(*amrAB-oprA*) efflux pump mutation (Choi et al. 2008; Qiu et al. 2008). However, this system exhibited leaky expression, as the complementation was observed in uninduced cells. This leaky expression is likely caused by the basal transcription from the P_{BAD} promoter (Qiu et al. 2008).

Prior et al. (2010) developed several protein expression vectors for various Gram-negative hosts, demonstrating the use of one of these vectors, pBTBX-5, in *B. cepacia* for the expression of GFPuv protein. This vector features a broad-host-range pBBR1 replicon and an arabinose-inducible P_{BAD} promoter for protein expression. They also showed that the empty vector control, when supplemented with arabinose, did not exhibit fluorescence (Prior et al. 2010).

1.5.10 Reporter systems

Fluorescent proteins have been widely used as marker systems in bacteria to study various biological processes. One of the applications of fluorescent proteins is bacterial tagging, which enables the tracking of bacteria, such as during cellular infection (Su et al. 2014). Norris et al. (2010) optimized a site-specific stable fluorescent tagging construct for *Burkholderia.* This system leverages the mini-Tn*7* site-specific transposition system, where a gene of interest is fused with a fluorescent protein, allowing insertion at one of the *glmS* sites in the chromosome. This method allows stable fluorescent labelling of *B. pseudomallei* and *B. thailandensis* in four unique colours (green, cyan, red, and yellow) using fluorescent protein genes *gfp*, *cfp*, *rfp*, and *yfp*, respectively. The ability to tag *Burkholderia* spp. with various colours allows for the localization and tracking of one or more strains expressing different

colours (Norris et al. 2010). Su et al. (2014) developed another chromosomal GFP and RFP tagging system for *B. mallei* and *B. pseudomallei*, which also employed a mini-Tn7 vector to deliver a reporter fusion into the genome. This system demonstrated improved fluorescent signal intensity compared to the earlier system developed by Norris et al. (2010). While the earlier system could not be detected with an exposure time of 200 msec, the method developed by Su et al. exhibited bright fluorescence at an exposure time of less than 200 msec (Su et al. 2014). The difference in detectability could be attributed to the choice of promoter used. Norris et al. (2010) utilized the rpsL promoter PS12 to drive the expression of the fluorescent protein genes, while Su et al. (2014) demonstrated that P1 was a more potent exogenous promoter for driving reporter fusion.

In addition to these developments, *FRT*-reporter fusion vectors expressing *lacZ*, *GFP*, and *luxCDABE* reporter genes have been developed in *Burkholderia* species. These vectors allow Flp-catalyzed recombination and the expression of fluorescence and bioluminescence proteins (Kang et al. 2009). Furthermore, fluorescent reporter gene expression has been coupled with transposon mutagenesis to select mutants that have activated silent clusters, a technique termed reporter-guided mutant selection (Mao et al. 2020).

1.6 Uncovering *Burkholderia* catabolic potential in degrading bioplastic

Accumulation of petroleum-derived plastics in the environment is a major global problem ("Plastics – the Facts 2018 An analysis of European plastics production, demand and waste data" 2018) as these materials are recalcitrant to natural biodegradation processes. Polyhydroxyalkanoates (PHAs) are biological polyesters, produced by microorganisms as storage compounds (Anderson and Dawes 1990), that could replace petroplastics because they have similar properties to petroplastics (Madison and Huisman 1999). PHAs can be classified based on the length of the R-alkyl sidechain, either short-chain length (scl-PHA) or medium-chain length (mcl-PHA). Scl-PHAs consist of subunits with 3-5 carbon atoms, the most

common type of scl-PHA is polyhydroxybutyrate (PHB), where the R-alkyl side chain is a methyl group. Instead, mcl-PHAs are characterized by an R-alkyl side chain of 6 to 14 carbon atoms. One of the representatives of the mcl-PHA family is polyhydroxyoctanoate (PHO), where the monomer is 3-hydroxyoctanoic acid, which contains eight carbon atoms (**Figure 1.2**) (Muneer et al. 2020).

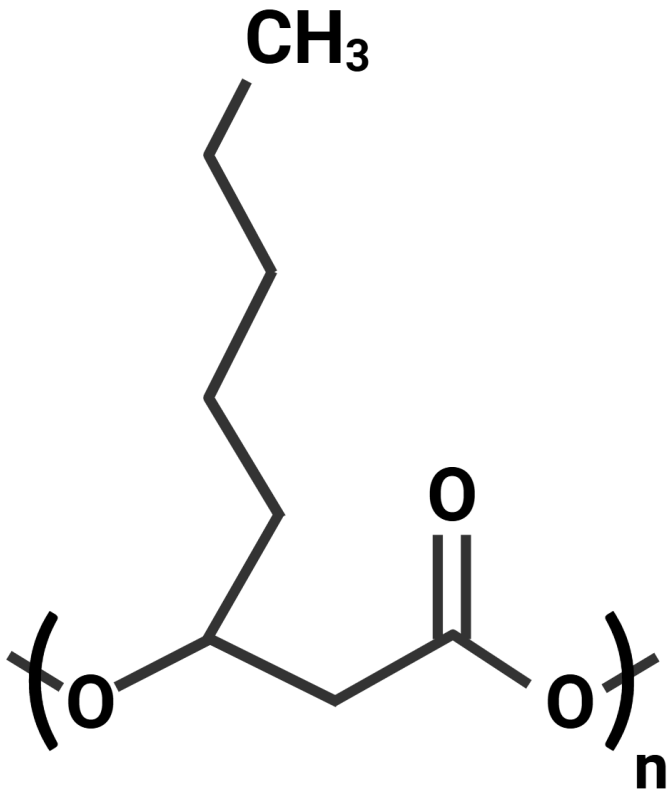


Figure 1. 2 General chemical structure of polyhydroxyoctanoate (PHO).

Figure 1.2 was created with https://biorender.com/.

However, the high diversity of chemical structures observed in PHAs requires different enzyme specificities for degradation. For example, PHO is resistant to degradation in natural environments and typically requires controlled industrial composting conditions to break down

(Narancic et al. 2018; Narancic and O'Connor 2019; W. Meereboer et al. 2020). Additionally, enzymes that degrade mcl-PHA are scarce (Knoll et al. 2009), limiting industrial degradation of PHA. Most of the extracellular mcl-PHA depolymerases that have been purified and biochemically validated belong to *Pseudomonas* sp (Schirmer and Jendrossek 1994; Kim et al. 2005; Rhee et al. 2006), an obligate predator *Bdellovibrio bacteriovorus* (Martínez et al. 2012), *Thermus thermophilus* (Papaneophytou et al. 2011), and the Actinobacteria *Streptomyces* spp. (Gangoiti et al. 2012; Santos et al. 2013; Martínez et al. 2015). BLASTp-based similarity searches using biochemically validated extracellular mcl-PHA depolymerases as queries against metagenomes suggest that extracellular mcl-PHA depolymerase producers are in the taxonomic groups Myxococcota, Proteobacteria, Actinobacteriota and Bdellovibrionota (Viljakainen and Hug 2021). Overall, mcl-PHA degradation is not widely distributed among Bacteria.

There is no significant homology between mcl-PHA depolymerases, scl-PHA depolymerases and lipases other than the presence of a catalytic triad consisting of histidine, aspartate, and either serine or cysteine. Moreover, the catalytic triad is not specific as it is shared by all carboxylesterases (Sood et al. 2016; Viljakainen and Hug 2021). Generally, lipases and PHA depolymerases differ functionally with respect to substrate preference because lipases show a preference for lipids, while PHA depolymerases have a preference for PHA polymers (Sharma et al. 2019). In fact, some known bioplastic-degrading enzymes are often members of lipase, proteinase, cutinase, or esterase families (Suzuki et al. 2020; Mohanan et al. 2022; Shalem et al. 2024). Some extracellular lipases purified from various species, including *Bacillus subtilis, Pseudomonas aeruginosa, Pseudomonas alcaligenes, Pseudomonas fluorescens, and Burkholderia cepacia*, were able to hydrolyze polyesters such as polyhydroxyhexanoate or polyhydroxybutyrate (Jaeger et al. 1995). Since the *Burkholderia* genus is one of the well-known lipase producers, for example, *B. cepacia* (Rathi et al. 2001),

B. lata (Oliveira et al. 2015), *Burkholderia sp.* ZYB002 (Shu et al. 2012), and *Burkholderia* sp. HL-10 (Lo et al. 2012). As discussed in section 1.2, *Burkholderia* has the ability to produce diverse enzymes that break down various substrates for carbon utilization. This enzymatic diversity suggests *Burkholderia*'s potential capability to degrade polymers such as mcl-PHA, even when they are not their natural substrates.

1.7 Rationale of the Thesis Research

Members of *Burkholderia* have extraordinary genomic and metabolic plasticity, making them biotechnologically relevant. However, their utilization in industrial applications has been hindered by their opportunistic pathogenic nature and the limited genetic tools available for their manipulation. This work addresses part of these challenges through two interconnected themes. This thesis aims to narrow down the mechanism of PHO degradation in *Burkholderia*. The detection of the genes involved and their regulation requires the development of molecular tools to facilitate this search. The first theme focuses on developing a genetic tool for *Burkholderia*, while the second explores *Burkholderia*'s potential for bioplastic degradation.

There is a need for more efficient and versatile genetic tools in non-model bacteria like *Burkholderia*. Chapter 2 of the thesis focuses on developing a genetic manipulation system for *Burkholderia.* While members of *Burkholderia* offer great promise for various biotechnological applications, the lack of sophisticated genetic manipulation techniques has constrained our ability to harness their potential. In order to address this, this work developed a system based on a CRISPR-associated transposase that aims to overcome these limitations by providing a faster and more adaptable method for targeted insertional mutagenesis.

The second part of this work builds on the genetic tool development by applying these techniques to investigate *Burkholderia*'s capacity for bioplastic degradation, specifically mcl-PHA. As the world seeks alternatives to petroleum-based plastics, understanding the

biodegradation pathways of these materials is important. Since *Burkholderia* species hold great potential as sources of novel enzymes, such as lipases, for bioplastic degradation. Chapter 3 of this thesis aims to identify *Burkholderia* strains capable of degrading mcl-PHA and elucidate the genetic basis of this activity. The genetic tool developed in Chapter 2 of this thesis was directly applied in Chapter 3 to validate the role of specific genetic elements in mcl-PHA degradation. This work demonstrates the practical application of the new genetic manipulation system and enhances our understanding of bioplastic biodegradation mechanisms.

1.8 Hypotheses and Objectives

The hypotheses that underlay this research were that:

1. *Burkholderia* species cultured under certain environmental conditions will adapt to the available nutrients and turn on different metabolic processes, including extracellular mcl-PHA degradation.
2. Molecular tools will facilitate the identification of potential genetic elements associated with extracellular mcl-PHA degradation.

The objectives of this research were to:

1. To develop a CRISPR-associated transposase genetic manipulation tool for targeted insertional mutagenesis in *Burkholderia cepacia complex* (Bcc) species;
2. To screen and identify *Burkholderia* strains capable of degrading mcl-PHA;
3. To identify genes and regulatory elements associated with extracellular mcl-PHA degradation in *Burkholderia*.

CHAPTER 2: A CRISPR-CAS ASSOCIATED TRANSPOSON SYSTEM FOR GENOME EDITING IN *BURKHOLDERIA CEPACIA* COMPLEX SPECIES

2.1 Abstract

Genome editing in non-model bacteria is important to understand gene-to-function links that may differ from those of model microorganisms. Although species of the *Burkholderia cepacia* complex (Bcc) have great biotechnological capacities, the limited genetic tools available to understand and mitigate their pathogenic potential hamper their utilization in industrial applications. To broaden the genetic tools available for Bcc species, we developed RhaCAST, a targeted DNA insertion platform based on a CRISPR-associated transposase driven by a rhamnose-inducible promoter. We demonstrated the utility of the system for targeted insertional mutagenesis in the Bcc strains *B. cenocepacia* K56-2 and *B. multivorans* ATCC17616. We showed that the RhaCAST system can be used for loss- and gain-of-function applications. Importantly, the selection marker could be excised and reused to allow iterative genetic manipulation. The RhaCAST system is faster, easier, and more adaptable than previous insertional mutagenesis tools available for Bcc species and may be used to disrupt pathogenicity elements and insert relevant genetic modules, enabling Bcc biotechnological applications.

2.2 Importance

Species of the Bcc have great biotechnological potential but are also opportunistic pathogens. Genetic manipulation of Bcc species is necessary to understand gene-to-function links. However, limited genetic tools are available to manipulate Bcc, hindering our understanding of their pathogenic traits and their potential in biotechnological applications. We developed a genetic tool based on a CRISPR-associated transposase that can be used for loss- and gain-of-function in Bcc species. The significance of our work is in expanding currently available tools to manipulate Bcc.

2.3 Introduction

Species in the genus *Burkholderia* have potential use in agriculture, bioremediation, and as cell factories, but are also opportunistic pathogens (Eberl and Vandamme 2016; Depoorter et al. 2016; Morya et al. 2020). One example is the subgroup *Burkholderia cepacia* complex (Bcc), which comprises species with plant protective and growth promotion properties and produces enzymes and metabolites of commercial interest (Mahenthiralingam et al. 2005; Eberl and Vandamme 2016; Depoorter et al. 2016; Morya et al. 2020). Unfortunately, all Bcc species can cause severe infections in people with cystic fibrosis (CF) and compromised immune systems (Mahenthiralingam et al. 2005), which hampers their utilization in biotechnological applications.

Developing genetic tools for genome editing could help streamline Bcc genomes, eliminating their pathogenic potential and enhancing biotechnological capacities. However, genome editing in Bcc species is challenging due to the characteristics of their genomes, which range from 6 to 9 Mb, have approximately 65% GC content and repetitive DNA elements (Mahenthiralingam et al. 2005). In addition, many antibiotic-resistance genetic markers are ineffective for mutant selection due to Bcc intrinsic resistance to most antibiotics (Rhodes and Schweizer 2016; Scoffone et al. 2017). Despite these difficulties, several genetic tools have been developed, which include methods for gene deletion (Flannagan et al. 2008), allelic replacement (Shastri et al. 2017), insertional mutagenesis (Flannagan et al. 2007), plasmid-based gene expression (Cardona and Valvano 2005; Hogan et al. 2021), CRISPR-based gene silencing or CRISPRi (Hogan et al. 2019), and transposon mutagenesis (Scoffone et al. 2021). Except for CRISPRi, all site-directed editing tools in Bcc species are based on homologous recombination, which requires PCR amplification and cloning of homologous DNA flanking regions in suitable vectors. Examples of homologous recombination-based systems applied to Bcc are gene disruption with the pGPΩ (Flannagan et al. 2007) or pKNOCK (Alexeyev 1999;

Castonguay-Vanier et al. 2010) plasmid series, allelic replacement with the pSHAFT-vector series (Shastri et al. 2017), and gene deletion with pGPI-SceI and pDAI-SceI (Flannagan et al. 2008). For genomic DNA integration, transposon *Tn*7-based mini-*Tn*7 is inserted in the chromosome at an *attTn*7 site downstream of the essential *glmS* gene (Heacock-Kang et al. 2018). While the *Tn*7 tool is valuable for genomic DNA integration, this system only allows integration at specific sites in the genome.

Recently, the CRISPR-associated transposases (CAST) from *Scytonema hofmannii* (ShCAST) (Strecker et al. 2019) and *Vibrio cholerae* (VchCAST) (Klompe et al. 2019) have been developed into genetic tools that allow DNA sequence integration at targeted region(s) without the need for homologous recombination. In these systems, the transposases provide DNA integration properties while the CRISPR-Cas effectors allow programmable, RNA-guided specific insertion of a DNA fragment or cargo DNA (Park et al. 2022; Zeng et al. 2023). ShCAST was the first programmable tool for genomic insertion of desired cargo DNA in a recombination-independent manner (Strecker et al. 2019). ShCAST consists of a V-K CRISPR effector (Cas12k) and the transposition proteins TnsB, TnsC and TniQ. The V-K CRISPR effector forms a complex with TnsB, TnsC, and TniQ and catalyzes the RNA-guided DNA transposition by unidirectionally inserting DNA segments 60 to 66 bp downstream of protospacer adjacent motif (PAM) sequences (Strecker et al. 2019). ShCAST was first used to introduce DNA insertions in *Escherichia coli* (Strecker et al. 2019) and later in *Burkholderia thailandensis*, *Agrobacterium fabrum* (Trujillo Rodríguez et al. 2023) and *Shewanella oneidensis* (Cheng et al. 2022). On the other hand, the *V. cholerae* VchCAST employs a type I-F CRISPR-Cas cascade consisting of the Cas6, Cas7 and Cas8 proteins and four transposases named TnsB, TnsC, TniQ and TnsA (Klompe et al. 2019; Vo et al. 2020) and was also first applied to insert DNA in the *E. coli* genome (Klompe et al. 2019). An improved version of VchCAST, called INTEGRATE, was later demonstrated to produce DNA insertions in

Klebsiella oxytoca, *Pseudomonas putida* (Vo et al. 2020) and *Agrobacterium tumefaciens* (Aliu et al. 2022). The overall lengths of the ShCAST and the INTEGRATE system are approximately 5,800 and 8,500 bp, respectively.

In this work, we develop RhaCAST, a ShCAST-based genetic tool driven by a rhamnose-inducible promoter, for targeted insertional mutagenesis in Bcc species. We chose ShCAST based on its smaller overall size compared to INTEGRATE and its previous successful use in a non-Bcc *Burkholderia* species, *B. thailandensis* (Trujillo Rodríguez et al. 2023). We demonstrate the applicability of RhaCAST for targeted-chromosomal gene integration in two Bcc species, *B. cenocepacia* K56-2 and *B. multivorans* ATCC 17616. RhaCAST was designed to allow multiple genetic manipulations by the recycling of selection markers.

2.4 Materials and Methods

2.4.1 Strains, Selective Antibiotics, and Growth Conditions

Strains and plasmids are shown in **Table 2.1**. Primers used in this study are listed in **Table 2.2**. All strains were grown in LB-Lennox medium (Difco). *B. cenocepacia* K56-2, *B. multivorans* ATCC 17616 and the strains of *E. coli* were grown at 37°C, except for *E. coli* Stbl2, which was grown at 30°C. The following selective antibiotics were used: Cm (Sigma; 20 μg/mL for *E. coli*), Tp (Sigma; 100 μg/mL for strains of *Burkholderia*, 50 μg/mL for *E. coli*), gentamicin (Sigma; 50 μg/mL for all strains of *Burkholderia*).

Table 2. 1 Strains and plasmids used in Chapter 2.

Strain or plasmid	Features	Source
Burkholderia cenocepacia K56-2	Clinical isolate from cystic fibrosis patient; ET12 lineage	(Darling et al. 1998)
K56-2 *fliF*::pAH26	Derived from K56-2; pAH26 integrated into *fliF*; Tp^r	(Hogan et al. 2019)
K56-2 *phbC*::pAH27	Derived from K56-2; pAH27 integrated into *phbC*; Tp^r	(Hogan et al. 2019)

K56-2 *paaA*::CAST-Tp (3390)	Derived from K56-2; Cargo containing Tp^r integrated into *paaA*; made with crRNA 3390	This study
K56-2 *paaA*::CAST-Tp (3422)	Derived from K56-2; Cargo containing Tp^r integrated into *paaA*; made with crRNA 3422	This study
K56-2 *paaA*::CAST-Tp (3423)	Derived from K56-2; Cargo containing Tp^r integrated into *paaA*; made with crRNA 3423	This study
K56-2 *fliF*::CAST-Tp (3463)	Derived from K56-2; Cargo containing Tp^r integrated into *fliF*; made with crRNA 3463	This study
K56-2 *fliF*::CAST-Tp (3466)	Derived from K56-2; Cargo containing Tp^r integrated into *fliF*; made with crRNA 3466	This study
K56-2 *phbC*::CAST-Tp (3469)	Derived from K56-2; Cargo containing Tp^r integrated into *phbC*; made with crRNA 3466	This study
K56-2 *phbC*::CAST-Tp (3472)	Derived from K56-2; Cargo containing Tp^r integrated into *phbC*; made with crRNA 3472	This study
K56-2::CAST-*fugfp-Tp* (3475)	Derived from K56-2; Cargo containing *fugfp* and Tp^r integrated into intergenic region RS16895-90; made with crRNA 3475	This study
K56-2::CAST-*fugfp-Tp* (3478)	Derived from K56-2; Cargo containing *fugfp* and Tp^r integrated into intergenic region RS16895-90; made with crRNA 3478	This study
K56-2::CAST-*fugfp*	Derived from K56-2::CAST-*fugfp-Tp* (3475); Tp^r flanking by the FRT region excised via Flp recombination using pFLP3	This study
K56-2::CAST-*fugfp* *fliF*::CAST-Tp	Derived from K56-2::CAST-*fugfp* (3475); Cargo containing Tp^r integrated into *fliF*; made with crRNA 3463	This study
Burkholderia multivorans ATCC 17616	Soil sample	ATCC
ATCC 17616 *paaA*::CAST-Tp (3390)	Derived from ATCC17616; Cargo containing Tp^r integrated into *paaA*; made with crRNA 3390	This study
ATCC 17616 *paaA*::CAST-Tp (3422)	Derived from ATCC17616; Cargo containing Tp^r integrated into *paaA*; made with crRNA 3422	This study
ATCC 17616 *paaA*::CAST-Tp (3424)	Derived from ATCC17616; Cargo containing Tp^r integrated into *paaA*; made with crRNA 3424	This study

ATCC 17616 *fliF*::CAST-Tp (3463)	Derived from ATCC17616; Cargo containing Tp^r integrated into *fliF*; made with crRNA 3463	This study
E. coli DH5α	*F- Φ80lacZΔM15 Δ(lacZYAargF) U169 recA1 endA1 hsdR17 (rH^-, mK^+) phoA supE44 λ^- thi-1 gyrA96 relA1*	Cardona lab collection
E. coli Stbl2	*F- mcrA Δ(mcrBC-hsdRMS-mrr) recA1 endA1lon gyrA96 thi supE44 relA1 λ^- Δ(lac-proAB)*	Invitrogen
E. coli PIR1	*F-* Δ*lac169 rpoS(Am) robA1 creC510 hsdR514 endA recA1 uidA(*Δ*MluI)::pir-116*	Cardona lab collection
E. coli SY327	*F− araD Δ(lac-proAB) argE(Am) recA56 Rif^r nalA λpir*	(Miller and Mekalanos 1988)
pHelper_ShCAST_crRNA	Amp^R, ori_{colE1}, *Sh-cas12K-tnsBC-tniQ*, PJ23119-gRNA	(Strecker et al. 2019)
pDonor_ShCAST_kanR	Km^R, ori_{R6K}, Tn-neo	(Strecker et al. 2019)
pSCrhaB2plus	ori_{pBBR1} *rhaR*, *rhaS*, PrhaB Tp^R mob^+, rhaI1-rhaI1 permutation of rhaS binding sites upstream of PrhaBAD and bacteriophage T7 gene 10 stem loop inserted upstream of native rhaBAD 5′ UTR	(Hogan et al. 2021)
pKD3	Cm^r ori_{R6K} rgnB	(Datsenko and Wanner 2000)
pRK2013	ori_{colE1} RK2 derivative Kan^r mob^+ tra^+	(Figurski and Helinski 1979)
pZLrhaB2plus	pSCrhaB2plus with modifications of resistance cassette to Cm^R	This study
pDonorTp	pDonor_ShCAST_kanR with modification of Km^R to Tp^R	This study
pDonorTp-fugfp	pDonorTp with addition of *fugfp* gene from pUS252 outside of the FRT sites	This study
pUS252	ori_{pUC}, Km^R, fuGFP	Addgene plasmid #127674
pFLP3	Amp^r, Tet^r, *Flp*	(Choi et al. 2005)
pRhaCAST	pZLrhaB2plus with *Sh-cas12K-tnsBC-tniQ* cloned into, which drives by the rhamnose inducible promoter	This study
pRhaCAST-3390	Modified from pRhaCAST. crRNA targeting *B. cenocepacia* K56-2 and *B. multivorans* ATCC17616 *paaA*	This study
pRhaCAST-3422	Modified from pRhaCAST. crRNA targeting *B. cenocepacia* K56-2 and *B. multivorans* ATCC17616 *paaA*	This study
pRhaCAST-3423	Modified from pRhaCAST. crRNA targeting *B. cenocepacia* K56-2 *paaA*	This study

pRhaCAST-3424	Modified from pRhaCAST. crRNA targeting *B. multivorans* ATCC17616 *paaA*	This study
pRhaCAST-3466	Modified from pRhaCAST. crRNA targeting *B. cenocepacia* K56-2 *fliF*	This study
pRhaCAST-3469	Modified from pRhaCAST. crRNA targeting *B. cenocepacia* K56-2 *phaC*	This study
pRhaCAST-3472	Modified from pRhaCAST. crRNA targeting *B. cenocepacia* K56-2 *phaC*	This study
pRhaCAST-3475	Modified from pRhaCAST. crRNA targeting *B. cenocepacia* K56-2 intergenic region RS16895-90	This study
pRhaCAST-3478	Modified from pRhaCAST. crRNA targeting *B. cenocepacia* K56-2 RS16895-90 intergenic region	This study

Table 2. 2 Primers/templates used for cloning and verification in Chapter 2.

Number	Sequence	Description
876	TGATGATATCTCATCGCAGTACTGTTGTATTC	Forward primer for CAT gene
877	TATAATGCATAAGTATAGGAACTTCGGCGC	Reverse primer for CAT gene
3145	ATTACATATGATGAACAGTCAGCAAAATCCTGATTTAG	Forward primer targeting CAST genes from pHelper_ShCAST_crRNA
3146	ATTATCTAGACTGCGCAGAAAGGCCCAC	Reverse primer targeting CAST genes from pHelper_ShCAST_crRNA
848	CCGCCAGGCAAATTCTGTTT	Colony PCR reverse primer for pZLrhaB2plus and pRhaCAST
1120	AGACTGGTCGTAAGGGAGAC	Colony PCR forward primer for pZLrhaB2plus and pRhaCAST
3392	ACTAACGGCTCTTCGAG	Reverse primer to amplify single stranded nucleotide template containing the crRNA
3421	CATTGGCTCTTCGAAAG	Forward primer to amplify single stranded nucleotide template containing the crRNA
1025	ATAATAGGTACCCGCACGAACCCAGTTGAC	Forward primer to amplify *dhfr* cassette from pKD3
1001	ATAATACTCGAGTAGAATTCTGACTCTTATACACAAG	Reverse primer to amplify *dhfr* cassette from pKD3
1540	ATCATGCTCGAGGGAAGAGTATGAGGATCCAACATTTC	Forward primer to remove kanR and add XhoI site in the pDonor-shCAST_KanR
1541	CATGCAGGTACCCCTCATCCTGTCTCTTGATCAGATC	Reverse primer to remove kanR and add XhoI site in the pDonor-shCAST_KanR
1542	GGCTTAGGGGATCGCGTAC	Forward primer for colony PCR of pDonorTp

1543	ACTAGTGATTGGAAATGTTGGATCC	Reverse primer for colony PCR of pDonorTp
3481	ATTACCCGGGTTGACAGCTAGCTCAGTCCTAGGTATAATACTAGTAGATTAAAGAGGAGAAAGAGTCC	To amplify fugfp gene from and add restriction site and PJ23119 promoter
3482	ATTACATATGGGAAACAGCTATGACGGTACC	To amplify fugfp gene and add restriction site
3483	ATTACCCGGGGATCTCGAATTGGGGATCTTG	Inverse PCR of pDonorTp at FRT-rrnB terminator
3484	ATTACATATGCCTAGCGGCGGATTTGTC	Inverse PCR of pDonorTp at FRT-rrnB terminator
3485	CCAACATTTCCAATCACTAGTG	Colony PCR for ligation into pDonorTp
Oligonucleotides for cloning crRNA into pRhaCAST (crRNA is in bold, *sapI* restriction site is in italics)		
3390	CATTG*GCTCTTC*GAAAG**GACGGCGCCGCGATCATGAACCAG**GGCTC*GAAGAGC*CGTTAGT	Targeting *paaA* in K56-2 and ATCC17616
3422	CATTG*GCTCTTC*GAAAG**CGATGCGGTGATGGCCGCGGACGG**GGCTC*GAAGAGC*CGTTAGT	Targeting *paaA* in K56-2 and ATCC17616
3423	CATTG*GCTCTTC*GAAAG**GATGATGAAGGGCAGCGACGCGCA**GGCTC*GAAGAGC*CGTTAGT	Targeting *paaA* in K56-2
3424	CATTG*GCTCTTC*GAAAG**GGCATGCTGCCGGAAGGCAACTGG**GGCTC*GAAGAGC*CGTTAGT	Targeting paaA in ATCC17616
3463	CATTG*GCTCTTC*GAAAG**GGCTTCGAGCTGATGGACAACCAG**GGCTC*GAAGAGC*CGTTAGT	Targeting *fliF* in K56-2 and ATCC17616
3466	CATTG*GCTCTTC*GAAAG**GAGCACAACACGCAGAAGCGCATC**GGCTC*GAAGAGC*CGTTAGT	Targeting *fliF* in K56-2
3469	CATTG*GCTCTTC*GAAAG**GCCGCGATTCCGCCCGAACGGCTC**GGCTC*GAAGAGC*CGTTAGT	Targeting *phaC* in K56-2
3472	CATTG*GCTCTTC*GAAAG**CAGCAATGGACGGCCGCCGCCGCG**GGCTC*GAAGAGC*CGTTAGT	Targeting *phaC* in K56-2
3475	CATTG*GCTCTTC*GAAAG**GGTAATGGCCGCCAGCGCCTTTTT**GGCTC*GAAGAGC*CGTTAGT	Targeting K562_RS16895-90 intergenic region in K56-2
3478	CATTG*GCTCTTC*GAAAG**TCGAGTCGCCGCGGAACGGGATAT**GGCTC*GAAGAGC*CGTTAGT	Targeting K562_RS16895-90 intergenic region in K56-2
Oligonucleotides for colony PCR to verify genomic insertion		
2500	CAATCCCTCGACATTCCCGG	Colony PCR for *paaA* of ATCC17616
2997	ATGTACACGCAATCCCTCGA	Colony PCR for *paaA* of K56-2
2998	GTTCCATTTCAGGTCGGGGT	Colony PCR for *paaA* of K56-2
3001	GGTGGGTTGAAAGCAAGTCC	LE primer upstream

3464	CTTCGAGCTGATGGACAACC	Colony PCR 1 for *fliF* of K56-2 and ATCC17616
3435	GTAGAGGTCGACGAACACC	Colony PCR 1 for *fliF* of K56-2
3467	GAGCACAACACGCAGAAG	Colony PCR 2 for *fliF* of K56-2
3468	GCTGGTCTGCTGGCTG	Colony PCR 2 for *fliF* of K56-2
3470	CGATTCCGCCCGAACG	Colony PCR 1 for *phaC* of K56-2
3471	TTGAGCAGATACCAGGCG	Colony PCR 1 for *phaC* of K56-2
3473	CAGCAATGGACGGCCG	Colony PCR 2 for *phaC* of K56-2
3474	GGTACATCCGAGGTTCTTGC	Colony PCR 2 for *phaC* of K56-2
3476	GGTAATGGCCGCCAGC	Colony PCR 1 for neutral intergenic insertion of K56-2
3479	TCGAGTCGCCGCGGA	Colony PCR 2 for neutral intergenic insertion of K56-2

2.4.2 Construction of the RhaCAST system

pRhaCAST. First, the *dhfr* resistance marker gene of pSCrhaB2plus (Addgene plasmid #164226) was changed by the chloramphenicol acetyltransferase (*cat)* gene. Briefly, the *cat* gene was PCR-amplified from pKD3 (Addgene plasmid #45604) using primers 876 and 877. This PCR product was introduced into pSCrhaB2plus by restriction cloning with *NsiI* and *EcoRV*, replacing the original *dhfr* with *cat*. The resulting construct was transformed into *E. coli* DH5α and Cm-resistant colonies were screened by colony PCR with primers 876 and 877 to isolate clones harbouring the resulting plasmid, pZLrhaB2plus. Next, components of the ShCAST (*tnsB, tnsC, tniQ,* and *Cas12k*) and the crRNA region were PCR-amplified from pHelper_ShCAST_crRNA (Addgene plasmid #127921) (Strecker et al. 2019) using primers 3145 and 3146. This PCR product was introduced into pSCrhaB2plus by restriction cloning with *NdeI* and *XbaI*. The resulting construct was transformed into *E. coli* Stbl2 and Cm-resistant colonies were screened by colony PCR with primers 848 and 1120. The obtained plasmid was called pRhaCAST.

pDonorTp. To replace the antibiotic resistance marker of pDonor_ShCAST_kanR (Addgene plasmid # 127924) from *neo* (kanamycin resistance) to *dhfr*, the *dhfr* gene was first PCR-amplified from pTnMod-STp (GenBank Accession: AF061932) (Dennis and Zylstra

1998) using primers 1025 and 1001. Next, pDonor_ShCAST_kanR was inverse PCR-amplified using primers 1540 and 1541 to remove the *neo* gene. The two DNA fragments were restricted with *KpnI* and *XhoI*, ligated, and the ligation products transformed into *E. coli* PIR1. Tp-resistant colonies were determined by colony PCR with primers 1542 and 1543. The obtained plasmid was called pRhaCAST. The sequences of pZLrhaB2plus, pRhaCAST, and pDonorTp were confirmed by whole plasmid sequencing performed by Plasmidsaurus using Oxford Nanopore Technology (ONT).

2.4.3 Cloning of crRNAs into pRhaCAST

crRNAs were ordered as single-stranded oligos from Integrated DNA Technologies (IDT) and PCR-amplified to create double-stranded DNA fragments. The PCR products were then introduced into pRhaCAST using Golden Gate cloning with *SapI*, with the following cycle parameters: (5 mins 37°C → 5 min 16°C) x 50 cycles followed by 5 mins at 60°C and 5 mins at 85°C. The newly constructed plasmids were then transformed into *E. coli* Stbl2. Cm-resistant colonies were screened by colony PCR with either primers 848 and 1120 or primers 848 and the spacer-specific primers.

2.4.4 Construction of pDonorTp-fugfp

The *fugfp* gene was PCR-amplified from pUS252 with primers 3481 and 3482, adding *Xma*I and *Nde*I restriction sites. pDonorTp was inverse PCR-amplified with primers 3483 and 3484 harbouring the same restriction sites. The *fugfp* gene was then introduced outside the FRT sites in pDonorTp by restriction cloning with the *Xma*I and *Nde*I sites. Successful *E. coli* SY327 transformants were determined by colony PCR with primers 3482 and 3485 and screening for fuGFP fluorescence. pDonorTp-*fugfp* sequence was confirmed by whole plasmid sequencing performed by Plasmidsaurus using Oxford Nanopore Technology (ONT).

2.4.5 Tetra-parental mating

Tetra-parental mating was performed similarly to tri-parental mating, previously described (Hogan et al. 2018). *E. coli* MM290/pRK2013 (helper strain), *E. coli* Stbl2/pRhaCAST with corresponding crRNA, and *E. coli* PIR1/pDonorTp or pDonorTp-*fugfp* were conjugated into *Burkholderia*. Briefly, each 5 mL of the subculture of the recipient was made from 100µL overnight culture and was grown to an OD of 0.3-0.6. *E. coli* containing plasmids was harvested and resuspended in LB and adjusted to a 1.5 mL suspension with an OD600 of 0.3. An overnight culture of the recipient was subcultured in 5 mL of LB and grown to the OD600 of 0.3-0.6. The resulting culture was adjusted to a 0.5 mL suspension in LB with an OD600 of 1.0. All the cultures were mixed and centrifuged at 5000 x g for 5 min. The pellet was then resuspended in 100µL of LB broth and spotted onto an LB agar plate containing 0.05% rhamnose. The plate was incubated at 37°C or 23°C, depending on the recipient strain, for 24 hours. The cells were collected and resuspended in 1 mL of LB, and 100µL of the cell suspension was plated (without diluting) in LB plates with gentamicin and Tp.

2.4.6 Removal of antibiotic resistance cassette using Flp-FRT recombination

The Flp expression vector pFLP3 (Choi et al. 2005) was introduced into *Burkholderia*::CAST-*fugfp*-Tp by tri-parental mating using *E. coli* MM290/pRK2013 as a helper strain. Tetracycline and gentamicin-resistant colonies were selected and patched onto LB agar plates with Tp to check for sensitivity. The resulting strain has the Tp resistance cassette excised and is left with *fugfp* in the genome. The exconjugants sensitive to Tp were used for subsequent mutagenesis.

2.4.7 Phenotypic characterization of phenylacetic acid auxotroph mutant

Colonies obtained from tetra-parental mating were patched onto M9 medium agar with 10 mM phenylacetic acid or 20 mM glucose,100 µg/mL Tp and 50 µg/mL gentamicin. Plates were incubated for 24 h at 37°C. The phenylacetic acid auxotroph mutants were identified by

the absence of growth in the medium containing phenylacetic acid as the carbon source and the presence of growth in the glucose-containing medium.

2.4.8 Flagellum staining

Cells were prepared for flagellum staining as previously described (Hogan et al. 2019). Briefly, an overnight culture was incubated statically at room temperature for 20-25 min. A 1:10 dilution of this culture was prepared in sterile water, carefully mixed by tapping for 30 sec, and left to sit statically for 20-25 min. A drop of the diluted culture was placed on a glass slide and rested for 20 min. A cover glass was applied gently to the samples. Flagella were stained using the Ryu stain (Kodaka et al. 1982). Ryu flagellum stain was added in excess towards one side of the coverslip and allowed to dry for 2-3 h at room temperature. Slides were observed by light microscopy at 1000× total magnification on an upright AxioImager Z1 (Zeiss).

2.4.9 Nile red staining and detection of PHA granules

PHA granules were detected, as previously reported (Hogan et al. 2019), with some modifications. Briefly, overnight cultures of the appropriate strains were inoculated to an OD600 of 0.025 and grown at 37°C for 3 hours with shaking at 230 rpm. One mL of the resulting culture was washed twice and resuspended in PBS; 3.7% formaldehyde + 1% methanol (Sigma) was used to fix the cells at room temperature for 10 minutes; excess formaldehyde was quenched by the addition of an equal volume of 0.5 M glycine. Cells were washed, resuspended in PBS and stained at room temperature with 0.5 µg/mL Nile red (Carbosynth) for 20 minutes. Excess stain was removed by washing with PBS; then, cells were mounted on 1.5% agarose pads and imaged by fluorescence microscopy at 1000X on an upright AxioImager Z1 (Zeiss). Nile red was excited at 546/12 nm and detected at 607/33 nm.

2.4.10 FuGFP detection

Fluorescence microscopy was performed as previously described (Hogan et al. 2019). Overnight cultures of cells expressing FuGFP were first diluted to an OD_{600} of 0.025 and grown for 3 hours to an OD_{600} of 0.15 (early exponential phase). Cells were immobilized on 1.5% agarose pads and imaged with an AxioImager Z1 (Zeiss). FuGFP was excited at 470/40 nm and detected at 525/50 nm.

2.4.11 Plate-based motility assay

The plate-based motility assay was performed as previously described (Hogan et al. 2019), with some modifications. Briefly, strains were grown on LB agar with the appropriate antibiotics, and single colonies were selected to stab-inoculate into a motility medium consisting of nutrient broth (Difco) with 0.3% agar. Plates were incubated right-side up for 22 hours at 37°C. The motility halos were recorded quantitatively by measuring the diameter of turbidity, corresponding to the bacteria swimming away from the point of inoculation. The images of the motility assay performed on *fugfp*-expressing mutants were taken with a FluorChemQ system (Cell Biosciences, Santa Clara, CA).

2.4.12 Genome sequencing and data analysis

Genomic DNA was extracted using the PureLink microbiome DNA purification kit (Invitrogen) according to the manufacturer's instructions. Long-read sequencing was performed by Plasmidsaurus using Oxford Nanopore Technologies (ONT) with custom annotations. Briefly, the genomic DNA was minimally fragmented, and the amplification-free long-read sequencing library was constructed using the v14 library prep chemistry. The library was then sequenced using R10.4.1 flow cells (ONT); genome assemblies were performed with Flye v2.9.1 (Kolmogorov et al. 2019) using high-quality ONT reads and were polished with Medaka v1.8.0. The genome annotations were performed using Bakta v1.6.1 (Schwengers et al. 2021). Sequences were analyzed with Geneious 8.1.9.

2.5 Results

2.5.1 Construction of the RhaCAST system for use in Bcc strains

The RhaCAST system developed in this work (**Figure 2.1A**) consists of two elements: a replicative plasmid pRhaCAST, encoding the ShCAST-associated machinery under the control of a rhamnose-inducible promoter, and a suicide plasmid pDonorTp, housing the cargo DNA. While pRhaCAST contains a chloramphenicol (Cm) resistance marker to facilitate plasmid maintenance, pDonorTp harbours a trimethoprim (Tp) resistance marker, *dhfr*, as the cargo DNA, flanked by the ShCAST-recognition sites Left End (LE) and Right End (RE), along with the Flippase Recombination Target (FRT) sites (Hoang et al. 1998; Strecker et al. 2019). pRhaCAST also harbours a constitutive promoter PJ23119 to drive the expression of the CRISPR RNA (crRNA), which guides the site-directed insertion of the DNA cargo sequence located in pDonorTp.

We constructed RhaCAST based on the following considerations.

1) The antibiotic resistance marker for selecting the insertion of the cargo DNA: we opted for the *dhfr* gene as a selectable cargo DNA due to previous evidence that the *dhfr* gene provides Tp resistance as a single copy from a chromosomal location (Gislason et al. 2017). The plasmid pDonor of the original ShCAST system utilized a kanamycin-resistance selection marker as the cargo DNA (Strecker et al. 2019). However, the members of the Bcc species often exhibit intrinsic resistance to aminoglycosides (Buroni et al. 2009);

2) The expression system for the ShCAST machinery: We first considered the P_{lac} of ShCAST, as used in most species, including *E. coli, A. fabrum, B. thailandensis,* and *P. putida* to express the genetic elements of ShCAST (Strecker et al. 2019; Cheng et al. 2022; Trujillo Rodríguez et al. 2023). However, the P_{lac} promoter is non-functional in at least three Bcc species, namely *B. multivorans, B. cenocepacia* and *B. vietnamiensis* (genomovars II, III, and V, respectively)

(Lefebre and Valvano 2002). The L-arabinose and L-rhamnose-inducible promoter systems from *E. coli* are the only inducible promoter systems that have been reported to be functional in Bcc (Hogan et al. 2021). The arabinose-inducible system requires high arabinose concentrations for gene expression, resulting in osmotic stress-like bloated cell morphology (Lefebre and Valvano 2002). Instead, the L-rhamnose-inducible system of the expression vector pSCrhaB2 allows strong gene expression in Bcc at low concentrations of rhamnose (as low as 0.02%) (Cardona and Valvano 2005). Therefore, the L-rhamnose inducible system was selected for the expression of the ShCAST system. We used a modified version of the rhamnose-inducible promoter from the plasmid pSCrhaB2plus (Hogan et al. 2021) in which the promoter P_{rhaBAD} was modified to combine the bacteriophage T7 gene *10* stem-loop and engineered *rhaI* transcription factor-binding sites for enhanced gene expression (Hogan et al. 2021). The rhamnose-inducible expression system in pSCrhaB2plus is tightly controlled in *B. cenocepacia* and related species and has a wider dynamic range than that of pSCrhaB2 (Cardona and Valvano 2005; Hogan et al. 2021).

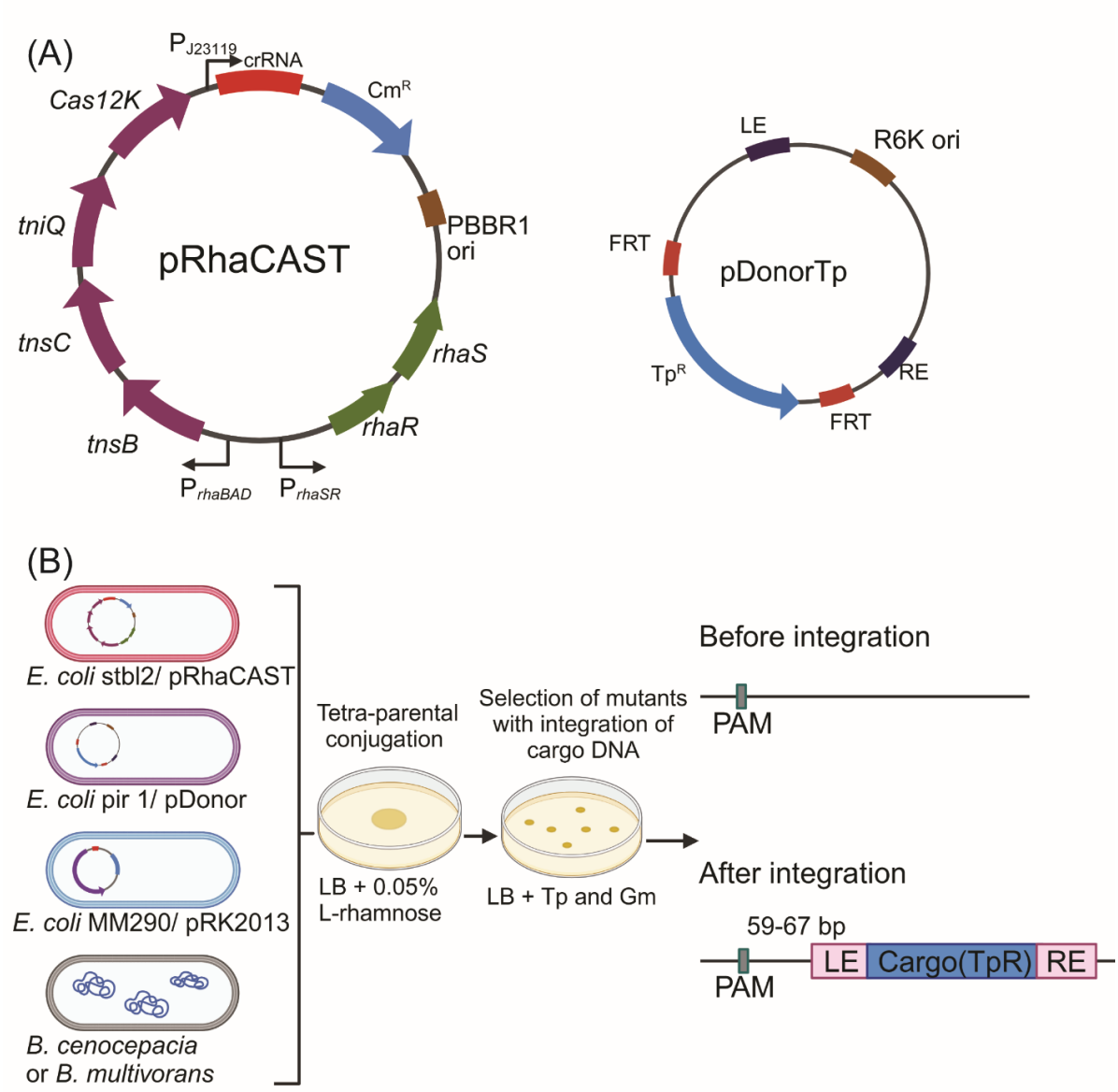


Figure 2. 1 Schematics of RNA-guided DNA integration by ShCAST developed for *Burkholderia cenocepacia* complex (Bcc) (RhaCAST).

A) Two-plasmid ShCAST system encodes protein-RNA components. pRhaCAST encodes for *tnsB*, *tnsC*, *tniQ*, *Cas12k*, and crRNA scaffold, which form the complex needed for RNA-guided DNA integration driven by rhamnose inducible system (*rhaR*, *rhaS*) pDonorTp encodes for the cargo gene (*TpR*), encoding trimethoprim resistance flanked by the flippase recognition target (FRT) internal to the transposon left end (LE) and right end (RE); B) Schematic of experimental overview for CAST-mediated genomic insertion. Plasmid

pRhaCAST and pDonorTp would be introduced into *B. cenocepacia* K56-2 or *B. multivorans* ATCC 17616 with a helper strain carrying pRK2013 via tetra-parental conjugation. The transposition event is induced by L-rhamnose. The cargo flanking with LE and RE insert directionally with LE integrating close to the PAM. Figure 2.1 was created with https://biorender.com/.

2.5.2 Use and validation of the RhaCAST system for insertional mutagenesis in *B. cenocepacia* K56-2

To evaluate the use of RhaCAST in Bcc species, we first analyzed possible PAM sequences based on the original systems. For ShCAST, the highest insertion frequencies in *E. coli* were obtained using the GGTT and GGTC PAMs (Strecker et al. 2019). Also, the previous study that used the ShCAST system in *B. thailandensis*, found that using a TGTC PAM resulted in high on-target insertion efficiency (Trujillo Rodríguez et al. 2023). Thus, we decided to target DNA regions containing GGTT, GGTC and TGTC PAMs in *B. cenocepacia* K56-2 and aimed to interrupt genetic elements that would result in observable phenotypes.

We first targeted the *paaA* gene, which encodes the phenylacetyl-CoA oxygenase subunit PaaA (Teufel et al. 2010). This gene is part of the *paaABCDE* operon, which enables phenylacetic acid (PAA) degradation and its utilization as a sole carbon source (Law et al. 2008). Three crRNAs were designed to target *paaA* in *B. cenocepacia* K56-2 using intragenic GGTT, GGTC and TGTC PAMs. The pRhaCAST plasmids containing the crRNAs targeting *paaA* were introduced into *B. cenocepacia* K56-2 via tetra-parental mating in media containing L-rhamnose alongside pDonorTp and the conjugal helper plasmid, pRK2013 (**Figure 2.1B**). Colonies yielded from the tetra-parental mating were selected on media containing Tp and then their phenotype was studied by replica plating in phenylacetic acid (PAA) or glucose as the sole carbon source. We observed that 92, 82, and 64% percent of the colonies in which the

paaA gene had been targeted using GGTC, TGTC and GGTT PAMs, respectively, had the expected phenotype, growth on glucose but no growth on PAA (**Table 2.3)**. Integration of the cargo DNA on target in clones with the desired phenotype was further confirmed by colony PCR (**Figure S2.1**). In summary, we confirmed that the GGTC PAM yielded the highest number of transformants with on-target insertions.

Table 2. 3 Summary of targeting *paaA* with RhaCAST system in *B. cenocepacia* K56-2.

PAM	Distance between ATG and downstream PAM sequence (bp)	Conjugation efficiency (conjugant/recipient)	Colonies on target (Mutants with expected phenotype/isolates screened)	Percent (%) on target
GGTC	436	5.95×10^{-7}	46/50	92
TGTC	564	1.07×10^{-8}	41/50	82
GGTT	81	2.47×10^{-8}	39/61	64

2.5.3 Further application of the RhaCAST system to target *fliF* and *phbC* in *B. cenocepacia* K56-2

Next, we applied this system to disrupt other genes in *B. cenocepacia* K56-2. Specifically, we targeted *fliF*, a gene encoding a transmembrane protein crucial for the formation of the S and M rings within the basal body complex of the flagellum (Francis et al. 1992). Disrupting *fliF* is expected to yield non-flagellated cells since *fliF* plays a crucial role in flagellum formation (Yang et al. 2017; Hogan et al. 2019). Out of the 10 Tp-resistant colonies tested by colony PCR, 9 yielded the expected PCR product, indicating integration of the cargo DNA at the correct position within *fliF* (**Figure S2.2**). While wild-type cells exhibited motility in a plate-based assay, the mutants created with the RhaCAST system (*fliF*::CAST-Tp) showed complete abrogation of swimming motility (**Figure 2.2A and B**). The lack of motility was similar to the effect observed in a control *fliF* mutant created with a homologous

recombination-based system (*fliF*::pAH26) (**Figure 2.2A and B**). Microscopy images also show that *fliF* mutants did not bear flagella (**Figure 2.2C**).

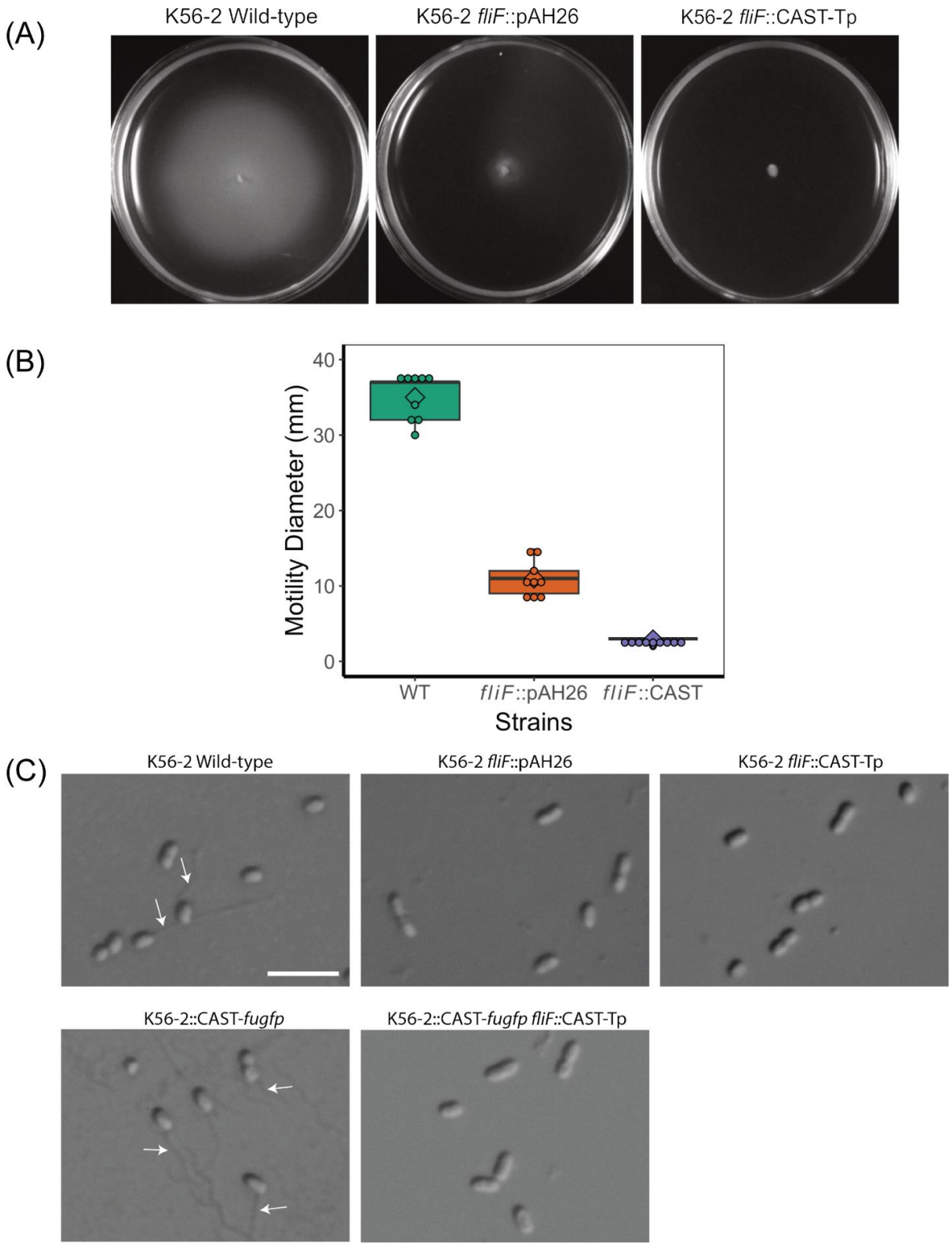


Figure 2. 2 Targeting *fliF* by shCAST in *B. cenocepacia* K56-2 abolishes swimming motility.

A) Representative plate of motility assay performed in nutrient broth with 0.3% agar. Motility was determined by the growth of bacteria around the point of inoculation, exhibited as the wild type. Motility was ablated by CAST targeting of *fliF* in K56-2 Wild-type (WT): *filF*::pAH26 (insertional mutant) and *fliF*::CAST-Tp; B) Diameter of the swimming motility halos in (A). Data is representative of three biological replicates repeated in triplicate. Diamond shapes in the boxplot represent the diameter mean; C) The indicated strains were grown overnight and used for flagellum staining. The flagellum was stained with Ryu flagellum stain. Cells were imaged by differential interference contrast (DIC). The white arrows indicate the presence of flagellum. The scale bar is 5 μm.

To further assess the utility of RhaCAST in *B. cenocepacia* K56-2, *phbC* was targeted, which encodes poly-β-hydroxybutyrate polymerase, an enzyme required for PHB synthesis. We tested ten Tp-resistant colonies obtained from conjugation by colony PCR, and 9 showed the expected PCR product, indicating correct integration (**Figure S2.3**). PHB granule accumulation was assessed by fluorescence microscopy following Nile Red staining. Wild-type K56-2 formed large intracellular PHB granules. However, the mutants created with the RhaCAST system were unable to produce PHB granules, similar to a control mutant created with a homologous recombination-based system (*phbC*::pAH27) (Hogan et al. 2019) (**Figure 2.3**).

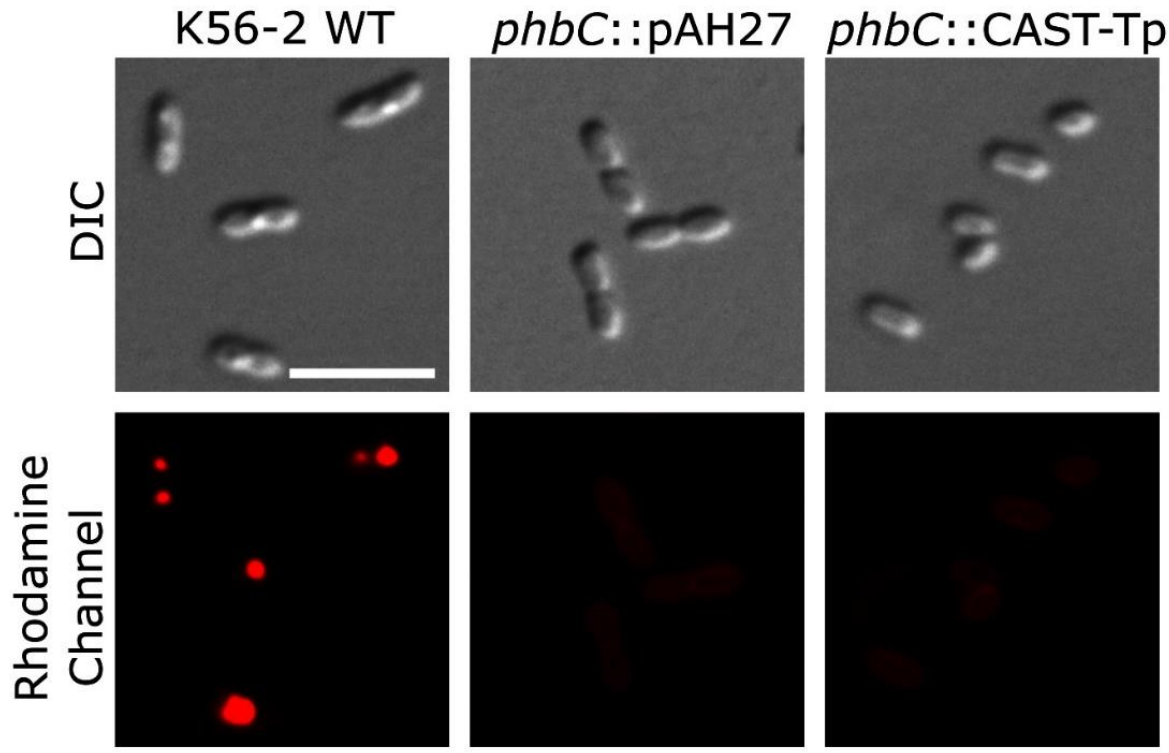


Figure 2. 3 Targeting *phbC* with shCAST abolishes poly-β-hydroxybutyrate granule accumulation in *B. cenocepacia* K56−2.

PHA granules are stained with Nile Red, as seen on the bottom panels. WT, an insertional mutant of the *phbC* gene made homologues recombination-based plasmid (*phbC*::pAH27) and an insertional mutant of the *phbC* gene made with pRhaCAST (*phbC*::pAH27) are shown. The scale bar is 5 μm.

2.5.4 RhaCAST-mediated gain-of-function, recycling of resistance marker for subsequent mutagenesis, and plasmid curing

To demonstrate the utility of the RhaCAST system for gain-of-function studies, we introduced a genetic element, free-use GFP (*fugfp*), into *B. cenocepacia* K56-2. We constructed pDonorTp-*fugfp* by cloning *fugfp* (Choi et al. 2005) into pDonorTp (**Figure 2.1; Figure 2.4A**). The cargo was delivered to a genetically neutral loci of the *B. cenocepacia* K56-2 genome, the intragenic region between RS16895 and RS16900 (Hogan et al. 2018). The RhaCAST-enabled insertion of *fugfp* resulted in a mutant *B. cenocepacia* K56-2::CAST-*fugfp*-Tp exhibiting the characteristic fluorescence (**Figure 2.4B and C**).

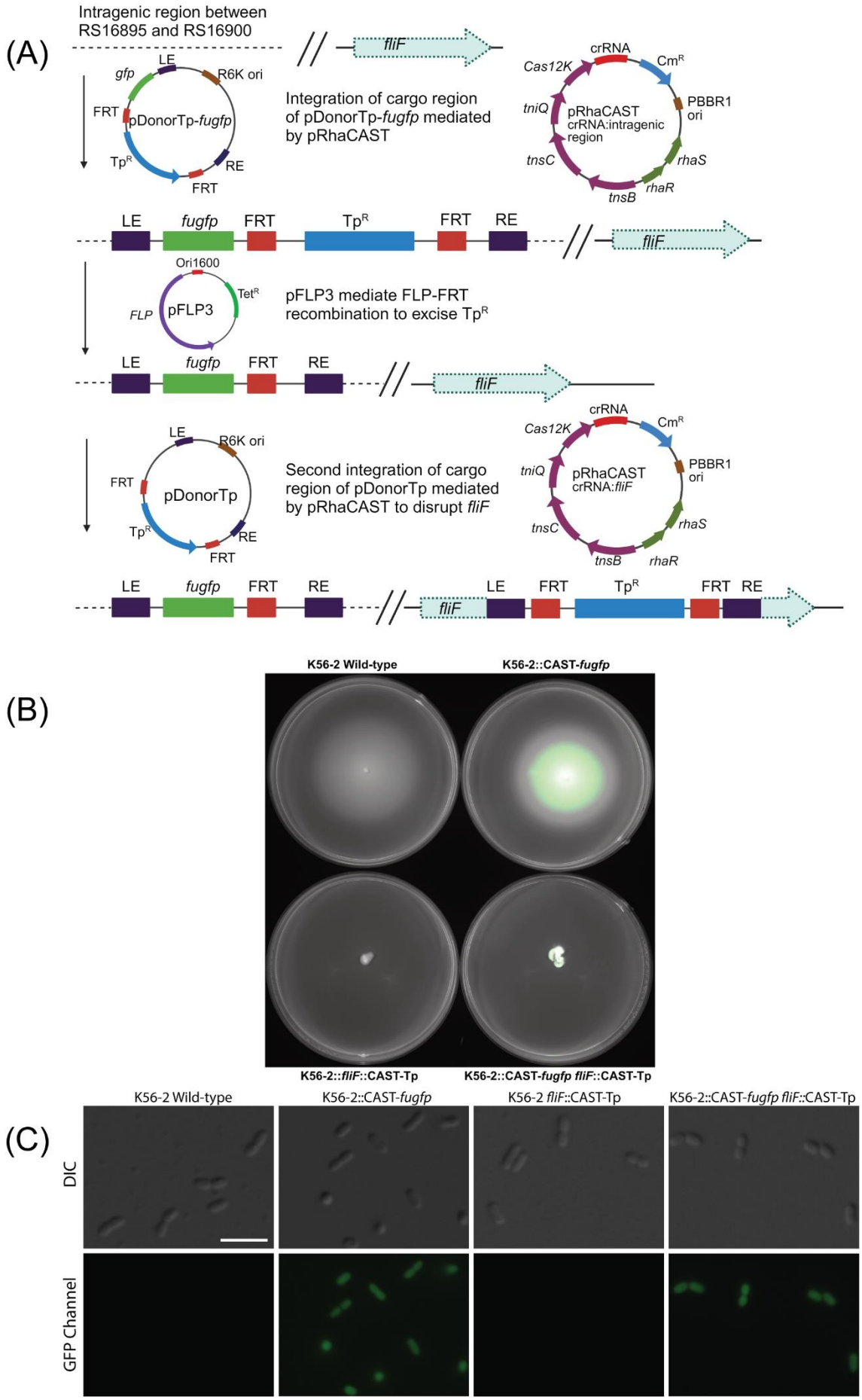

(A)
Intragenic region between RS16895 and RS16900
fliF
LE
gfp
R6K ori
FRT
pDonorTp-fugfp
Tp^R
RE
FRT
Integration of cargo region of pDonorTp-fugfp mediated by pRhaCAST
crRNA
Cas12K
Cm^R
tniQ
pRhaCAST
crRNA:intragenic region
PBBR1 ori
tnsC
rhaS
tnsB
rhaR
LE fugfp FRT Tp^R FRT RE
fliF
Ori1600
FLP
pFLP3
Tet^R
pFLP3 mediate FLP-FRT recombination to excise Tp^R
LE fugfp FRT RE
fliF
pDonorTp
Second integration of cargo region of pDonorTp mediated by pRhaCAST to disrupt fliF
pRhaCAST
crRNA:fliF
LE fugfp FRT RE fliF LE FRT Tp^R FRT RE
(B)
K56-2 Wild-type
K56-2::CAST-fugfp
K56-2::fliF::CAST-Tp
K56-2::CAST-fugfp fliF::CAST-Tp
(C)
K56-2 Wild-type
K56-2::CAST-fugfp
K56-2 fliF::CAST-Tp
K56-2::CAST-fugfp fliF::CAST-Tp
DIC
GFP Channel

Figure 2. 4 RhaCAST-mediated gain of function and recycling of antibiotic resistance cassette.

A) Schematics of the *fugfp* insertion into *B. cenocepacia* K56-2 chromosome after co-transformation of pRhaCAST and pDonorTp-*fugfp*. The Tp^R marker is excised by FLP-FRT recombination mediated by pFLP3, resulting in Tp-sensitive cells that express *fugfp*. The second integration event targets *fliF* in *B. cenocepacia* K56-2 CAST::*fugfp* by co-transformation of pRhaCAST and pDonorTp, resulting in *B. cenocepacia* K56-2 CAST::*fugfp fliF*::CAST-Tp. B) Phenotypic characterization of motility and GFP signals in K56-2 Wild-type (Top left), K56-2::CAST-*fugfp* (Top right), K56-2::*fliF*::CAST-Tp (Bottom left) and K56-2::CAST-*fugfp fliF*::CAST-Tp (Bottom right). The motility was determined by the presence of a halo surrounding the point of inoculation in nutrient broth with 0.3% agar. Expression of GFP was captured with FluorChemQ. C) Micrographs showing green fluorescence of the K56-2::CAST-*fugfp* and K56-2::*fliF*::CAST-Tp mutants. The scale bar is 5 μm. Figure 2.4A was created with https://biorender.com/.

Burkholderia species display intrinsic resistance to many antibiotics commonly used as selectable markers. Thus, recycling the same antibiotic marker for subsequent mutagenesis would be ideal. We took advantage of the Flp-FRT system (Hoang et al. 1998) to excise the *dhfr* gene between the FRT sites, thus rendering the mutants sensitive to Tp. In the case of the K56-2::CAST-*fugfp-Tp* mutant, expression of Flp from the pFLP3 plasmid left the *fugfp* cargo in the chromosome (K56-2::CAST-*fugfp*) (**Figure S2.10**). This strain was then used as the background for subsequent mutagenesis of *fliF*. The resulting strain, *B. cenocepacia* K56-2::CAST-*fugfp fliF*::CAST-Tp, was fluorescent and lacked swimming motility (**Figure 2.4B and 2.4C**).

A common step immediately after mutant construction with a plasmid-based genetic tool is plasmid curation, usually performed by subculturing the obtained mutants without selective pressure to facilitate plasmid removal. However, a specific procedure for curing pRhaCAST from the CAST-Tp mutants was unnecessary. After tetra-parental mating, Tp-resistant colonies were selected with Tp and gentamicin (not Cm). Therefore, pRhaCAST was not maintained. We demonstrated the absence of pRhaCAST by replica-plating the mutants *B. cenocepacia* K56-2::CAST-*fugfp*-Tp in solid media with and without Cm (data not shown). The absence of pRhaCAST was also confirmed by whole genome sequencing. Similarly, after the subsequent integration on *fliF* that resulted in *B. cenocepacia* K56-2::CAST-*fugfp fliF*::CAST-Tp, cells were tetracycline-sensitive, indicating the absence of pFLP3. Genome sequencing results confirmed that pFLP3 was no longer present in the strains tested.

2.5.5 Optimized RhaCAST for *B. multivorans* ATCC 17616

Having shown that the RhaCAST could mutagenize *B. cenocepacia* K56−2, we next focused on another species of Bcc, *B. multivorans* ATCC 17616. We employed a similar strategy as *B. cenocepacia* K56-2, targeting the *paaA* gene of *B. multivorans* ATCC 17616. However, we obtained no colonies following conjugation via tetra-parental mating at 37°C. It has been reported that conducting transposition using VchCAST at temperatures lower than 37°C (30°C or 25°C) can strongly enhance integration efficiencies in *E. coli* (Vo et al. 2020) due to a slower growth rate, allowing longer transposition times. To determine if lowering incubation temperature would increase the integration efficacy of RhaCAST, we targeted the *paaA* gene in *B. multivorans* by performing tetra-parental matings at three different temperatures, 37°C, 30°C and 23°C. We only observed Tp-resistant clones when the conjugation was performed at 23°C.

The phenotypic characterization of the *B. multivorans* ATCC17616 putative *paaA* mutants was performed similarly to *B. cenocepacia* K56-2, where we patched Tp-resistant

transformants onto M9 minimal media with phenylacetic acid or glucose as the sole carbon sources. Targeting the chromosome with two PAMs (GGTC and CGTC) resulted in 97 and 92% DNA cargo insertion efficiency, respectively. However, targeting with GGTT resulted in successful integration only in 11 % of the colonies tested (**Table 2.4**). Integration of the cargo DNA on target in clones with the desired phenotype was further confirmed by colony PCR (**Figure S2.4**). We also targeted *fliF* of *B. multivorans* ATCC 17616 and confirmed the insertion site with colony PCR. From the ten colonies tested, 9 exhibited the expected size of the PCR product for integration (**Figure S2.5**). As expected, the mutant shows complete abolishment of the flagellum (**Figure 2.5**).

Table 2. 4 Summary of targeting *paaA* with RhaCAST system in *B. multivorans* ATCC 17616.

PAM	**Distance between ATG and downstream PAM (bp)**	**Conjugation efficiency (conjugant/recipient)**	**Colonies on target (Mutant with expected phenotype/isolate screened)**	**Percent (%) on target**
CGTC	435	7.22×10^{-9}	12/13	92
GGTT	80	4.33×10^{-9}	1/9	11
GGTC	193	1.60×10^{-8}	30/31	97

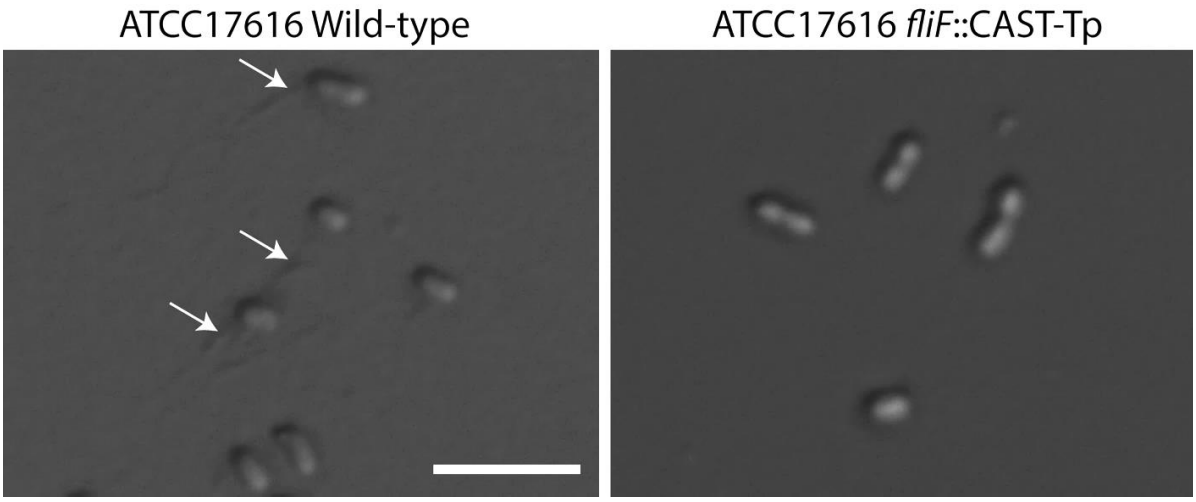


Figure 2. 5 Targeting *fliF* by shCAST in *B. multivorans* ATCC 17616 abolished flagellum formation.

The indicated strains were grown overnight and used for flagellum staining. Cells were imaged by differential interference contrast (DIC). The white arrows indicate the presence of flagellum. The scale bar is 5 μm.

2.5.6 Long-read sequencing confirms on-site insertional mutagenesis and detects the frequency of whole plasmid integration

It has been observed that the ShCAST system can sometimes result in the co-integration of the entire donor plasmid into the targeted site (Vo et al. 2021; Trujillo Rodríguez et al. 2023). To explore this possibility, we performed long-read sequencing of several mutants created with our RhaCAST system (**Table 2.5**). Of 15 genomes sequenced, 100% contained the DNA cargo on target, but in 3 of them, the insertion consisted of whole-plasmid integration. While all single insertional mutants showed integration of cargo DNA only (**Figure S2.6, S2.7, S2.8, S2.9**), one of two double mutants sequenced showed co-integration of the whole plasmid into the target site (**Figure S2.11**). In *B. multivorans* ATCC17616, two of the four sequenced mutants had the whole plasmid integrated into the genome (**Figure S2.12**). For the mutants with the cargo-only insertion, the distances of the PAM and LE were between 59 to 67 bp, similar to the previously reported integration distance from PAM in *E. coli*, which is 60 to 66 bp (Strecker et al. 2019).

Table 2. 5 Long read sequencing summary of mutants created using RhaCAST system in *B. cenocepacia* K56-2 and *B. multivorans* ATCC17616.

Mutants	crRNA's primer number	Summary	Distance of cargo integration (bp)**
K56-2 *paaA*::CAST-Tp	3390	On-target, integration of cargo only	63
K56-2 *paaA*::CAST-Tp	3422	On-target, integration of cargo only	61
K56-2 *paaA*::CAST-Tp	3423	On-target, integration of cargo only	63
K56-2 *fliF*::CAST-Tp	3463	On-target, integration of cargo only	67
K56-2 *fliF*::CAST-Tp	3466	On-target, integration of cargo only	64
K56-2 *phbC*::CAST-Tp	3469	On-target, integration of cargo only	64
K56-2 *phbC*::CAST-Tp	3472	On-target, integration of cargo only	64
K56-2::CAST-*fugfp*-Tp	3475	On-target, integration of cargo only	63
K56-2::CAST-*fugfp*-Tp	3478	On-target, integration of cargo only	64
K56-2::CAST-*fugfp* *fliF::*CAST-Tp	3475	On-target, integration of cargo only	60
K56-2::CAST-*fugfp* *fliF::*CAST-Tp	3475	On-target, whole plasmid integration*	63
ATCC 17616 *paaA*::CAST-Tp	3390	On-target, integration of cargo only	59
ATCC 17616 *paaA*::CAST-Tp	3422	On-target, whole plasmid integration*	65
ATCC 17616 *paaA*::CAST-Tp	3424	On-target, integration of cargo only	59
ATCC 17616 *fliF*::CAST-Tp	3463	On-target, whole plasmid integration*	60

*Co-integration of the cargo DNA and the whole plasmid; **From PAM to LE

2.6 Discussion

Genetic tools are necessary to dissect genotype-phenotype relationships, especially in organisms like Bcc species, which display a duality of beneficial and pathogenic traits. Here, we report the application of the ShCAST system to the Bcc for targeted DNA insertion without homologous recombination. Several research groups have optimized ShCAST for various species, including *S. oneidensis* (Cheng et al. 2022), *B. thailandensis, P. putida* and *A. fabrum* (Trujillo Rodríguez et al. 2023). Most ShCAST systems have the constitutive P_{lac} promoter to drive the expression of *tnsB, tnsC, tniQ,* and *cas12k* genes, except for *S. oneidensis* MR-1, where the endogenous promoters were used (Cheng et al. 2022). The P_{lac} promoter is non-functional in several *Burkholderia* species strains, including *B. cenocepacia* and *B. multivorans* (Flannagan et al. 2007). This work employed a rhamnose-inducible, tightly regulated expression system (Hogan et al. 2021) to drive tnsB-tnsC-tniQ-Cas12k-tracrRNA expression.

To introduce the pRhaCAST and pDonor into *B. cenocepacia* K56-2, we performed tetra-parental conjugation with the helper plasmid pRK2013 at a conjugation temperature of 37°C. However, conjugation for *B. multivorans* ATCC 17616 only yielded transformants when the conjugation was performed at 23°C. It has been suggested that lower temperatures could exhibit higher integration efficiencies (Vo et al. 2020). In *E. coli*, incubation times at either 30°C or 25°C can enhance integration efficiencies with VchCAST (Gelsinger et al. 2023). However, the mechanistic explanation for the temperature effect on CAST systems has not been thoroughly studied.

It has been described that the use of ShCAST for site-specific genome targeting resulted in whole plasmid integration into the target site due to the lack of functional TnsA (Vo et al. 2021). This issue has been observed in various species, including *E. coli, B. thailandensis, P. putida,* and *A. fabrum* (Rice et al. 2020; Strecker et al. 2020; Trujillo Rodríguez et al. 2023). We also observed a few instances of co-integration of full-length plasmid in *B. cenocepacia*

and *B. multivorans*. Using linear or 5′-nicked DNA donors could prevent co-integration formation (Strecker et al. 2020). However, these approaches cannot be applied if the plasmid is introduced into the recipient via conjugation. While the incorporation of whole plasmids has a low frequency, it is a limitation of the system. To rule out whole plasmid integration in selected mutants, PCR amplification of the target gene should reveal a PCR product that includes the cargo DNA's expected size. A failed PCR reaction or a longer-than-expected PCR product may signal whole plasmid integration. To confirm the suspected whole plasmid integration, we recommend whole genome sequencing. Alternatively, multiple studies have shown that the ShCAST system has off-target activity and lower fidelity than the INTEGRATE system in various species. Whether the INTEGRATE system can overcome some of the limitations of RhaCAST in any Bcc species remains to be demonstrated.

The RhaCAST system developed for Bcc provides an improved targeted integration system compared to available targeted mutagenesis and Tn7 tools for chromosomal integration. Current site-directed genome editing tools are based on homologous recombination, which requires the cloning of long homology arms (Flannagan et al. 2007). As for genomic integration with *Tn7* tools, the integration could be only at specific sites (Heacock-Kang et al. 2018). RhaCAST allows targeting any genomic region with only 24 bp of crRNA to deliver a cargo DNA. The delivered DNA fragment can be aimed to disrupt a functional element or to introduce a genetic element into the chromosome at a specific site. In addition, the pRhaCAST plasmid is easily cured as opposed to the plasmid described by Strecker et al., which cannot be cured easily after transformation (Trujillo Rodríguez et al. 2023). Other systems developed based on ShCAST require extra curing steps dependent on the temperature-sensitive origin (Trujillo Rodríguez et al. 2023) or via counter selection (Cheng et al. 2022). The spontaneous curing of pRhaCAST allows the system to be used iteratively without additional steps of

plasmid curation. It should be noted, however, that while we observed high integration efficiency of selected genes, other genomic regions may be more challenging to target.

In summary, the RhaCAST system is a versatile tool that can be used for both loss- and gain-of-function applications in Bcc species. Additionally, this system allows for the excision and reuse of the selection marker, enabling iterative genetic manipulation without additional selection markers. The RhaCAST system is faster, easier, and more adaptable than existing insertional mutagenesis tools for Bcc species. RhaCAST may be used to disrupt and insert relevant genetic elements, paving the way for future Bcc biotechnological applications.

2.7 Plasmid and data availability

For ease of distribution, the following plasmids are deposited to AddGene: pZLrhaB2plus (#211787), pRhaCAST (#211791), pDonorTp (#211788), and pDonorTp-*fugfp* (#211790). All the genome sequences of the mutants from this study are available in the NCBI database under BioProject PRJNA1041412.

CHAPTER 3: IDENTIFYING BIOPLASTIC DEGRADATION GENES IN BURKHOLDERIA EMPLOYING TN-SEQ AND CRISPR-CAS

3.1 Abstract

Bioplastics represent promising alternatives to petroleum-based plastics, yet their biodegradation remains insufficiently understood. Identifying bacteria and enzymes capable of degrading bioplastics could enhance end-of-life management practices. To investigate *Burkholderia's* capacities for degradation of medium-chain-length polyhydroxyalkanoate (mcl-PHA), we screened a panel of *Burkholderia* strains and identified *B. gladioli*, *B. multivorans* and *B. vietnamiensis* as capable of degrading extracellular mcl-PHA. To elucidate the genetic basis of this activity, we performed transposon mutagenesis followed by Tn-seq on *B. vietnamiensis* LMG 16232. Transposon insertions were identified in genes encoding a triacylglycerol lipase, a lipase chaperone, type II secretion system components, HTH-type transcriptional activators, and a polyhydroxyalkanoate synthesis repressor. To validate the involvement of these genetic elements in mcl-PHA degradation, we generated insertional mutants using a CRISPR-associated transposase system (CAST). Complete loss or reduced extracellular mcl-PHA depolymerase activity was observed in the CAST mutants, validating their involvement in mcl-PHA degradation. In addition, the interruption of these genetic elements showed a loss of lipase activity, suggesting that the enzymes responsible for mcl-PHA depolymerase are lipases with substrate ambiguity. Together, we identify *Burkholderia* genetic determinants for mcl-PHA degradation, which indicates that this *Burkholderia* lipase might also be the catalyst for the degradation of extracellular mcl-PHA.

3.2 Introduction

Polyhydroxyalkanoates (PHAs) are bioplastics made from biological polyesters and have a wide-range of applications in various sectors, such as packaging, agriculture, and biomedical devices (Muneer et al. 2020). Depending on the number of carbon atoms on each

monomer, PHAs can be broadly classified as either short-chain-length PHAs (scl-PHA), which consist of 3-5 carbon atoms or medium-chain length (mcl-PHA) with 6-15 carbon atoms per monomer, in the 3-hydroxyalkanoate units (Li et al. 2016).

PHAs are degraded by either intracellular or extracellular PHA depolymerases. Intracellular PHA depolymerases hydrolyze the endogenous carbon reservoir, carbonosomes, and the native amorphous PHA granules with a surface layer of proteins and phospholipids (Jendrossek 2009). Extracellular PHA depolymerases are secreted from the cell to degrade exogenous denatured granules that are semi-crystalline and lack the surface layer (Jendrossek and Handrick 2002). Both intracellular and extracellular PHA depolymerases are carboxylesterases and belong to the α/β-hydrolase fold family (Knoll et al. 2009). PHA depolymerases have been isolated and biochemically characterized from species belonging to phyla Ascomycetes, Firmicutes, Proteobacteria, and Actinobacteria (Viljakainen and Hug 2021).

The ability to degrade extracellular PHA to release oligomers and monomers as carbon and energy sources relies on the secretion of specific extracellular depolymerase (Martínez et al. 2015). Many studies have found microorganisms that degrade scl-PHA in various environments, purified, and characterized these enzymes (Knoll et al. 2009; Viljakainen and Hug 2021). However, microorganisms that can degrade mcl-PHA are relatively rare compared to those that can degrade scl-PHA (Viljakainen and Hug 2021). Most of the extracellular mcl-PHA depolymerases that have been purified and biochemically validated belong to *Pseudomonas* sp (Schirmer and Jendrossek 1994; Kim et al. 2005; Rhee et al. 2006), an obligated predator *Bdellovibrio bacteriovorus* (Martínez et al. 2012), *Thermus thermophilus* (Papaneophytou et al. 2011) and the Actinobacteria *Streptomyces* sp (Gangoiti et al. 2012; Santos et al. 2013; Martínez et al. 2015). BLASTp-based similarity searches using biochemically validated extracellular mcl-PHA depolymerases as queries against

metagenomes suggest that extracellular mcl-PHA depolymerase producers are in the taxonomic groups Myxococcota, Proteobacteria, Actinobacteriota and Bdellovibrionota (Viljakainen and Hug 2021). In summary, mcl-PHA degradation is not widely distributed among Bacteria.

Both extracellular scl and mcl-PHA depolymerases are hydrolytic enzymes that break down PHAs into smaller components. However, extracellular mcl-PHA depolymerases show little overall sequence homology with scl-PHA despite both being involved in the degradation of PHAs (Martínez et al. 2012; Paloyan et al. 2025). The catalytic mechanism of these enzymes involves a common feature that is shared with other hydrolytic enzymes, such as lipases. Lipases are known for catalyzing the hydrolysis of carboxyl-ester bonds in triglycerides, such as oil and fats, into free fatty acid and glycerol (Gupta et al. 2004). Both scl and mcl-PHA depolymerases and lipases have a catalytic triad consisting of serine, histidine, and aspartic acid at the active site. The catalytic serine is located within the GxSxG sequence motif (also known as the lipase box), also found in other α/β-hydrolases. Furthermore, a conserved non-catalytic histidine near the oxyanion hole is analogous to lipases (Jaeger et al. 1995; Jendrossek and Handrick 2002; Knoll et al. 2009). Some bacterial genera, such as *Bacillus, Pseudomonas* and *Burkholderia* (Rathi et al. 2001), are well-known lipase producers (Gupta et al. 2004).

Some known bioplastic degrading enzymes are often members of lipase, proteinase, cutinase or esterase families (Suzuki et al. 2020; Mohanan et al. 2022; Shalem et al. 2024). Some extracellular lipases purified from various species, including *Bacillus subtilis, Pseudomonas aeruginosa, Pseudomonas alcaligenes, Pseudomonas fluorescens, and Burkholderia cepacia*, were able to hydrolyze polyesters such as polyhydroxyhexanoate or polyhydroxybutyrate (Jaeger et al. 1995). The extracellular lipases of *Pseudomonas chlororaphis* PA23 and *Acinetobacter lwoffii* can hydrolyze various PHA polymers, including mcl-PHA: polyhydroxyoctanoate (PHO) and polyhydroxydecanoate (Sharma et al. 2019). The

Burkholderia genus is one of the most well-known lipase producers. For example, *B. cepacia* (Rathi et al. 2001), *B. lata* (Oliveira et al. 2015), *Burkholderia sp.* ZYB002 (Shu et al. 2012), and *Burkholderia* sp. HL-10 (Lo et al. 2012). Specifically, *B. cepacia* lipase has been widely used in various industrial processes (Mello Bueno et al. 2015; Li et al. 2017; Sánchez et al. 2018).

As the production of PHAs is predicted to surge in the coming years, it becomes increasingly important to identify and better understand PHA-degrading microbes, the enzymes they produce, and the genes associated with PHA-degrading activity. In this context, *Burkholderia*, known for its remarkable metabolic versatility, presents a promising avenue for exploration (Eberl and Vandamme 2016). *Burkholderia* has the ability to produce diverse enzymes that break down various substrates for carbon utilization (Vial et al. 2007). This enzymatic diversity suggests *Burkholderia*'s potential capability to degrade polymers such as bioplastics, even when they are not their natural substrates.

In this work, we explored the degradation capabilities of *Burkholderia* extracellular mcl-PHA by using PHO as a representative substrate and identifying the genetic elements involved in this process. We first identified several *Burkholderia* strains, including *B. gladioli*, *B. multivorans and B. vietnamiensis,* capable of degrading extracellular mcl-PHA. To elucidate the genetic basis of this activity, we performed transposon mutagenesis on one of the strains, *B. vietnamiensis* and identified several putative genes associated with extracellular mcl-PHA degradation. These genes include triacylglycerol lipase, lipase chaperone, type II secretion system components, HTH-type transcriptional activator, and polyhydroxyalkanoate synthesis repressor. To validate these genetic elements, we generated insertional mutants using a CRISPR-associated transposase system (CAST). We have successfully adapted this system for several *Burkholderia* species and intend to leverage its capabilities to elucidate the genetic determinants of PHA degradation further.

3.3 Materials and Methods

3.3.1 Strains, Selective Antibiotics, and Growth Conditions

Strains and plasmids are shown in **Table 3.1**. Primers used in this study are listed in **Table 3.2**. All strains were grown in LB-Lennox medium (Difco). Strains of *Burkholderia* and the strains of *E. coli* were initially grown at 37°C, except for *E. coli* Stbl2, which was grown at 30°C. The following selective antibiotics were used: chloramphenicol (Sigma; 20 μg/mL for *E. coli*), trimethoprim (Sigma; 100 μg/mL for strains of *Burkholderia*, 50 μg/mL for *E. coli*), and gentamicin (Sigma; 50 μg/mL for *Burkholderia*).

Table 3. 1 List of bacterial strains and plasmids used in Chapter 3.

Strain or plasmid	**Features**	**Source**
Burkholderia cenocepacia K56-2	ET12 lineage cystic fibrosis clinical isolate from Toronto	(Darling et al. 1998)
Burkholderia cenocepacia F9141525	Cystic fibrosis clinical isolate from Toronto	SickKids, Toronto
Burkholderia cenocepacia F3071909	Cystic fibrosis clinical isolate from Toronto	SickKids, Toronto
Burkholderia cenocepacia G1181568-1	Cystic fibrosis clinical isolate from Toronto	SickKids, Toronto
Burkholderia cenocepacia F4200989-3	Cystic fibrosis clinical isolate from Toronto	SickKids, Toronto
Burkholderia cenocepacia VC14488	Canadian cystic fibrosis isolate	CBCCRRR
Burkholderia cenocepacia VC14543	Canadian cystic fibrosis isolate	CBCCRRR
Burkholderia cenocepacia VC10414	Canadian cystic fibrosis isolate	CBCCRRR
Burkholderia cenocepacia VC14761	Canadian cystic fibrosis isolate	CBCCRRR
Burkholderia cenocepacia 130723	Clinical respiratory isolate collected in Halifax	CANWARD/CARA database
Burkholderia cenocepacia 125007	Clinical respiratory isolate collected in Vancouver	CANWARD/CARA database
Burkholderia contaminans 21NG595759	Canadian cystic fibrosis isolate	H. Adam (Shared Health MB)
Burkholderia contaminans 21NG609698	Canadian cystic fibrosis isolate	H. Adam (Shared Health MB)
Burkholderia dolosa AU6940	Cystic fibrosis clinical isolate	SickKids, Toronto
Burkholderia dolosa AU2167	Cystic fibrosis clinical isolate	SickKids, Toronto

Burkholderia dolosa LM018941	Cystic fibrosis clinical isolate	SickKids, Toronto
Burkholderia dolosa AU0645	Cystic fibrosis clinical isolate	SickKids, Toronto
Burkholderia gladioli VC19233	Canadian cystic fibrosis isolate	CBCCRRR
Burkholderia gladioli VC14812	Canadian cystic fibrosis isolate	CBCCRRR
Burkholderia gladioli 132208	Clinical respiratory isolate collected in Montreal	CANWARD/CARA database
Burkholderia gladioli 113611	Clinical respiratory isolate collected in Saskatoon	CANWARD/CARA database
Burkholderia multivorans 21NH942533	Canadian cystic fibrosis isolate	H. Adam (Shared Health MB)
Burkholderia multivorans 21NJ503211	Canadian cystic fibrosis isolate	H. Adam (Shared Health MB)
Burkholderia multivorans V1120157	Cystic fibrosis clinical isolate	SickKids, Toronto
Burkholderia multivorans LM013010	Cystic fibrosis clinical isolate	SickKids, Toronto
Burkholderia multivorans F9091687	Cystic fibrosis clinical isolate	SickKids, Toronto
Burkholderia multivorans VC19694	Canadian cystic fibrosis isolate	CBCCRRR
Burkholderia multivorans VC15555	Canadian cystic fibrosis isolate	CBCCRRR
Burkholderia multivorans VC9825	Canadian cystic fibrosis isolate	CBCCRRR
Burkholderia multivorans 131077	Clinical respiratory isolate collected in Toronto	CANWARD/CARA database
Burkholderia stagnalis MSMB618	N/A	NAU-PMI
Burkholderia stagnalis MSMB642	N/A	NAU-PMI
Burkholderia vietnamiensis LMG 22486	Wastewater isolate	BCCM
Burkholderia vietnamiensis LMG 10929	Oryza sativa, rhizosphere soil isolate	BCCM
Burkholderia vietnamiensis LMG 16232	Clinical isolate from cystic fibrosis patient	BCCM
Burkholderia vietnamiensis VC11431	Canadian cystic fibrosis isolate	CBCCRRR
Burkholderia vietnamiensis VC18984	Canadian cystic fibrosis isolate	CBCCRRR

Burkholderia vietnamiensis LMG 16232 *lip1*::CAST-Tp	Derived from LMG 16232; Cargo containing Tp^r integrated into triacylglycerol lipase CDS (P4G95_16805)	This study
Burkholderia vietnamiensis LMG 16232 A24 family peptidase CDS:: CAST-Tp	Derived from LMG 16232; Cargo containing Tp^r integrated into A24 family peptidase CDS (P4G95_07805)	This study
Burkholderia vietnamiensis LMG 16232 *otsB*::CAST-Tp	Derived from LMG 16232; Cargo containing Tp^r integrated into *otsB* (P4G95_10885)	This study
Burkholderia vietnamiensis LMG 16232 *gspE*::CAST-Tp	Derived from LMG 16232; Cargo containing Tp^r integrated into *gspE* (P4G95_05530)	This study
Burkholderia vietnamiensis LMG 16232 TetR/AcrR family transcriptional regulator CDS::CAST-Tp	Derived from LMG 16232; Cargo containing Tp^r integrated into TetR/AcrR family transcriptional regulator CDS (P4G95_00865)	This study
E. coli Stbl2	*F- mcrA Δ(mcrBC-hsdRMS-mrr) recA1 endA1lon gyrA96 thi supE44 relA1 λ- Δ(lac-proAB)*	Invitrogen
pRBrhaBoutgfp	pSCrhaBoutgfp derivative, ori_{R6K}, *rhaR* *rhaS* PrhaB e-gfp	(Bloodworth et al. 2013)
pRK2013	ori_{colE1} RK2 derivative Kan^r mob^+ tra^+	(Figurski and Helinski 1979)
pDonorTp	pDonor_ShCAST_kanR with modification of Km^R to Tp^R	(Yap et al. 2024)
pRhaCAST	*Sh-cas12K-tnsBC-tniQ* drives by the rhamnose inducible promoter	(Yap et al. 2024)
pRhaCAST-3668	Modified from pRhaCAST. crRNA targeting *B. vietnamiensis* LMG 16232 triacylglycerol lipase CDS (P4G95_16805)	This study
pRhaCAST-3952	Modified from pRhaCAST. crRNA targeting *B. vietnamiensis* LMG 16232 A24 family peptidase CDS (P4G95_07805)	This study
pRhaCAST-3956	Modified from pRhaCAST. crRNA targeting *B. vietnamiensis* LMG 16232 *otsB* (P4G95_10885)	This study
pRhaCAST-3996	Modified from pRhaCAST. crRNA targeting *B. vietnamiensis* LMG 16232 *gspE* (P4G95_05530)	This study
pRhaCAST-4000	Modified from pRhaCAST. crRNA targeting *B. vietnamiensis* LMG 16232 TetR/AcrR family	This study

	transcriptional regulator CDS (P4G95_00865)	

Table 3. 2 Primers/templates used in Chapter 3.

Number	Sequence	Description
Oligonucleotides for Tn-seq		
683	CCGTAGTGAGTTCTTCGTCCGAGCCA CTCGGAGATGTGTATAAGAGACAGT	Tn-seq adapter (top strand)
684	CTGTCTCTTATACACATCTCCGAGTG GCTCGGACGAAGAACTCACTACGG	Tn-seq adapter (bottom strand)
682	CACAAGTGCGGCCGCACTAGTCTAG ATTTAAATTACCGTAGTGAGTTCTTC GTCCGAGCCAC	Tn-seq oligo probe
681	CAAGCAGAAGACGGCATACGAGATT CGCCTTAGTCTCGTGGGCTCGGAGAT GTGTATAAGAGACAG	Illumina Nextera index N701 (pool 1)
690	AATGATACGGCGACCACCGAGATCT ACACTAGATCGCTCGTCGGCAGCGTC AGATGTGTATAAGAGACAGNNNNAA TCTAGACTAGTGCGGCC	Illumina Nextera index N501 (pool 1)
718	CAAGCAGAAGACGGCATACGAGATA GGAGTCCGTCTCGTGGGCTCGGAGAT GTGTATAAGAGACAG	Illumina Nextera index N705 (pool 2)
719	AATGATACGGCGACCACCGAGATCT ACACCTCTCTATTCGTCGGCAGCGTC AGATGTGTATAAGAGACAGNNNNAA TCTAGACTAGTGCGGCC	Illumina Nextera index N502 (pool 2)
Oligonucleotides for cloning crRNA into pRhaCAST (crRNA is in bold, *sapI* restriction site is in italics)		
3392	ACTAACGGCTCTTCGAG	Reverse primer to amplify single stranded nucleotide template containing the crRNA
3421	CATTGGCTCTTCGAAAG	Forward primer to amplify single stranded nucleotide template containing the crRNA
3668	CATT*GGCTCTTC*GAAAG**ATCCTCGTG CACGGCCTTACCGGC**GGCTC*GAAGA GC*CGTTAGT	Targeting triacylglycerol lipase CDS (P4G95_16805) of LMG 16232
3952	CATT*GGCTCTTC*GAAAG**GTGATCGG TCTGTGCGTCGGCAGC**GGCTC*GAAG AGC*CGTTAGT	Targeting A24 family peptidase CDS (P4G95_07805) of LMG 16232
3956	CATT*GGCTCTTC*GAAAG**CCTGACCG ATACCGCGTTCTTTTT**GGCTC*GAAG AGC*CGTTAGT	Targeting *otsB* (P4G95_10885) of LMG 16232
3996	CATT*GGCTCTTC*GAAAG**TGCAAGGA AGAGCGACACGAGGAC**GGCTC*GAA GAGC*CGTTAGT	Targeting *gspE* (P4G95_05530) of LMG 16232

4000	CATT*GGCTCTTC*GAAAG**CCACCATCG ACGAGACCTGGTCGT**GGCTC*GAAGA GCC*GTTAGT	Targeting TetR/AcrR family transcriptional regulator CDS (P4G95_00865) of LMG 16232
Oligonucleotides for colony PCR to verify genomic insertion		
3001	GGTGGGTTGAAAGCAAGTCC	left end of the cargo insertion
3670	CTATCCGGTCATCCTCGTGC	Colony PCR for triacylglycerol lipase CDS (P4G95_16805) of LMG 16232
3953	GTGATCGGTCTGTGCGTCG	Colony PCR for A24 family peptidase CDS (P4G95_07805) of LMG 16232
3957	CTGACCGATACCGCGTTCTT	Colony PCR for *otsB* (P4G95_10885) of LMG 16232
3997	GCAAGGAAGAGCGACACGAG	Colony PCR for *gspE* (P4G95_05530) of LMG 16232
4001	CCACCATCGACGAGACCTG	Colony PCR for TetR/AcrR family transcriptional regulator CDS (P4G95_00865) of LMG 16232

3.3.2 Genomic and plasmid extraction

Genomic DNA of the *B. vietnamiensis* LMG 16232 mutants made with RhaCAST were extracted using the PureLink microbiome DNA purification kit (Invitrogen). Genomic DNA of the Tn-seq pools were extracted using standard isopropanol precipitation. Plasmid DNA was extracted using the EZNA Plasmid DNA Mini Kit (Omega Bio-tek). Both genomic and plasmid DNA were eluted or solubilized in Tris-HCl pH 8.5.

3.3.3 Substrate and media preparation

The Poly(3-hydroxyoctanoate) (PHO) colloidal suspension was created by dissolving 400 mg of PHO into 200 mL acetone (Polyferm Canada Inc., Canada). Once the PHO was dissolved, 40 mL of dH2O was added. The acetone was evaporated off using a speed evaporator. The colloidal suspension was stored at 4˚ C until needed.

The mcl-PHA containing medium consisted of an M9 minimal media agar with 2 mM phenylalanine, 2 mM $MgSO_4$, 10 mg/ mL of PHO and 0.3 µg/mL Nile red. PHO was added to the media by using a previously prepared colloidal suspension of PHO. The PHO, Nile red, $MgSO_4$, and phenylalanine were added after autoclaving to the M9 agar whilst melted. 25 mL

of media was then poured into petri plates. After solidifying, the plates were stored at 4°C until needed.

Tributyrin media was made using a minimal media with 2 mM phenylalanine and 2 mM $MgSO_4$ with tributyrin added to a final concentration of 4% (v/v) in the medium according to the Sigma-Aldrich instructions (Sigma, St. Louis, Missouri, USA). The tributyrin was added after autoclaving whilst the agar medium was around 80°C. The media with tributyrin was vigorously mixed until ready to pour into petri plates. After solidifying, the plates were stored at 4°C until needed.

3.3.4 Screening for mcl-PHA and tributyrin degradation

To determine the strain's ability to degrade mcl-PHA and tributyrin. The overnight cultures were grown at 30°C and washed twice with PBS. 20 µL of the culture was inoculated after being adjusted to an OD_{600} of 1. For mcl-PHA degradation determination, the plates were incubated for 7 days; For tributyrin degradation determination, the plates were incubated for 3 days, both incubated at 30°C. The visualization of the halo degradation was performed using AlphaImager EP (Cell Biosciences, Santa Clara, CA). For the mcl-PHA plates containing Nile red, the image was taken under UV excitation.

3.3.5 Transposon mutagenesis, Tn-seq library preparation and genome mapping

B. vietnamiensis LMG 16232 was subjected to transposon mutagenesis with pRBrhaBoutgfp (Cardona et al. 2006). A total of 50,000 single colonies were screened, and the colonies that appeared to have lost the PHO degradation activity on the first round of screening were then subjected to a secondary screening to rule out false positives. 66 and 18 transconjugants were isolated without or with weak PHO degradation activity, respectively.

Tn-seq was chosen to identify the transposon insertion site, as this method will simultaneously detect transposon-genome junctions in all 84 mutants by next-generation

sequencing. To enrich transposon-genome junctions and to determine the insertion site, an adapted Tn-seq method, Tn-seq circle, developed by Gallagher et al. (2011), was performed as previously described with some minor modifications (Gallagher et al. 2011; Gislason et al. 2017). Briefly, cultures of individual mutants were grown individually to approximately OD_{600} of 3 and were combined into two separate pools, based on without (pool 1) or with weak (pool 2) PHO degradation activity. The cultures were harvested, followed by the genomic DNA extraction. The DNA was sheared to an average size of 300 bp via ultrasonication with a Covaris M220 (duty factor of 20%, a peak incident power of 50W, 200 cycles per burst, and a duration of 75s), followed by end repair with the NEBNext End Repair Module (NEB) and A-tailing. Next, the products were ligated with adaptors, consisting of annealing oligos 683 and 684 with the Quick Ligation Kit (NEB) and digested with *PacI* (NEB). Probe 682 in the presence of Ampligase (Lucigen) was used to circularize fragments containing the transposon sequence. The exonuclease treatment was carried out with a mix of T7 gene 6 exonuclease (ThermoFisher), Lambda exonuclease (NEB), and Exonuclease I (NEB) to digest the linear fragments. The enrichment of the transposon–genome junctions was confirmed by comparing the amplification of the transconjugant's pools with wild-type *B. vietnamiensis* LMG 16232 using qPCR with iTaq Universal SYBR Green Supermix (Bio-Rad). The number of PCR cycles corresponding to ~50% saturation by qPCR was chosen to amplify transposon-genome junctions with iTaq DNA polymerases (Bio-Rad) for Illumina sequencing. PCR primers 681, 690, 718, and 719 contain the Nextera indices and were used in appropriate pairs (**Table 3.2**). The indexed samples were then cleaned-up with the SeraMag beads (Cytiva), analysed on a TapeStation4150 (Agilent Technologies) and sequenced with an Illumina MiSeq 2500. Raw reads were deposited in the NCBI Sequence Read Archive (SRA) repository under BioProject: PRJNA1082765, accession: SRR28216496 (pool 1), SRR28216495 (pool 2).

The sequenced reads of these mutants were mapped to the *B. vietnamensis* LMG 16232 genome with the Galaxy bioinformatics platform (https://usegalaxy.org). Using Cutadapt (Galaxy v2.9+galaxy0)(Martin 2011), the transposon sequence 5'-NNNNAATCTAGACTAGTGCGGCCGCACTTGTGTATAAGAGTCA-3' was removed from the FASTQ file. Next, using Burrows-Wheeler transform (BWA) (Galaxy v0.7.17.4) (Li and Durbin 2010), the reads were mapped to the closed genome of *B. vietnamiensis* LMG 16232 (Yap et al. 2023). The BWA's BAM output was then converted to SAM using BAM-to-SAM (Galaxy 2.0.2) (Li et al. 2009). The output was visualized using Geneious 8.1.9.

3.3.6 Determination of the PHO content beneath inoculated culture

The inoculated culture from the phenotypic assay was scraped off from the agar. An agar disk beneath the inoculated culture was cut using the back of the P1000 pipette tip. For control, a disk was cut where no cell was inoculated. The samples were dried at 60°C for 16 hours, and the PHO was extracted in chloroform using the acid-catalyzed methanolysis procedure as previously described (Braunegg et al. 1978; Fu et al. 2014). The determination of PHO in the agar was performed using an Agilent 7890A gas chromatograph equipped with a DB-23 capillary column (30 m × 250 μm × 0.25 μm) and a flame ionization detector (Agilent Technologies, Santa Clara, CA). Method operating parameters and peak quantification have been previously described (Fu et al. 2014; Blunt et al. 2024).

3.3.7 *In silico* analysis

The calculated molecular weight and theoretical isoelectric point (pI) of the putative enzyme were computed with Expasy (Gasteiger et al. 2005). The putative catalytic amino acid was predicted with Phyre2 server (Protein Homology/analogY Recognition Engine V 2.0) (Kelley et al. 2015). Signal peptides were predicted for predicted PHA depolymerases using Signal P 5.0 (https://services.healthtech.dtu.dk/service.php?SignalP) with default settings using both Gram-negative and Gram-positive predictions (Almagro Armenteros et al. 2019).

The alignment of amino acid sequences was performed using Clustal Omega (https://www.ebi.ac.uk/jdispatcher/msa) (Madeira et al. 2024).

3.3.8 Construction of *B. vietnamiensis* LMG 16232 insertional mutants

Genes were interrupted using the RhaCAST method reported previously (Yap et al. 2024). Briefly, 24 bp crRNAs were designed from the genes to be targeted, and the templates were ordered as single-stranded oligos and PCR-amplified using PCR primers 3392 and 3421 to create double-stranded DNA fragments. The PCR products were then introduced into pRhaCAST using Golden Gate cloning with SapI (NEB). The newly constructed plasmids were then transformed into *E. coli* Stbl2. pRhaCAST was then introduced to *B. vietnamiensis* LMG 16232 by tetra-parental mating (Yap et al. 2024, see chapter 2). *E. coli* MM290/pRK2013 helper strain, *E. coli* Stbl2/pRhaCAST with corresponding crRNA, and *E. coli* PIR1/pDonorTp were conjugated into *B. vietnamiensis* LMG 16232 on LB agar plate containing 0.05% rhamnose. The plate was incubated at 37°C for 24 hours. Successful exconjugants were selected on LB plates containing trimethoprim and gentamicin to select against the *E. coli*. Colonies that appeared within 48 h at 37°C were screened by colony PCR. All insertional mutants constructed with RhaCAST were verified by whole genome sequencing using Oxford Nanopore Technologies platforms with v14 library prep chemistry and R10.4.1 flow cells by Plasmidsaurus (Oregon, USA). The genomic sequence of the insertional mutants is available under BioProject: PRJNA1205771.

3.4 Results

3.4.1 Diversity of extracellular mcl-PHA degradation activity in *Burkholderia* strains

An initial screen for mcl-PHA degradation activity was performed on several *Burkholderia* strains. To identify mcl-PHA degradation activity, *Burkholderia* were inoculated in a solid minimal medium containing PHO and phenylalanine (as another carbon source to aid growth), supplemented with Nile red to enhance the visualization of PHO. Phenylalanine was

chosen as a secondary carbon source in the media because (i) it is known to be catabolized by the model *Burkholderia* species, *B. cenocepacia* (Yudistira et al. 2011), and (ii) its metabolism can influence several bacterial pathways, including those associated with quorum sensing (Tung et al. 2024). Therefore, we hypothesize that the addition of this amino acid could potentially induce extracellular mcl-PHA degradation by *Burkholderia*. The plates were incubated for 20 days to ensure cells grew densely and sufficient enzyme production to degrade mcl-PHA. After dense growth was achieved, a clear halo was observed around some colonies, suggesting extracellular PHO degradation. Using this medium, we screened a panel of *Burkholderia* species and found several strains, including *B. gladioli*, *B. multivorans*, and *B. vietnamiensis,* that could degrade extracellular mcl-PHA (**Table 3.3, Figure S3.1**). Of the strains with activity, *B. gladioli* strain VC19233, *B. multivorans* 21NH942533, and VC9825 exhibit weak activity in degrading mcl-PHA; *B. stagnalis* strains MSMB618, MSMB642, and *B. vietnamiensis* LMG 16232 have moderate activity in degrading mcl-PHA. There are two strains, *B. multivorans* F9091687 and *B. gladioli* 132208, where the temperature affects the activity. No mcl-PHA depolymerase activity was observed for *B. cenocepacia*, *B. contaminans,* and *B. dolosa* isolates tested (**Table 3.3**). *B. vietnamiensis* LMG 16232 was selected for further study for this activity for a few reasons: first, the extracellular mcl-PHA degradation of this strain is one of the highest among other *Burkholderia* strains that exhibit this activity. Secondly, we were able to implement transposon mutagenesis in this strain. Thirdly, this strain was genetically amenable using the RhaCAST system, allowing us to create insertional mutants to verify transposon mutagenesis results. Finally, the genome sequence of this strain is available (Yap et al. 2023, see Appendix 6.3).

Table 3. 3 *Burkholderia* isolates that exhibit extracellular mcl-PHA degradation activity.

Species	Strain	Ability to degrade PHO after 20 days	
		30˚C	37˚C
Burkholderia cenocepacia	K56-2	-	-
	F9141525	-	-
	F3071909	-	-
	G1181568-1	-	-
	F4200989-3	-	-
	VC14488	-	-
	VC14543	-	-
	VC10414	-	-
	VC14761	-	-
	130723	-	-
	125007	-	-
Burkholderia contaminans	21NG595759	-	-
	21NG609698	-	-
Burkholderia dolosa	AU6940	-	-
	AU2167	-	-
	LM018941	-	-
	AU0645	-	-
Burkholderia gladioli	VC19233	+	+

	VC14812	-	-
	132208	+	-
	113611	-	-
Burkholderia multivorans	21NH942533	+	+
	21NJ503211	+	-
	V1120157	-	-
	LM013010	-	-
	F9091687	+	-
	VC19694	-	-
	VC15555	-	-
	VC9825	+	+
	131077	-	-
Burkholderia stagnalis	MSMB618	++	++
	MSMB642	++	++
Burkholderia vietnamiensis	LMG 22486	-	-
	LMG 10929	-	-
	LMG 16232	++	++
	VC11431	-	-
	VC18984	-	-

mcl-PHA degradation was ranked based on (–) no clearing, (+) weak clearing, (++) moderate clearing.
Figure S3.1 is the source of the data interpretation.

3.4.2 Genetic basis of *B. vietnamiensis* LMG 16232 extracellular mcl-PHA degradation activity

To determine the gene elements involved in the extracellular mcl-PHA degradation activity by *B. vietnamiensis* LMG 16232, we performed transposon mutagenesis, followed by Illumina sequencing (Tn-seq) (**Figure 3.1**). We first optimized the screening method to allow for the visualization of mcl-PHA degradation from a single isolated transconjugant. The transconjugants were directly plated from the conjugation mix on agar containing the antibiotic for the selection of transposon conjugants and mcl-PHA degradation. The screening method now only took only 7 days, in contrast to the initial screening, which took 20 days. The media also contained phenylalanine to aid growth. To ensure genomic coverage of transposon insertions in *B. vietnamiensis* LMG 16232, we determined the estimated transposon insertion density using an analytical model based on a Poisson distribution of transposon insertions (Baym et al. 2016). We screened ~50,000 transposon mutants in LMG 16232, where the expected average transposon insertion density from the model is ~8 transposon insertions per gene. Using this model, assuming a genome with N=6000 non-essential gene and a collection of N=50,000 transposon insertion mutants, the probability that a single gene will see no transposon insertion is: P(0, k, N) = e^(-50,000/ 6,000)= 2.4×10^{-4}; the total number of genes that will see no insertions is: N* e^(-k/N) =6,000 x 2.4×10^{-4}= 1.4 genes; and the total number of genes will be found with this transposon density is n(insertion) 6,000* (1-e ^(-50,000/ 6,000))=5,999 genes. From the primary screening of single isolated transconjugants, we identified 84 colonies that did not produce a visible halo. These colonies were subjected to secondary screening, where each isolated transconjugant was grown individually and screened on solid media containing mcl-PHA. The secondary screening was performed as it is more reliable, because it does not imply using a single colony as in the primary screening. We observed that 66 transconjugants had lost the ability to degrade extracellular mcl-PHA,

showing no halo. In contrast, 18 transconjugants exhibited severely reduced halo formation around the cells growing on the media consisting of mcl-PHA.

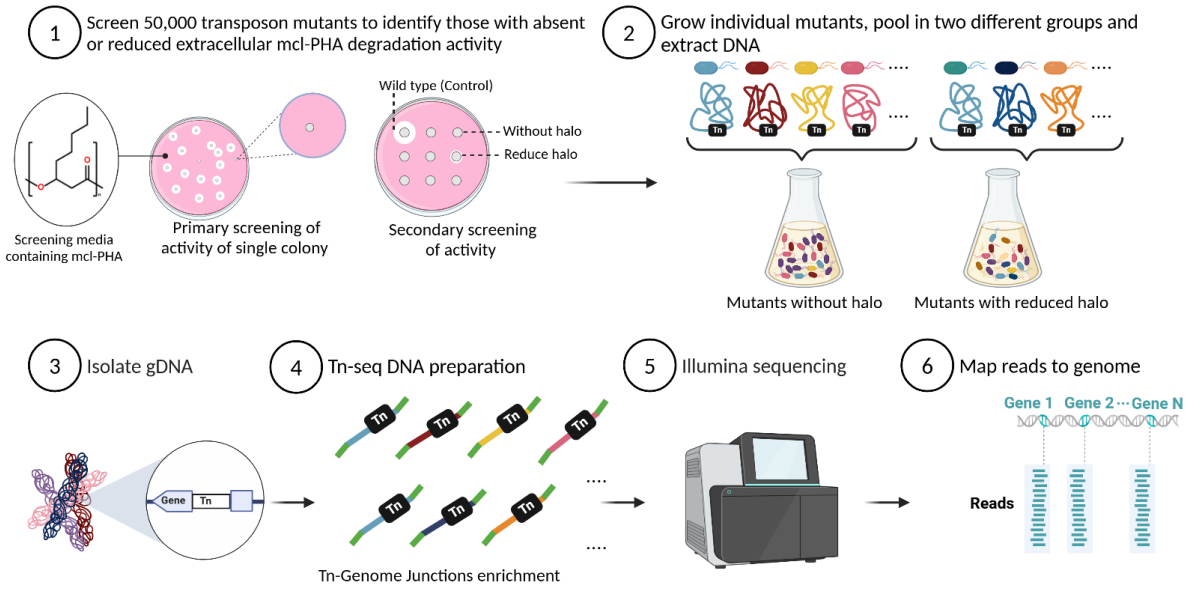


Figure 3. 1 Overview of transposon mutagenesis and Tn-seq workflow to identify genetic elements involved in the extracellular mcl-PHA degradation activity in *B. vietnamiensis* LMG 16232.

B. vietnamiensis LMG 16232 was subjected to transposon mutagenesis, and 50,000 colonies were screened for those with absent or reduced extracellular mcl-PHA degradation activity. Colonies showing reduced or no degradation activity were selected for further analysis. Selected mutants were grown individually and then grouped into two pools based on their mcl-PHA degradation activity (pool 1 for no activity, pool 2 for weak activity). Genomic DNA (gDNA) was extracted from each pool. The gDNA was prepared for Tn-Genome junction enrichment. The enriched DNA fragments were sequenced using Illumina MiSeq. The sequencing data were analyzed by mapping the reads to the *B. vietnamiensis* LMG 16232 genome. Figure 3.1 was created with https://biorender.com/.

The transconjugants were grouped into two pools. Pool 1 consisted of the 66 transconjugants that completely lost mcl-PHA degradation activity, while Pool 2 included the 18 transconjugants with severely reduced mcl-PHA degradation activity. To identify the transposon insertion sites, we chose Tn-seq, a method that simultaneously detects transposon-genome junctions in all 84 mutants through next-generation sequencing. An adapted Tn-seq method, Tn-seq circle (Gallagher et al. 2011), was used to enrich transposon-genome junctions and identify the insertion sites.

In pool 1, which consists of transconjugants that have completely lost their ability to degrade mcl-PHA, 34 transposons were mapped to chromosome 1. Of these, 27 transposons were inserted into 11 genes within a gene cluster that encodes a type II secretion system (P4G95_05485, P4G95_05490, P4G95_05495, P4G95_05500, P4G95_05505, P4G95_05510, P4G95_05515, P4G95_05520, P4G95_05525, P4G95_05530, P4G95_05535) (**Figure 3.2A**). Additionally, three transposons were mapped to the gene encoding the TetR/AcrR family transcriptional regulator (P4G95_00865), and three transposons were mapped to the gene encoding an A24 family peptidase (P4G95_07805). One transposon mapped to a gene encoding trehalose-6-phosphate phosphatase activity (P4G95_10885). From pool 1, three transposons were mapped to chromosome 2, where two of the transposons mapped to the lipase gene cluster of *B. vietnamiensis* LMG 16232, encoding for triacylglycerol lipase, *lip1* (P4G95_16805) and a lipase chaperone, *lipO* (P4G95_16815) (**Figure 3.2B**). Another transposon was mapped to a hypothetical protein (P4G95_20805). Furthermore, only one transposon was mapped to chromosome 3, annotated as *gspD*, encoding the secretin for the type II secretion system (P4G95_28980). However, since the insertion site of this transposon has the same sequence as the *gspD* gene found on chromosome 1, we speculate that this may be an artifact of the transposon mapping (**Table 3.4**).

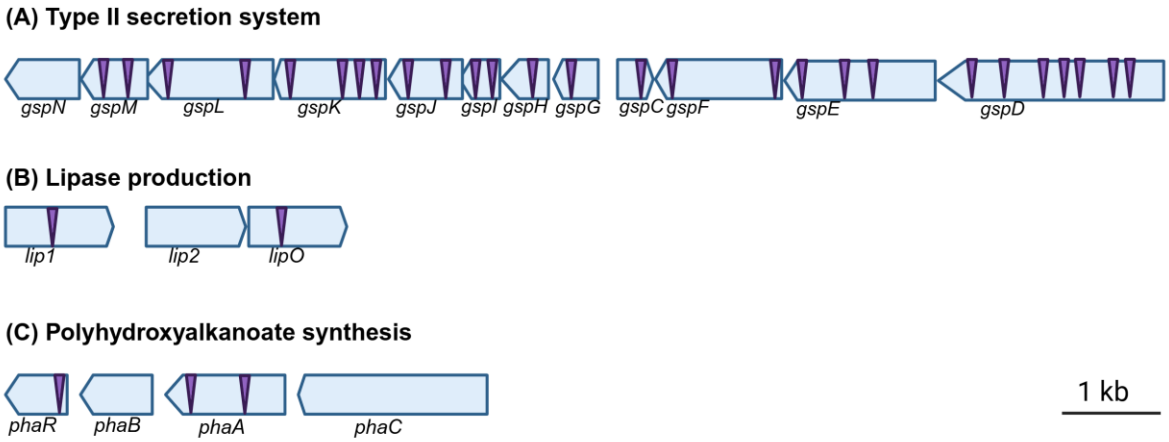


Figure 3. 2 Genetic Organization of the *B. vietnamiensis* LMG 16232 gene clusters that affect the extracellular mcl-PHA degradation upon interruption by transposon.

The purple triangle indicates transposon insertions that resulted in the complete loss or severe reduction of extracellular mcl-PHA degradation activity in *B. vietnamiensis* LMG 16232. (A) The type II secretion system of *B. vietnamiensis* LMG 16232 is arranged in a gene cluster containing 12 genes (P4G95_05480, P4G95_05485, P4G95_05490, P4G95_05495, P4G95_05500, P4G95_05505, P4G95_05510, P4G95_05515, P4G95_05520, P4G95_05525, P4G95_05530, P4G95_05535). All genes of the gene cluster are interrupted except for *gspN*. (B) lipase gene cluster consists of three genes, *lip1*, *lip2* and *lipO* (P4G95_16805, P4G95_16810, and P4G95_16815). Interruption of *lip1* and *lipO* by transposon abolishes *B. vietnamiensis* LMG 16232 ability to degrade extracellular mcl-PHA. (C) The polyhydroxyalkanoate synthesis gene cluster of *B. vietnamiensis* LMG 16232 consists of four genes, *phaR, phaB, phaA, and phbC* (P4G95_13560, P4G95_13565, P4G95_13570, and P4G95_13575). Transposon interruption on *phaR* and *phaA* severely reduces *B. vietnamiensis* LMG 16232 to degrade extracellular mcl-PHA. The genes are depicted to scale, as indicated by the bars on the right side of the panels. The putative function

of genes interrupted by the transposon is provided in Table 3.4. Figure 3.2 was created with https://biorender.com/.

Table 3. 4 Transposon mutant of *B. vietnamiensis* LMG 16232 with abolished (Pool 1) or reduced (Pool 2) extracellular mcl-PHA activity.

Chromosome location	Locus tag	Gene name	Putative function
Pool 1			
1	P4G95_00865	TetR/AcrR family transcriptional regulator CDS	TetR/AcrR family transcriptional regulator
1	P4G95_05485	gspM	type II secretion system protein M
1	P4G95_05490	gspL	type II secretion system protein GspL
1	P4G95_05495	gspK	type II secretion system minor pseudopilin GspK
1	P4G95_05500	gspJ/prepilin-type N-terminal cleavage/methylation domain-containing protein CDS	prepilin-type N-terminal cleavage/methylation domain-containing protein
1	P4G95_05505	gspI	type II secretion system minor pseudopilin GspI
1	P4G95_05510	GspH/FimT family pseudopilin CDS	GspH/FimT family pseudopilin
1	P4G95_05515	gspG	type II secretion system major pseudopilin GspG
1	P4G95_05520	general secretion pathway protein GspC CDS	general secretion pathway protein GspC CDS
1	P4G95_05525	gspF	type II secretion system inner membrane protein GspF
1	P4G95_05530	gspE	type II secretion system ATPase GspE
1	P4G95_05535	gspD	type II secretion system secretin GspD
1	P4G95_07805	A24 family peptidase CDS	A24 family peptidase
1	P4G95_10885	otsB CDS	trehalose-phosphatase
2	P4G95_16805	lip1/triacylglycerol lipase CDS	triacylglycerol lipase
2	P4G95_16815	lipO/lipase secretion chaperone CDS	lipase secretion chaperone
2	P4G95_20805	hypothetical protein CDS	hypothetical protein
3	P4G95_28980	gspD CDS	type II secretion system secretion GspD
Pool 2			
1	P4G95_03530	nagA	N-acetylglucosamine-6-phosphate deacetylase

1	P4G95_05495	gspK	type II secretion system minor pseudopilin GspK
1	P4G95_05505	gspI	type II secretion system minor pseudopilin GspI
1	Between P4G95_05555 and P4G95_05560	Between mnmC and cation: proton antiporter CDS	cation: proton antiporter
1	P4G95_05570	MarR family winged helix-turn-helix transcriptional regulator CDS	MarR family winged helix-turn-helix transcriptional regulator
1	P4G95_06510 and P4G95_06515	paaK and paaJ CDS	phenylacetate-CoA oxygenase/reductase subunit PaaK and phenylacetate-CoA oxygenase subunit PaaJ
1	P4G95_13560	phaR	polyhydroxyalkanoate synthesis repressor PhaR
1	P4G95_13570	phaA/acetyl-CoA C-acetyltransferase CDS	acetyl-CoA C-acetyltransferase
1	Between P4G95_15285 and P4G95_15290	Between cupin domain-containing protein CDS and hypothetical protein	
2	P4G95_16325	helix-turn-helix domain-containing protein CDS	helix-turn-helix domain-containing protein
2	P4G95_20810	hypothetical protein CDS	hypothetical protein
3	Between P4G95_29770 and P4G95_29775	Between porin CDS and helix-turn-helix domain-containing protein CDS	

For the transconjugants with weak activity (pool 2), ten transposons are mapped to chromosome 1. These include: *nagA* (P4G95_03530), encoding for N-acetylglucosamine-6-phosphate deacetylase; *gspK* (P4G95_05495), encoding for type II secretion system minor pseudopilin GspK; *gspI* (P4G95_05505), encoding for type II secretion system minor pseudopilin GspI; the intragenic region between downstream of *mnmC*, and upstream of a cation: proton antiporter CDS (Between P4G95_05555 and P4G95_05560); MarR family winged helix-turn-helix transcriptional regulator CDS (P4G95_05570); the intragenic region between *paaK* and *paaJ* (Between P4G95_06510 and P4G95_06515), which encoded for phenylacetate-CoA oxygenase subunit PaaJ and paaK. Additionally, three transposons mapped to the Pha gene cluster, one transposon mapped to *PhaR* (P4G95_13560), the polyhydroxyalkanoate synthesis repressor, while another two transposons mapped to *phaA* (P4G95_13570), which encodes for Acetyl-CoA acetyltransferase involved in the biosynthesis of polyhydroxybutyrate (**Figure 3.2C**). The last transposon from chromosome 1 was mapped to an intragenic region between a gene that encodes for a cupin domain-containing protein and a hypothetical protein (Between P4G95_15285 and P4G95_15290). Two transposons are mapped to chromosome 2, corresponding to genes that encode a helix-turn-helix domain-containing protein CDS (which functions as a transcriptional activator) (P4G95_16325) and a hypothetical protein (P4G95_20810), respectively. Moreover, two transposons are located in intragenic regions between a porin CDS and helix-turn-helix domain-containing protein CDS in chromosome 3 (Between P4G95_29770 and P4G95_29775) (**Table 3.4**).

Based on the information we gathered from Tn-seq, we can deduce that the enzyme that is responsible for extracellular mcl-PHA is triacylglycerol lipase, *lip1* (P4G95_16805), and this activity could be affected by four transcriptional regulators in *B. vietnamiensis* LMG 16232, which are TetR/AcrR family transcriptional regulator (P4G95_00865), MarR family winged helix-turn-helix transcriptional regulator CDS (P4G95_05570), *PhaR* (P4G95_13560), the

polyhydroxyalkanoate synthesis repressor, and helix-turn-helix domain-containing protein CDS (P4G95_16325). The lipase is encoded by *lip1* (P4G95_16805) and contains a predicted secretion signal peptide, which directs the protein into the secretory pathway. During secretion, this signal peptide is likely to be cleaved by an A24 family peptidase (P4G95_07805). In the periplasm, the lipase chaperone *lipO* (P4G95_16815) may assist in folding and activating the lipase prior to secretion (Hobson et al. 1993). Finally, the lipase is predicted to be excreted into the extracellular space via the type II secretion system (P4G95_05485, P4G95_05490, P4G95_05495, P4G95_05500, P4G95_05505, P4G95_05510, P4G95_05515, P4G95_05520, P4G95_05525, P4G95_05530, P4G95_05535). However, direct experimental validation, such as secretion assays or protein interaction studies, will be required to confirm this pathway. There are a few elements that we obtained from Tn-seq where the relationship with extracellular mcl-PHA degradation in *B. vietnamiensis* LMG 16232 is unknown, including trehalose-6-phosphate phosphatase activity (P4G95_10885), hypothetical proteins (P4G95_20805 and P4G95_20810), N-acetylglucosamine-6-phosphate deacetylase, *nagA* (P4G95_03530), Phenylacetate-CoA oxygenase/reductase subunit PaaK and PaaJ (P4G95_06510 and P4G95_06515) and Acetyl-CoA acetyltransferase PhaA (P4G95_13570).

3.4.3 Characteristic of mcl-PHA degrading enzyme in *B. vietnamiensis* LMG 16232 predicted via *in silico* analysis

Some lipases from various organisms are known to be capable of degrading polymers, such as polycaprolactone, polyethylene terephthalate, and mcl-PHA (Jaeger et al. 1995; Mohanan et al. 2020). In the genome of *B. vietnamiensis* LMG 16232, there are three genes putatively associated with lipase function: P4G95_16805 and P4G95_16810, both coding for triacylglycerol lipase, and P4G95_14150, coding for a lipase family protein. While these candidate genes could encode the enzyme for mcl-PHA degradation, from transposon mutagenesis, all the transconjugants from pool 1 have completely lost the ability to degrade

mcl-PHA. One of the genes that got inactivated is a gene annotated as triacylglycerol lipase (locus tag: P4G95_16805, protein ID: WHU94860.1, EC 3.1.1.3). The sequence of this triacylglycerol lipase shows common features to those previously identified enzymes that can degrade extracellular mcl-PHA, such as containing a signal peptide and a catalytic triad composed of a serine (embedded in a lipase box motif), histidine and aspartic acid (Knoll et al. 2009). This enzyme is predicted to have 364 amino acids, with a calculated molecular weight of 37.6 kDa and a theoretical isoelectric point (pI) of 6.43, computed with Expasy (Gasteiger et al. 2005). The computed molecular mass and isoelectric point are in the range of currently known mcl-PHA depolymerase, where the molecular range is approximately 25 to 41 kDa, and the pI value is mostly in the acidic range (Papaneophytou et al. 2011). This enzyme was predicted via SignalP 5.0 to be secreted via secretory signal peptides transported by the Sec translocon and cleaved by Signal Peptidase I (Lep) with a probability of 0.83. Signal peptidase I is essential in many bacterial functions, and it could be the reason why the *LepB* (P4G95_10750) in *B. vietnamiensis* LMG 16232 was not interrupted by the transposon. Cleavage site position was predicted between 43-44 with a probability of 0.5069. The occurrence of a motif (G-H-S-Q-G) in the amino acid sequence agrees with the lipase box consensus sequence that could also be found in previously identified in a novel subgroup of extracellular mcl-PHA depolymerase identified from Actinobacteria, as those from *S. roseolus* and *S. venezuelae,* and *S. exfoliates* (Gangoiti et al. 2012; Santos et al. 2013; Martínez et al. 2015), in contrast of those that are identified from the genus *Pseudomonas* (Schirmer and Jendrossek 1994; Kim et al. 2005; Rhee et al. 2006), as well as in *Bdellovibrio* (Martínez et al. 2012), where the lipase consensus sequence is (G-I-S-S-G) (Knoll et al. 2009). However, this putative protein sequence shows very little sequence similarity to currently known enzymes, which can degrade mcl-PHA from the genus *Streptomyces*, *Pseudomonas*, and *Bdellovibrio,* where there is only 9 to 12 % sequence identity (**Figure 3.3**). The enzyme also has a putative

catalytic amino acid (Ser131-Asp308-His330). These characteristics suggest that this gene codes for a lipase that is also a putative extracellular mcl-PHA depolymerase in *B. vietnamiensis* LMG 16232.


WHU94860.1 MVRSMRSRV----------VAAAVACAMSGAQFAGTTAVM 30
AFQ93688.1 ---------- 0
AFQ93689.1 ---------- 0
CAE81078.1 ----MKKLLAGVFGVVAMSLSAQAAKKASNCEVT----GLVDRMTCPYLEKL-VSGP-HL 50
AAA64538.1 --MPLRTLLCGLLLAVCLGQHALA---ASRCSERPRTLLRPAEVSCSYQSTWLDSGL-VG 54
WHU94860.1 TLATTHAATAATAATDDYAATRYPVILVH-GL-TGTDKYA---GVL-EYW--YGIQEDLQ 82
AFQ93688.1 ----VHTF-YH-PRAMGASGERHPVVIW----------GNGTGAVPGIY--SSLLRHWA 41
AFQ93689.1 ----VHTF-YH-PRSMGASGERHPVVIW----------GNGTGAVPGIY--SSLLRHWA 41
CAE81078.1 ---TRHVK-YSLPKGKTPKA-GWPTVILYQGSLFPVE-FSRSSLMIAGGYNEIRLIQTLL 104
AAA64538.1 ---QRKII-YQTPLGTPPAG-GWPVVLIYQGSFFPLNDFSYHSNLPFGGYYEGKLVQNLL 109
WHU94860.1 RHGATVY----------VANLSGFQSD----DGPNGRGEQLLAYVKTVLAATGATKVNLI 128
AFQ93688.1 SHGFIVAAANTPTSNFALS----------MRAGIDVLERRNADPGSEYFGRVDLARIGSA 91
AFQ93689.1 SHGIIVAAANTPTSNFAIS----------MRAGIDVLERRNADPGSEYFGRVDLEHIGSA 91
CAE81078.1 DSGFAVIAPPAIEGVAWMTNIVGI--DYDTSEDFYFVEELLVAMGNGEFGKLNMDRLYAT 162
AAA64538.1 DHGYAVIAPSAPADLFWQTNIPGLAQAYELSTDYDFLGNVLAAIASGHFGPLNAQRQYAT 169
WHU94860.1 GHSQGGLTSRYVAAVAPDLVASVTTIGTPHRGSEFADFVQSVLAYDPTGLSSSVIATFFN 188
AFQ93688.1 GHSQGGAAAVNAAVDAR-VDTAVPIQ-----PG--------PL-----TDP--------- 123
AFQ93689.1 GHSQGGAAAVNAAIDAR-VDTAVPIQ-----PG--------PL-----TDP--------- 123
CAE81078.1 GISSGGYHSSRMAVAFPGVFKALAVH-----SASYADCGG-PMCFVPAQVP--------- 207
AAA64538.1 GISSGGYNTSRMAVSFPGKFRALAVQ-----SGSYATCSG-PLCVVPDQLP--------- 214
WHU94860.1 VFGILTSSSNNTNQDALAALKTLTTSQAAAYNQNYPSAGLGAPGSCQTGAPTETVGGNTH 248
AFQ93688.1 ----------DLTGVPVFY------ 132
AFQ93689.1 ----------DLTDVPMFY------ 132
CAE81078.1 ----------ENHPPTIF------ 215
AAA64538.1 ----------ADHPPTLF------ 222
WHU94860.1 LLYSWAGTAIQPTVSMFGVTGAKDVSTIPVIDPANALDLSTLALLGTGTVMINRGAGQND 308
AFQ93688.1 ----------LAGERDLTVWPAL----VKALYRDSD---------- 154
AFQ93689.1 ----------LAGQRDLTVWPAL----VKALYRDSS---------- 154
CAE81078.1 ----------LHGRLDPVV-PVR----TMYPYHETL---------- 236
AAA64538.1 ----------LHGFVDAVV-PWW----SMDLYYDRL---------- 243
WHU94860.1 GLVSKCSALYGQVLGTRYKWNHLDEINQLLGVRGAYAEDPVAVIRTHANRLKLAGV 364
AFQ93688.1 ----HLPAVYGEVRGAGHLS--------SIGDGGDFRAPT-TA---------- 184
AFQ93689.1 ----HLPAVYGEVRGAGHLS--------SIGDGGDFRAPT-T---------- 183
CAE81078.1 ----KNQG----VETEMFVS--------PWARHEWLEEAPELITNWFINHK----- 271
AAA64538.1 ----LHQG----IETARYTE--------PLGGHEWFAASPGKVLAWFNAHP----- 278

Figure 3. 3 Amino acid sequence alignment of putative lipase that is able to degrade extracellular mcl-PHA depolymerase of *B. vietnamiensis* LMG 16232 (protein ID: WHU94860.1) with other mcl-PHA depolymerase sequences.

The sequences analyzed include those from *Streptomyces roseolus* (GenBank: AFQ93688.1), *Streptomyces venezuelae* (GenBank: AFQ93689.1), *Bdellovibrio bacteriovorus* HD100 (GenBank: CAE81078.1), *Pseudomonas fluorescens* (GenBank: AAA64538.1). The lipase box consists of the pentapeptide sequence (G-X1-S-X2-G), which is indicated in the red box. The signal peptide of *B. vietnamiensis* LMG 16232 was predicted by the SignalP (version 5.0) program (purple box). The main putative catalytic amino acids Ser131-Asp308-His330 of *B. vietnamiensis* LMG 16232, predicted with Phyre 2, are marked with a dark blue box.

3.4.4 Validation of genetic elements responsible for mcl-PHA degradation identified from transposon mutagenesis

To validate the genetic elements involved in extracellular mcl-PHA degradation activity obtained with transposon mutagenesis, we created insertional mutants using RhaCAST and investigated the phenotypes. RhaCAST is a genetic tool we recently developed for targeted insertional mutagenesis in *Burkholderia cepacia* complex and previously applied to *B. cenocepacia* and *B. multivorans.* In this work, we have applied RhaCAST in *B. vietnamiensis* LMG 16232 for the first time. We targeted genes that encode for the putative lipase (P4G95_16805), A24 family peptidase (P4G95_07805), TetR/AcrR family transcriptional regulator (P4G95_00865), trehalose-phosphatase (P4G95_10885), and a gene from type II secretion system, *gspE* (P4G95_05530) to validated the phenotype obtained from transposon mutagenesis (**Figure S2-S6**). These mutants did not produce a halo around the mutant strain in an agar plate containing mcl-PHA (**Figure 3.4**).

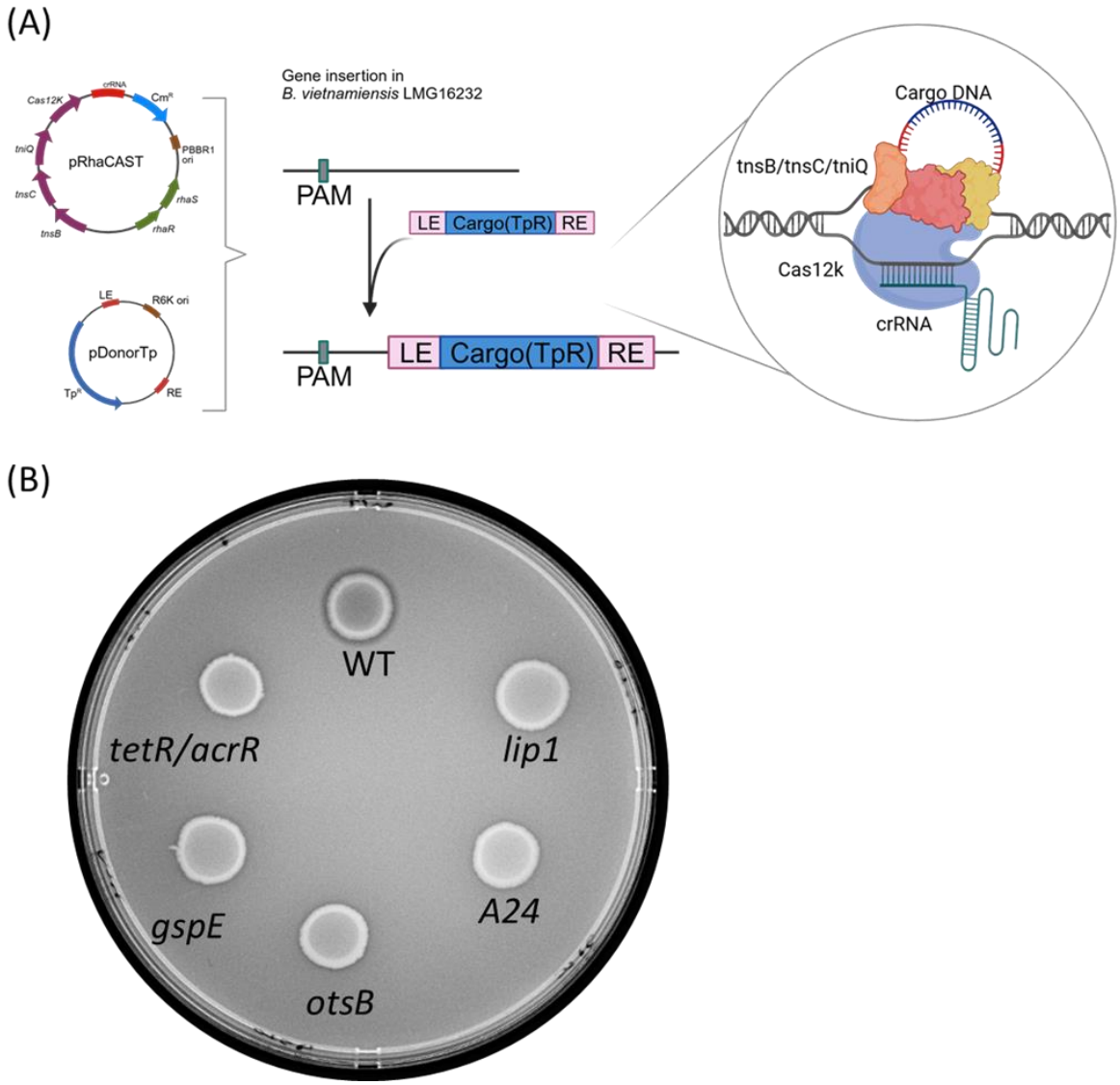


Figure 3. 4 Targeting genes involved in mcl-PHA degradation in *B. vietnamiensis* LMG 16232 abolish the strain's ability to degrade mcl-PHA.

(A) Schematic model of RNA-guided DNA transposition by RhaCAST applied to *B. vietnamiensis* LMG 16232. The two plasmids of the RhaCAST system, pRhaCAST and pDonorTp, encode all the necessary components, tnsB, tnsC, tniQ, Cas12k, crRNA scaffold, and the cargo gene (TpR) that is flanked by the transposon left end (LE) and right end (RE). (B) The ability to degrade mcl-PHA was ablated by CAST targeting triacylglycerol lipase CDS, A24 family peptidase CDS, *otsB, gspE,* TetR/AcrR family transcriptional regulator CDS in LMG 16232 Wild-type (WT). This figure shows a representative plate of the mcl-

PHA degradation assay of three biological replicates in duplicates. Figure 3.4A was created with https://biorender.com/.

To further confirm if the halo of degradation observed resulted from the putative lipase is mcl-PHA degradation, we took a disk underneath the inoculated mutant, *lip1::CAST-Tp* and wild type as control from the agar-based assay. We determined the absence and presence of PHO in the agar with gas chromatography with flame ionization detection (GC-FID). As expected, no PHO was detected in the agar beneath the WT strain, whereas PHO was detected under the *lip1*::CAST-Tp strain, indicating that PHO was not being degraded (**Figure 3.5**).

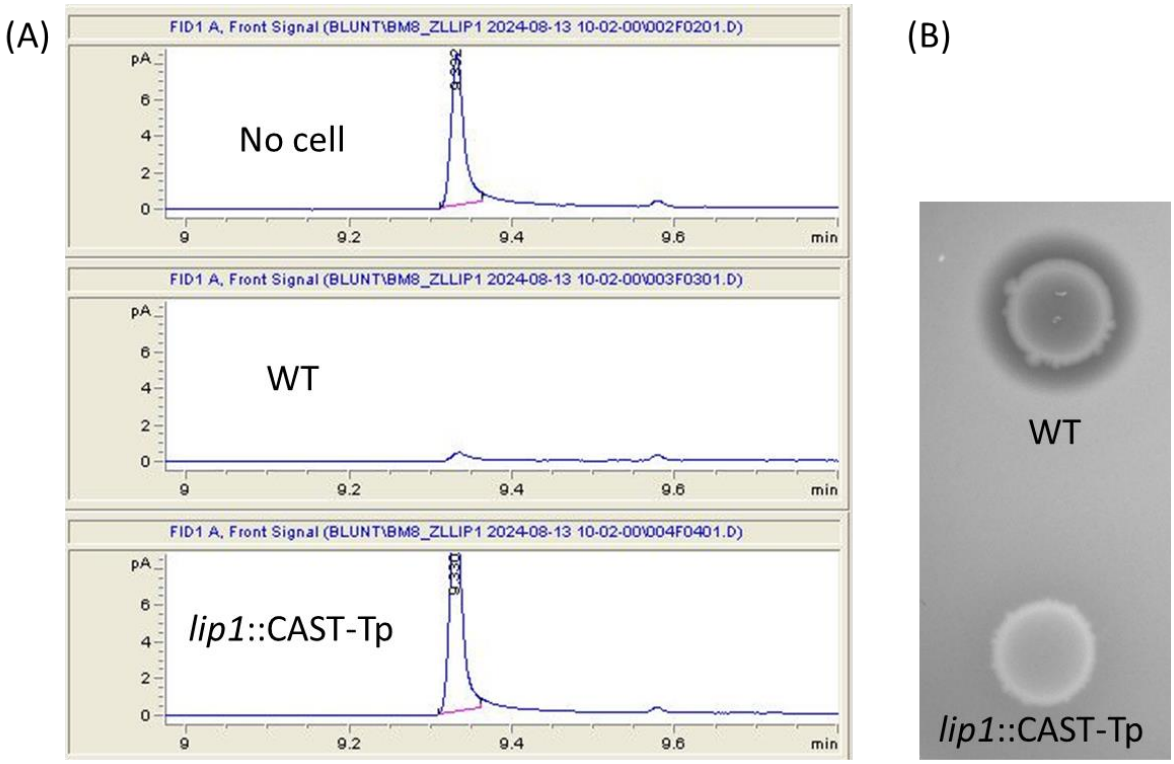


Figure 3. 5 Targeting the putative *lipase* gene (locus tag: P4G95_16805) in *B. vietnamiensis* LMG 16232 abolishes the ability to degrade mcl-PHA.

(A) The absence or presence of PHO in the agar after strain inoculation was determined with gas chromatography with flame ionization detection (GC-FID). Samples were obtained by cutting an agar disk under the strain. For control, a disk was cut at an area of the agar where no cell was inoculated. The peak at ~9.3 minutes retention time corresponds to PHO, which can be observed at the no cell control (Top). The absence of a peak corresponds to PHO in WT, and the presence of PHO in *lip1::CAST-Tp* supports the phenotypic test. (B) Strains were grown on an agar plate containing Nile red and PHO and visualized under UV irradiation. Inoculation of wild type (WT) results in a clear halo around the strain, whereas the inoculation of the mutant *lip1::CAST-Tp* does not have a halo around the strain.

To determine if *B. vietnamiensis* LMG 16232 putative lipase and the genes that we choose to make an insertional mutant are involved in mcl-PHA degradation are also involved in lipid degradation, we tested the ability of *B. vietnamiensis* LMG 16232 and the mutants in tributyrin degradation. The wild type *B. vietnamiensis* LMG 16232 exhibits the highest activity against tributyrin. The mutant *lip1::CAST-Tp* exhibits reduced activity in degrading tributyrin, suggesting other lipases or esterases might be produced and secreted. By disrupting *gspE*, which is part of the gene cluster encoding for the type II secretion system, the mutant (*gspE::CAST-Tp*) showed complete abrogation of tributyrin degradation, indicating that the lipases or esterases might be produced and secreted via type II secretion system. Disrupting the gene encoding for A24 family peptidase also completely abolishes tributyrin degradation, suggesting that the lipases or esterases responsible for tributyrin degradation are extracellular enzymes with a leader peptide. For the TetR/AcrR family transcriptional regulator insertional mutant, the ability to degrade tributyrin was reduced to residual activity (**Figure 3.6**).

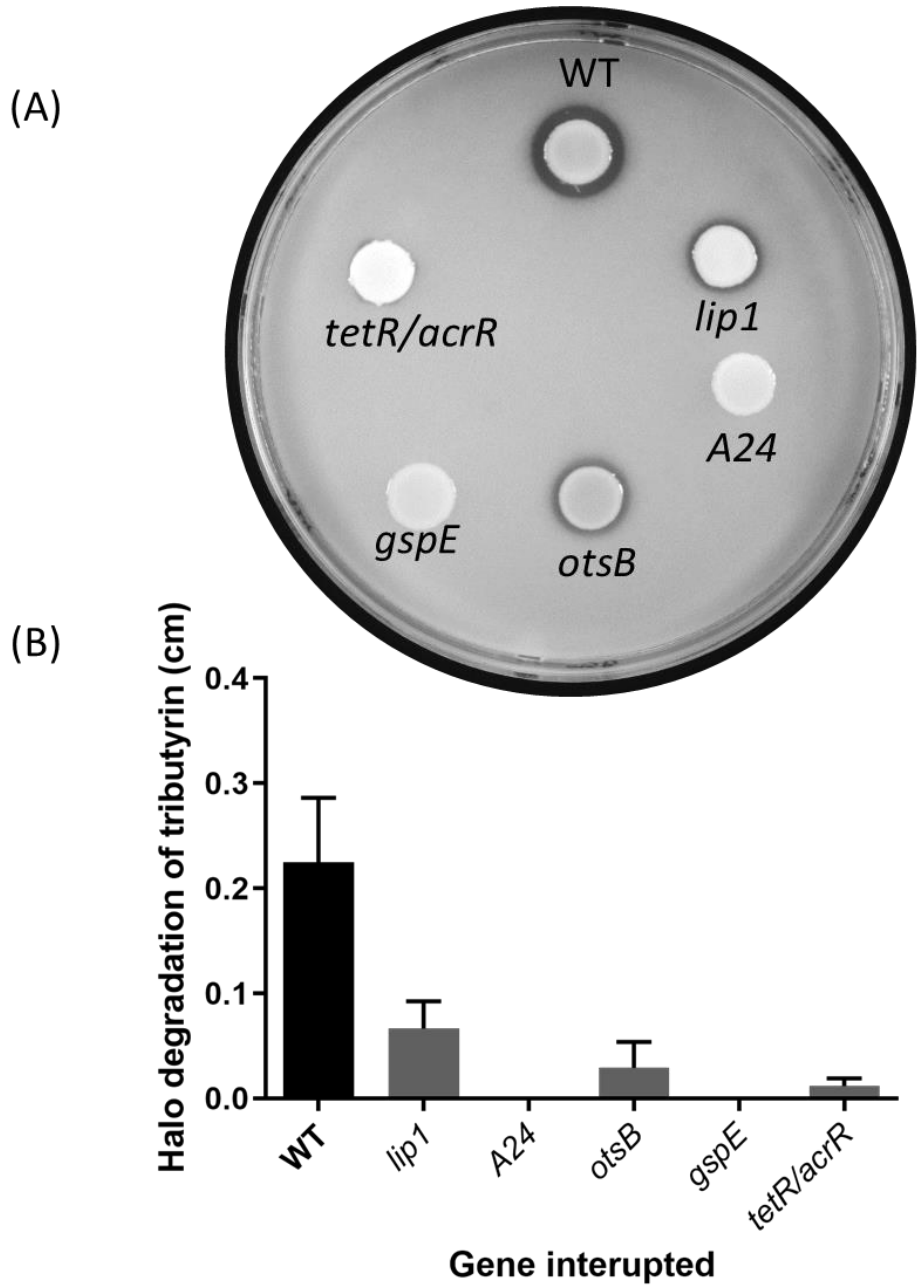


Figure 3. 6 Targeting genes involved in mcl-PHA degradation in *B. vietnamiensis* LMG 16232 affects the ability to degrade tributyrin.

A) Representative plate of tributyrin degradation assay; B) Diameter of the halos degradation in (A). The ability to degrade tributyrin was ablated by CAST targeting triacylglycerol lipase CDS, A24 family peptidase CDS, *otsB, gspE,* TetR/AcrR family transcriptional regulator CDS in LMG 16232 wild-type (WT). Data is representative of two biological replicates repeated in technical triplicate.

3.5 Discussion

The production and use of bioplastic, including mcl-PHA, has increased recently. These materials are considered alternatives to petroleum-based plastics because they can be derived from renewable resources and have a wide range of applications (Muneer et al. 2020). Despite growing interest, microorganisms and enzymes capable of degrading mcl-PHA remain relatively understudied (Viljakainen and Hug 2021). Extracellular mcl-PHA depolymerases have been found in various genera, including *Pseudomonas* (Schirmer and Jendrossek 1994; Kim et al. 2005; Rhee et al. 2006), *Bdellovibrio* (Martínez et al. 2012), *Thermus* (Papaneophytou et al. 2011) and *Streptomyces* (Gangoiti et al. 2012; Santos et al. 2013; Martínez et al. 2015). However, to date, the mechanism of action for extracellular mcl-PHA by microorganisms has not been thoroughly explored. Here, we report that several *Burkholderia* strains, including *B. gladioli*, *B. multivorans*, and *B. vietnamiensis*, can degrade mcl-PHA. Through transposon mutagenesis combined with Tn-seq analysis, we identified genetic elements associated with mcl-PHA degradation in *B. vietnamiensis* LMG 16232. We further validated some of these genetic elements by generating insertional mutants using a CRISPR-associated transposase system (CAST) in extracellular mcl-PHA degradation activity. Our findings indicate that the enzyme responsible for extracellular mcl-PHA degradation is a lipase with wider range of substrates.

A technique commonly used to enhance the visualization of mcl-PHA degradation involves incorporating Nile red, a lipophilic fluorescent dye, into agar plates (Mohanan et al. 2022). Thus, we adopted this visualization method in our screening media to increase sensitivity. In comparison to other studies, where the degradation of extracellular mcl-PHA can be observed within 2 to 3 days, *Burkholderia vietnamiensis* LMG16232 exhibited a slower degradation process, requiring approximately 7 days for observable activity. Some strains of *Burkholderia* from the initial screening showed weak activity, with degradation taking up to

20 days, despite the use of Nile red to enhance detection. Nevertheless, by implementing this visualization technique and alongside transposon mutagenesis in *B. vietnamiensis* LMG 16232, we were able to screen 50,000 individual colonies in a rapid manner. This approach enabled us to identify transconjugant colonies that had lost the ability to degrade mcl-PHA, providing a sensitive and efficient screening method. This method may be applicable to other polymers that can be stained with suitable dyes, enhancing assay sensitivity.

According to the data on PHA depolymerase engineering database, several species of *Burkholderia,* including *Burkholderia thailandensis, Burkholderia ambifaria, Burkholderia graminis*, *Burkholderia cenocepacia*, *Burkholderia dolosa*, *Burkholderia multivorans*, *B. vietnamiensis* and *Burkholderia oklahomensis* have genes encoding proteins putatively capable of degrading extracellular scl-PHA (Knoll et al. 2009). While *B. cepacia* DP1 has been shown to degrade extracellular scl-PHA (Nor Azura Azam et al. 2018; Azura Azami et al. 2019), there are no reports of *Burkholderia* species that degrade extracellular mcl-PHA. Thus, this study represents the first evidence of *Burkholderia*'s capability to degrade extracellular mcl-PHA.

The results of this work indicated that the putative lipase gene, *lip1* from *B. vietnamiensis* LMG 16232, encodes an enzyme that degrades mcl-PHA. It was known that *Burkholderia* is a well-known lipase producer, and those lipases are capable of degrading various compounds. For example, lipases from *Burkholderia* MC 16-3 (GenBank: AY772173) and 99-2-1 (GenBank: AY772174) can degrade methyl(R)-N-(2,6-dimethyl-phenyl)alaninate (Park and Lee 2005). Additionally, lipase from *B. cepacia* PBSA-1 (GenBank: EF189714.1) has been shown to degrade poly(butylene succinate-co-butylene adipate) (Lee and Kim 2010), while *B. cepacia* lipase can degrade Polycaprolactone (PCL) (Jaeger et al. 1995). These lipases, including the one identified in this work, share a conserved lipase consensus sequence of G-H-S-Q-G, resembling the oxyanion hole consensus sequence. Enzymes that degrade extracellular mcl-PHA exhibit similar characteristics to extracellular lipases, including the presence of the

lipase box and a conserved non-catalytic histidine near the oxyanion hole (Jaeger et al. 1995; Jendrossek and Handrick 2002; Knoll et al. 2009). Lipases are known for catalyzing the hydrolysis of carboxyl-ester bonds in triglycerides, such as oil and fats, breaking them down into free fatty acids and glycerol (Gupta et al. 2004). Bacteria genera, such as *Bacillus*, *Pseudomonas* and *Burkholderia* (Rathi et al. 2001), are well-known producers of lipases (Gupta et al. 2004). Consequently, this study suggests that the mcl-PHA degrading enzymes from *Burkholderia* are lipases that also possess the capability to degrade mcl-PHA.

In this work, transposon mutagenesis combined with Tn-seq on *B. vietnamiensis* LMG 16232 identified the genetic elements involved in the degradation of mcl-PHA, which can be broadly characterized into three main groups: a) lipase/chaperone gene cluster, b) components of type II secretion system, and c) regulatory elements. Based on this information, we hypothesize that the putative extracellular lipase, Lip1, is the enzyme responsible for extracellular mcl-PHA depolymerase activity. The genetic elements associated with the mcl-PHA degradation in *B. vietnamiensis* LMG 16232 are consistent with the findings in various *Burkholderia* lipases, particularly regarding the production and secretion of extracellular lipase. It is well established that *Burkholderia* extracellular lipases are secreted through the type II secretion system. In this process, the N-terminal signal peptide is transported across the inner membrane via the Sec secretion system. Once in the periplasm, a chaperone interacts with the lipase, facilitating the formation of the active form of the lipase (Khattabi et al. 2000; Knapp et al. 2015). This work also supports that the extracellular lipase of *Burkholderia* depends on a dedicated chaperone. A previous study on *Burkholderia glumae* has demonstrated that the chaperone resembles the propeptide of protease (Khattabi et al. 2000). Similar to the lipases in *B. cepacia* and *B. glumae,* the putative lipase responsible for degrading mcl-PHA from *B. vietnamiensis* LMG 16232 is predicted to have an N-terminal signal as well as a chaperone situated downstream of the putative lipase gene to help the correct folding and efficient

secretion (Frenken et al. 1993b; Wang et al. 2009). This putative enzyme is likely secreted via the general secretion pathway (GSP), also known as the type II secretion system, which relies on a signal sequence for translocation. This mechanism is similarly predicted for the excretion of the enzyme that degrades extracellular mcl-PHA (Martínez et al. 2012). One of the putative regulatory elements identified in this work is the TetR/AcrR family transcriptional regulator CDS (P4G95_00865). This regulator is widely distributed among bacteria and controls various cellular processes, including the metabolism of lipid compounds, such as the synthesis and degradation of fatty acid and the storage of polymer (Cuthbertson and Nodwell 2013). The involvement of other regulatory elements, such as HTH-type transcriptional activators and a PHA synthesis repressor, suggests that the extracellular mcl-PHA degradation activity of *B. vietnamiensis* LMG 16232 may be integrated with other metabolic pathways. While we did not identify a specific genetic element directly responsible for the uptake of mcl-PHA, we propose that mcl-PHA enters the cell through passive diffusion. This hypothesis is based on the structural similarity between mcl-PHA monomers and fatty acids, which both contain a hydrophobic alkyl chain (Kniewel et al. 2017). Medium-chain fatty acids (C_7-C_{11}) can enter bacteria through simple diffusion without the involvement of active transport systems or an unknown mechanism (Black and DiRusso 1994; Jimenez-Diaz et al. 2017) (**Figure 3.7**).

Overall, this study provides new insight into the degradation of extracellular mcl-PHA by the genus *Burkholderia*. This information could guide future directions involving enzyme purification and site-directed mutagenesis to optimize lipases for efficient bioplastic degradation or to develop synthetic enzymes for biotechnological processes. Although this work has identified key genes involved in mcl-PHA degradation, further studies are necessary to characterize their specific biochemical roles and regulatory pathways.

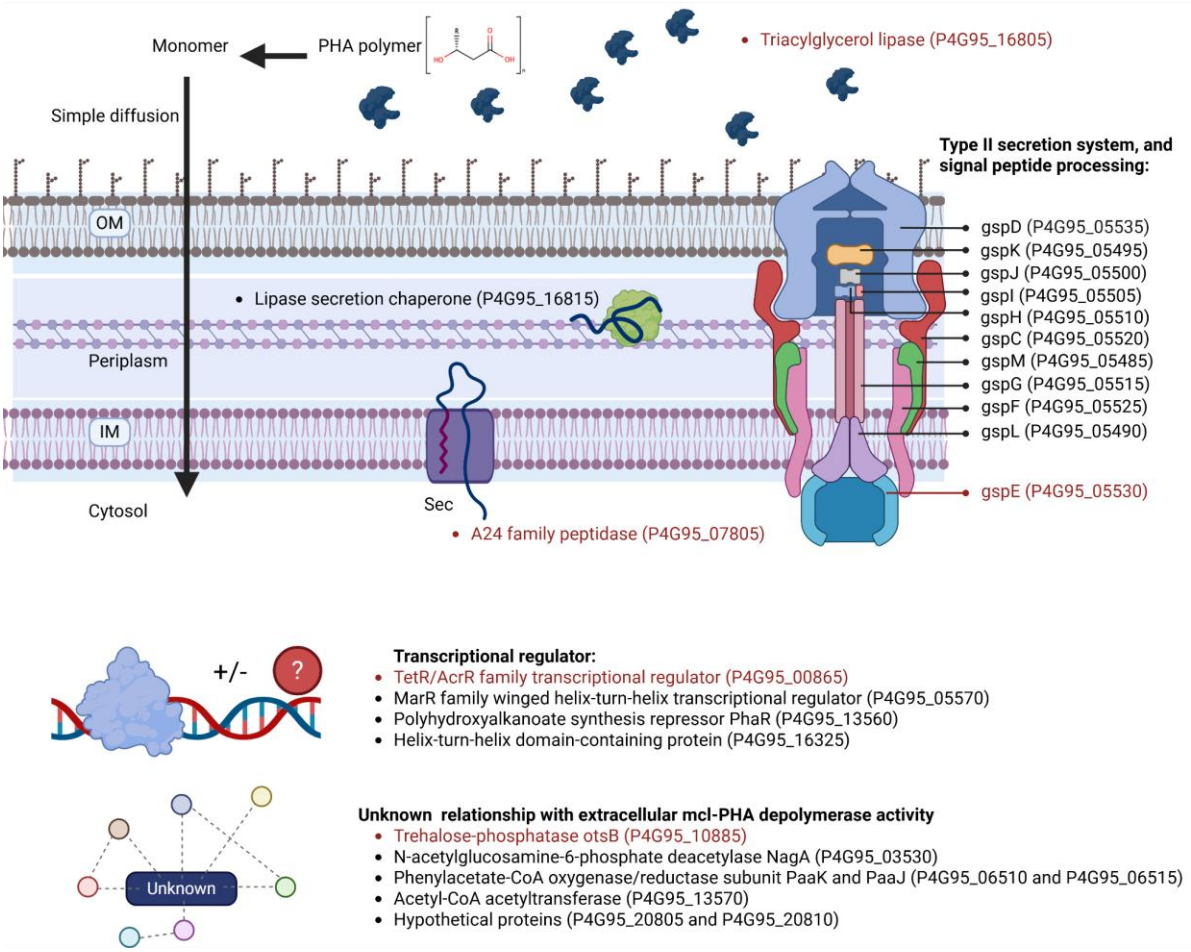


Figure 3. 7 Proposed model of components involved in *B. vietnamiensis* LMG 16232 extracellular mcl-PHA degradation activity.

The elements in this model were deduced from the transconjugants that either lost or showed severely reduced extracellular mcl-PHA depolymerase activity due to transposon insertion. The components where the text is in red have been verified via the creation of insertional mutagenesis using RhaCAST. The regulatory elements influencing this activity are TetR/AcrR family transcriptional regulator (P4G95_00865), Polyhydroxyalkanoate synthesis repressor (P4G95_13560) and HTH-type regulators (P4G95_05570 and P4G95_16325). The Sec system is responsible for transporting the unfolded protein into the periplasm, as the protein is predicted to contain a sec tag. The putative lipase chaperone (P4G95_16815) is responsible for folding the putative lipase into a mature protein and

excreting it to the outside of the cell via the type II secretion system. *B. vietnamiensis* LMG 16232 extracellular mcl-PHA degradation activity is also affected by the transposon interruption in genetic elements related to polyhydroxyalkanoate production and several genes involved in metabolism. Figure 3.7 was created with https://biorender.com/.

CHAPTER 4: DISCUSSION AND CONCLUSION

The *Burkholderia* genus presents a dual nature, being a “friend and foe” due to its dual nature. Some species within this genus can cause opportunistic infections in humans, while others exhibit lots of potential in biotechnological applications due to their vast metabolic capabilities. These capabilities include the production of novel enzymes and the degradation of various substrates (Eberl and Vandamme 2016; Morya et al. 2020). However, members of *Burkholderia* have the possibility of causing disease, thus hindering their broader use. To fully harness the advantages of this genus, it is crucial to deepen our understanding of the gene-to-function connection that governs their traits, which will allow us to maximize desirable characteristics while mitigating associated risks. Thus, genetic tools are vital for elucidating gene function and manipulating *Burkholderia* species. With the molecular biology tools available, many gene-to-function links of *Burkholderia* have been uncovered, increasing our understanding of this genus. This thesis focuses on the development and application of genetic tools for *Burkholderia* for biotechnology and bioremediation, with bioplastic degradation, specifically mcl-PHA, as an illustrative example and proof of principle.

Significant advancements in genetic editing technology for this non-model organism have been achieved despite the challenges of working on *Burkholderia* genetics. Techniques such as site-directed mutagenesis allow for marker-less gene deletions and knockdowns, plasmids and gene expression systems for gene complementation, and whole-genome approaches like random transposon-based mutagenesis have been employed. However, current site-directed genome editing tools rely on homologous recombination, which requires cloning long homology arms. Additionally, Tn7-based tools for genomic integration are restricted to the specific site(s). These limitations highlight the need for better molecular biology tools, specifically for *Burkholderia* species.

Motivated by reports on CRISPR-associated transposases being developed into genetic tools for targeted DNA sequence integration without the need for homologous recombination, as first demonstrated in *E. coli* (Strecker et al. 2019; Klompe et al. 2019), I reasoned that this approach could be adapted for *Burkholderia*. Thus, the first objective of this thesis was to develop a CRISPR-associated transposon system for *Burkholderia*, named RhaCAST. This targeted DNA insertion platform, based on a CRISPR-associated transposase, is driven by a rhamnose-inducible promoter that enables both loss- and gain-of-function applications. It also features marker excision and reuse capabilities, which enhance its utility for iterative genetic manipulations (Yap et al. 2024, see Chapter 2). This aspect is important for creating complex genetic modifications requiring multiple gene deletions or insertions. RhaCAST has been successfully applied in *B. cenocepacia* K56-2 and *B. multivorans* ATCC17616, demonstrating its versatility across different *Burkholderia* strains. I further extended its application to another species, *B. vietnamiensis* LMG 16232, validating the genetic elements responsible for the degradation of extracellular mcl-PHA as part of the third objective of this thesis.

Although the development of RhaCAST increases the genetic toolkit available for *Burkholderia*, several areas still require further investigation. For instance, while RhaCAST was successfully used in three *Burkholderia* species in this thesis, additional testing across a broader range of species is necessary to enable the use of this system in other species. Moreover, exploring multiplexing capabilities for the simultaneous editing of multiple genes or integrating RhaCAST with other genetic tools, such as CRISPRi, could further broaden its application. Overall, I anticipate that the development of RhaCAST for *Burkholderia* will facilitate precision gene editing, linking genotype to phenotype.

Members of the *Burkholderia* genus are known for their extensive catabolic abilities and the production of a wide range of enzymes that can break down various substrates for carbon utilization (Vial et al. 2007). This characteristic suggests that they may effectively degrade

polymers, including bioplastics, making *Burkholderia* a promising candidate for exploring bioplastic degradation.

Given the expected rise in global production of medium-chain-length polyhydroxyalkanoates (mcl-PHA) (Viljakainen and Hug 2021), it is crucial to identify microbes capable of degrading mcl-PHA, understand the enzymes they produce, and uncover the related genes for sustainable bioplastic management. Therefore, the second objective of this thesis was to investigate extracellular mcl-PHA degradation capacities in *Burkholderia*. To achieve this, I used a medium designed to enhance the visualization of mcl-PHA degradation and screened a panel of *Burkholderia* strains from the Cardona lab collection. Several strains, including *B. gladioli*, *B. multivorans*, and *B. vietnamiensis*, exhibit extracellular mcl-PHA degradation capability, highlighting the diverse metabolic capacities within the *Burkholderia* genus.

Building on this finding, the third objective of this thesis was to identify genes and regulatory elements associated with extracellular mcl-PHA degradation in *Burkholderia*. To elucidate the genetic basis of this activity, I selected *B. vietnamiensis* LMG 16232 for several reasons. First, the extracellular mcl-PHA degradation of this strain is one of the highest among other *Burkholderia* strains. Second, I was able to implement transposon mutagenesis in this strain. Third, this strain is genetically amenable through the RhaCAST system, which was developed in the first objective of this thesis, allowing us to create insertional mutants to verify the results of transposon mutagenesis. Additionally, the genome of this strain was sequenced as part of the analysis (Yap et al. 2023, see Appendix 6.3).

By performing transposon mutagenesis coupled with Tn-seq, I uncovered several genetic elements involved in mcl-PHA degradation, which can be broadly characterized into three main groups: a) lipase and chaperone gene cluster: The identification of genes encoding a

triacylglycerol lipase and a lipase chaperone suggests that lipases play a crucial role in mcl-PHA depolymerization. This finding aligns with previous studies on PHA depolymerases in other bacterial species and provides new insights specific to *Burkholderia*. b) Type II secretion system components: The involvement of components from the type II secretion system indicates that the extracellular degradation of mcl-PHA depends on enzyme secretion. c) Regulatory elements: The identification of regulatory elements, such as HTH-type transcriptional activators and a PHA synthesis repressor, points to a complex regulatory network governing mcl-PHA degradation. This suggests that the process may be integrated with other metabolic pathways.

I utilized the RhaCAST system developed in objective 1 to generate mutants for validating the genetic elements identified through Tn-seq. The absence of extracellular mcl-PHA depolymerase activity in the mutants confirms the involvement of the identified genes in mcl-PHA degradation. These findings point to future directions involving enzyme purification and site-directed mutagenesis to optimize lipases for efficient bioplastic degradation or to design synthetic enzymes. While this work has identified key genes involved in mcl-PHA degradation, further studies are necessary to characterize their specific biochemical roles and regulatory pathways.

Overall, this thesis shows how the development and application of genetic tools, such as RhaCAST and transposon mutagenesis for *Burkholderia*, can facilitate functional genomics studies in non-model bacteria such as *Burkholderia*. By applying these tools to investigate the mechanisms of bioplastic degradation, this work has identified and validated genetic elements involved in the degradation of extracellular mcl-PHA in *Burkholderia*. These findings suggest that *Burkholderia* has potential as a source of novel enzymes for future enzyme development.

Developing new genetic manipulation tools remains important for non-model bacteria like *Burkholderia*. Many efficient and advanced genetic tools have been developed in other organisms, and adapting some of these tools for *Burkholderia* would be beneficial. For instance, the CRISPR-based transcriptional activation system (CRISPRa) can be used for endogenous gene expression to activate genes of interest (Gilbert et al. 2014). The development of CRISPRa would expand our ability to regulate gene expression within this genus. Currently, the genetic toolbox for *Burkholderia* lacks strategies for simultaneously editing multiple genes. Targeted, continuous multigene editing strategies that have been successfully achieved in *E. coli,* which allow for the insertions and knock-outs of single and multiple targets, would be useful if applied to *Burkholderia* (Jiang et al. 2015). Additionally, a more rapid genetic editing tool is also desirable, the CRMAGE system, developed by combining CRISPR/Cas9 with λ Red recombineering-based MAGE technology, is a fast and multiplexable tool that has been implemented in *E. coli* (Ronda et al. 2016). Introducing CRMAGE into *Burkholderia* would accelerate the genetic engineering process within this genus. As genetic tools become more advanced and extensive, modifying and studying genes in *Burkholderia* will become faster and higher throughput. This progress will facilitate the exploration of *Burkholderia*'s biotechnological potential as cell factories for producing valuable products, such as biocontrol agents or bioremediation solutions.

CHAPTER 5: REFERENCES

Abdu, A., Juarez-Lara, G., and Dennis, J.J. 2018. Development of an Sce-I mutagenesis system for *Burkholderia cepacia* complex strains. Journal of Microbiological Methods **146**: 16–21. doi:10.1016/j.mimet.2018.01.011.

Agnoli, K., Lowe, C.A., Farmer, K.L., Husnain, S.I., and Thomas, M.S. 2006. The ornibactin biosynthesis and transport genes of *Burkholderia cenocepacia* are regulated by an extracytoplasmic function sigma factor which is a part of the Fur regulon. Journal of Bacteriology **188**(10): 3631–3644. doi:10.1128/JB.188.10.3631-3644.2006.

Agnoli, K., Schwager, S., Uehlinger, S., Vergunst, A., Viteri, D.F., Nguyen, D.T., Sokol, P.A., Carlier, A., and Eberl, L. 2012. Exposing the third chromosome of *Burkholderia cepacia* complex strains as a virulence plasmid. Mol Microbiol **83**(2): 362–378. doi:10.1111/j.1365-2958.2011.07937.x.

Alexeyev, M.F. 1999. The pKNOCK series of broad-host-range mobilizable suicide vectors for gene knockout and targeted DNA insertion into the chromosome of gram-negative bacteria. Biotechniques **26**(5): 824–826, 828. doi:10.2144/99265bm05.

Aliu, E., Lee, K., and Wang, K. 2022. CRISPR RNA-guided integrase enables high-efficiency targeted genome engineering in Agrobacterium tumefaciens. Plant Biotechnology Journal **20**(10): 1916–1927. doi:10.1111/pbi.13872.

Almagro Armenteros, J.J., Tsirigos, K.D., Sønderby, C.K., Petersen, T.N., Winther, O., Brunak, S., von Heijne, G., and Nielsen, H. 2019. SignalP 5.0 improves signal peptide predictions using deep neural networks. Nat Biotechnol **37**(4): 420–423. doi:10.1038/s41587-019-0036-z.

Anderson, A.J., and Dawes, E.A. 1990. Occurrence, metabolism, metabolic role, and industrial uses of bacterial polyhydroxyalkanoates. Microbiol. Rev. **54**(4): 450–472.

Araújo, W.L., Creason, A.L., Mano, E.T., Camargo-Neves, A.A., Minami, S.N., Chang, J.H., and Loper, J.E. 2016. Genome Sequencing and Transposon Mutagenesis of *Burkholderia seminalis* TC3.4.2R3 Identify Genes Contributing to Suppression of Orchid Necrosis Caused by *B. gladioli*. MPMI **29**(6): 435–446. doi:10.1094/MPMI-02-16-0047-R.

Azura Azami, N., Ira Aryani, W., Aik-Hong, T., and Amirul, A.A. 2019. Purification and characterization of new bio-plastic degrading enzyme from *Burkholderia cepacia* DP1. Protein Expression and Purification **155**: 35–42. doi:10.1016/j.pep.2018.10.008.

Barrett, A.R., Kang, Y., Inamasu, K.S., Son, M.S., Vukovich, J.M., and Hoang, T.T. 2008. Genetic tools for allelic replacement in *Burkholderia* species. Appl Environ Microbiol **74**(14): 4498–4508. doi:10.1128/AEM.00531-08.

Baugh, L., Gallagher, L.A., Patrapuvich, R., Clifton, M.C., Gardberg, A.S., Edwards, T.E., Armour, B., Begley, D.W., Dieterich, S.H., Dranow, D.M., Abendroth, J., Fairman, J.W., 3rd, D.F., Staker, B.L., Phan, I., Gillespie, A., Choi, R., Nakazawa-Hewitt, S., Nguyen, M.T., Napuli, A., Barrett, L., Buchko, G.W., Stacy, R., Myler, P.J., Stewart, L.J., Manoil, C., and Voorhis, W.C.V. 2013. Combining functional and structural genomics to sample the essential *Burkholderia* structome. PloS one **8**(1): e53851. doi:10.1371/journal.pone.0053851; 10.1371/journal.pone.0053851.

Baym, M., Shaket, L., Anzai, I.A., Adesina, O., and Barstow, B. 2016. Rapid construction of a whole-genome transposon insertion collection for *Shewanella oneidensis* by Knockout Sudoku. Nature Communications **7**(1): 1–13. doi:10.1038/ncomms13270.

Bazzini, S., Udine, C., Sass, A., Pasca, M.R., Longo, F., Emiliani, G., Fondi, M., Perrin, E., Decorosi, F., Viti, C., Giovannetti, L., Leoni, L., Fani, R., Riccardi, G., Mahenthiralingam, E., and Buroni, S. 2011. Deciphering the role of RND efflux

transporters in *Burkholderia cenocepacia*. PLoS ONE **6**(4): e18902. doi:10.1371/journal.pone.0018902.

Black, P.N., and DiRusso, C.C. 1994. Molecular and biochemical analyses of fatty acid transport, metabolism, and gene regulation in *Escherichia coli*. Biochim Biophys Acta **1210**(2): 123–145. doi:10.1016/0005-2760(94)90113-9.

Blokesch, M. 2016. Natural competence for transformation. Current Biology **26**(21): R1126–R1130. Elsevier. doi:10.1016/j.cub.2016.08.058.

Bloodworth, R.A., Gislason, A.S., and Cardona, S.T. 2013. *Burkholderia cenocepacia* conditional growth mutant library created by random promoter replacement of essential genes. MicrobiologyOpen **2**(2): 243–258. doi:10.1002/mbo3.71.

Blunt, W., Lagassé, A., Harvey, J., Sparling, R., Gapes, D., Levin, D., and Cicek, N. 2024. Semi-continuous non-sterile production of medium chain-length polyhydroxyalkanoates from fatty acids. The Canadian Journal of Chemical Engineering **102**(11): 3896–3908. doi:10.1002/cjce.25299.

Boekema, B.K.H.L., Beselin, A., Breuer, M., Hauer, B., Koster, M., Rosenau, F., Jaeger, K.-E., and Tommassen, J. 2007. Hexadecane and Tween 80 Stimulate Lipase Production in *Burkholderia glumae* by Different Mechanisms. Appl Environ Microbiol **73**(12): 3838–3844. doi:10.1128/AEM.00097-07.

Braunegg, G., Sonnleitner, B., and Lafferty, R.M. 1978. A rapid gas chromatographic method for the determination of polyhydroxybutyric acid in microbial biomass. European Journal of Applied Microbiology and Biotechnology **6**(1): 29–37. doi:10.1007/BF00500854.

Burkholder, W.H. 1950. Sour skin, a bacterial rot of onion bulbs. Phytopathology **40**: 115–117.

Buroni, S., Pasca, M.R., Flannagan, R.S., Bazzini, S., Milano, A., Bertani, I., Venturi, V., Valvano, M.A., and Riccardi, G. 2009. Assessment of three Resistance-Nodulation-

Cell Division drug efflux transporters of *Burkholderia cenocepacia* in intrinsic antibiotic resistance. BMC Microbiol. **9**: 200. doi:10.1186/1471-2180-9-200.

Burtnick, M.N., DeShazer, D., Nair, V., Gherardini, F.C., and Brett, P.J. 2010. *Burkholderia mallei* Cluster 1 Type VI Secretion Mutants Exhibit Growth and Actin Polymerization Defects in RAW 264.7 Murine Macrophages. Infect Immun **78**(1): 88–99. doi:10.1128/IAI.00985-09.

Cardona, S.T., Mueller, C., and Valvano, M.A. 2006. Identification of essential operons in *Burkholderia cenocepacia* with a rhamnose inducible promoter. Appl Environ Microbiol **72**(4): 2547–2555.

Cardona, S.T., and Valvano, M.A. 2005. An expression vector containing a rhamnose-inducible promoter provides tightly regulated gene expression in *Burkholderia cenocepacia*. Plasmid **54**(3): 219–228. doi:10.1016/j.plasmid.2005.03.004.

Castonguay-Vanier, J., Vial, L., Tremblay, J., and Déziel, E. 2010. *Drosophila melanogaster* as a Model Host for the *Burkholderia cepacia* Complex. PLoS One **5**(7): e11467. doi:10.1371/journal.pone.0011467.

Cauduro, G.P., Leal, A.L., Marmitt, M., de Ávila, L.G., Kern, G., Quadros, P.D., Mahenthiralingam, E., and Valiati, V.H. 2021. New benzo(a)pyrene-degrading strains of the *Burkholderia cepacia* complex prospected from activated sludge in a petrochemical wastewater treatment plant. Environ Monit Assess **193**(4): 163. doi:10.1007/s10661-021-08952-z.

Chandler, J.R., Duerkop, B.A., Hinz, A., West, T.E., Herman, J.P., Churchill, M.E.A., Skerrett, S.J., and Greenberg, E.P. 2009. Mutational Analysis of *Burkholderia thailandensis* Quorum Sensing and Self-Aggregation. J Bacteriol **191**(19): 5901–5909. doi:10.1128/JB.00591-09.

Chapalain, A., Groleau, M.-C., Le Guillouzer, S., Miomandre, A., Vial, L., Milot, S., and Déziel, E. 2017. Interplay between 4-hydroxy-3-methyl-2-alkylquinoline and N-acyl-homoserine lactone signaling in a *Burkholderia cepacia* complex clinical strain. Front Microbiol **8**: 1021. doi:10.3389/fmicb.2017.01021.

Chapalain, A., Vial, L., Laprade, N., Dekimpe, V., Perreault, J., and Déziel, E. 2013. Identification of quorum sensing-controlled genes in *Burkholderia ambifaria*. Microbiologyopen **2**(2): 226–242. doi:10.1002/mbo3.67.

Chen, F., Ye, J., Liu, W., Chio, C., Wang, W., and Qin, W. 2021a. Knockout of a highly GC-rich gene in *Burkholderia pyrrocinia* by recombineering with freeze-thawing transformation. Mol Plant Pathol **22**(7): 843–857. doi:10.1111/mpp.13058.

Chen, H., Sun, T., Bai, X., Yang, J., Yan, F., Yu, L., Tu, Q., Li, A., Tang, Y., Zhang, Y., Bian, X., and Zhou, H. 2021b. Genomics-Driven Activation of Silent Biosynthetic Gene Clusters in *Burkholderia gladioli* by Screening Recombineering System. Molecules **26**(3): 700. doi:10.3390/molecules26030700.

Chen, R., Barphagha, I.K., and Ham, J.H. 2015. Identification of potential genetic components involved in the deviant quorum-sensing signaling pathways of *Burkholderia glumae* through a functional genomics approach. Front Cell Infect Microbiol **5**: 22. doi:10.3389/fcimb.2015.00022.

Cheng, Z.-H., Wu, J., Liu, J.-Q., Min, D., Liu, D.-F., Li, W.-W., and Yu, H.-Q. 2022. Repurposing CRISPR RNA-guided integrases system for one-step, efficient genomic integration of ultra-long DNA sequences. Nucleic Acids Research **50**(13): 7739–7750. doi:10.1093/nar/gkac554.

Choi, K.H., DeShazer, D., and Schweizer, H.P. 2006. mini-Tn7 insertion in bacteria with multiple glmS-linked attTn7 sites: example *Burkholderia mallei* ATCC 23344. Nat Protoc **1**(1): 162–169. doi:10.1038/nprot.2006.25.

Choi, K.H., Gaynor, J.B., White, K.G., Lopez, C., Bosio, C.M., Karkhoff-Schweizer, R.R., and Schweizer, H.P. 2005. A Tn7-based broad-range bacterial cloning and expression system. Nat Methods **2**(6): 443–448. doi:10.1038/NMETH765.

Choi, K.H., Mima, T., Casart, Y., Rholl, D., Kumar, A., Beacham, I.R., and Schweizer, H.P. 2008. Genetic tools for select-agent-compliant manipulation of *Burkholderia pseudomallei*. Appl Environ Microbiol **74**(4): 1064–1075. doi:10.1128/AEM.02430-07.

Coenye, T., and LiPuma, J.J. 2002. Multilocus Restriction Typing: A Novel Tool for Studying Global Epidemiology of *Burkholderia cepacia* Complex Infection in Cystic Fibrosis. The Journal of Infectious Diseases **185**(10): 1454–1462. doi:10.1086/340279.

Cordova-Kreylos, A.L., Fernandez, L.E., Koivunen, M., Yang, A., Flor-Weiler, L., and Marrone, P.G. 2013. Isolation and Characterization of *Burkholderia rinojensis* sp. nov., a Non-*Burkholderia cepacia* Complex Soil Bacterium with Insecticidal and Miticidal Activities. Appl Environ Microbiol **79**(24): 7669–7678. doi:10.1128/AEM.02365-13.

Costa, S.G.V. a. O., Déziel, E., and Lépine, F. 2011. Characterization of rhamnolipid production by *Burkholderia glumae*. Lett Appl Microbiol **53**(6): 620–627. doi:10.1111/j.1472-765X.2011.03154.x.

Coutinho, B.G., Mitter, B., Talbi, C., Sessitsch, A., Bedmar, E.J., Halliday, N., James, E.K., Cámara, M., and Venturi, V. 2013. Regulon Studies and In Planta Role of the BraI/R Quorum-Sensing System in the Plant-Beneficial *Burkholderia* Cluster. Appl Environ Microbiol **79**(14): 4421–4432. doi:10.1128/AEM.00635-13.

Cuthbertson, L., and Nodwell, J.R. 2013. The TetR Family of Regulators. Microbiology and Molecular Biology Reviews **77**(3): 440–475. doi:10.1128/mmbr.00018-13.

Darling, P., Chan, M., Cox, A.D., and Sokol, P.A. 1998. Siderophore production by cystic fibrosis isolates of *Burkholderia cepacia*. Infection and immunity **66**(2): 874–877.

Datsenko, K.A., and Wanner, B.L. 2000. One-step inactivation of chromosomal genes in *Escherichia coli* K-12 using PCR products. Proc Natl Acad Sci **97**(12): 6640–6645.

Denef, V.J., Klappenbach, J.A., Patrauchan, M.A., Florizone, C., Rodrigues, J.L.M., Tsoi, T.V., Verstraete, W., Eltis, L.D., and Tiedje, J.M. 2006. Genetic and Genomic Insights into the Role of Benzoate-Catabolic Pathway Redundancy in *Burkholderia xenovorans LB400*. Appl Environ Microbiol **72**(1): 585–595. doi:10.1128/AEM.72.1.585-595.2006.

Denman, C.C., and Brown, A.R.Y. 2013. 2013. Mannitol promotes adherence of an outbreak strain of *Burkholderia multivorans* via an exopolysaccharide-independent mechanism that is associated with upregulation of newly identified fimbrial and afimbrial adhesins. Microbiology **159**(Pt_4): 771–781. Microbiology Society,. doi:10.1099/mic.0.064832-0.

Dennis, J.J., and Zylstra, G.J. 1998. Plasposons: modular self-cloning minitransposon derivatives for rapid genetic analysis of gram-negative bacterial genomes. Appl Environ Microbiol **64**(7): 2710–2715.

Depoorter, E., Bull, M.J., Peeters, C., Coenye, T., Vandamme, P., and Mahenthiralingam, E. 2016. *Burkholderia*: an update on taxonomy and biotechnological potential as antibiotic producers. Appl Microbiol Biotechnol **100**(12): 5215–5229. doi:10.1007/s00253-016-7520-x.

Donahue, J.P., Israel, D.A., Peek Jr, R.M., Blaser, M.J., and Miller, G.G. 2000. Overcoming the restriction barrier to plasmid transformation of *Helicobacter pylori*. Molecular Microbiology **37**(5): 1066–1074. doi:10.1046/j.1365-2958.2000.02036.x.

Dubeau, D., Déziel, E., Woods, D.E., and Lépine, F. 2009. *Burkholderia thailandensis* harbors two identical rhl gene clusters responsible for the biosynthesis of rhamnolipids. BMC Microbiol **9**: 263. doi:10.1186/1471-2180-9-263.

Eberl, L., and Vandamme, P. 2016. Members of the genus *Burkholderia*: good and bad guys. F1000Res **5**: 1007. doi:10.12688/f1000research.8221.1.

Elshafie, H.S., Devescovi, G., Venturi, V., Camele, I., and Bufo, S.A. 2019. Study of the Regulatory Role of N-Acyl Homoserine Lactones Mediated Quorum Sensing in the Biological Activity of *Burkholderia gladioli* pv. agaricicola Causing Soft Rot of *Agaricus* spp. Front Microbiol **10**: 2695. doi:10.3389/fmicb.2019.02695.

Espinosa-Victoria, D., López-Reyes, L., Carcaño-Montiel, M.G., Serret-López, M., Espinosa-Victoria, D., López-Reyes, L., Carcaño-Montiel, M.G., and Serret-López, M. 2020. The *Burkholderia* genus: between mutualism and pathogenicity. Revista mexicana de fitopatología **38**(3): 337–359. Sociedad Mexicana de Fitopatología A.C. doi:10.18781/r.mex.fit.2004-5.

Farmer, K.L., and Thomas, M.S. 2004. Isolation and Characterization of *Burkholderia cenocepacia* Mutants Deficient in Pyochelin Production: Pyochelin Biosynthesis Is Sensitive to Sulfur Availability. Journal of Bacteriology **186**(2): 270–277. doi:10.1128/JB.186.2.270-277.2004.

Fazli, M., Harrison, J.J., Gambino, M., Givskov, M., and Tolker-Nielsen, T. 2015. In-Frame and Unmarked Gene Deletions in *Burkholderia cenocepacia* via an Allelic Exchange System Compatible with Gateway Technology. Appl Environ Microbiol **81**(11): 3623–3630. doi:10.1128/AEM.03909-14.

Fazli, M., McCarthy, Y., Givskov, M., Ryan, R.P., and Tolker-Nielsen, T. 2013. The exopolysaccharide gene cluster Bcam1330-Bcam1341 is involved in Burkholderia cenocepacia biofilm formation, and its expression is regulated by c-di-GMP and Bcam1349. MicrobiologyOpen **2**(1): 105–122. doi:10.1002/mbo3.61.

Ferreira, M.R., Queiroga, V., and Moreira, L.M. 2024. Genomic editing in *Burkholderia multivorans* by CRISPR/Cas9. Appl Environ Microbiol **90**(2): e02250-23. doi:10.1128/aem.02250-23.

Figurski, D.H., and Helinski, D.R. 1979. Replication of an origin-containing derivative of plasmid RK2 dependent on a plasmid function provided in trans. Proc Natl Acad Sci **76**(4): 1648–1652.

Flannagan, R.S., Aubert, D., Kooi, C., Sokol, P.A., and Valvano, M.A. 2007. *Burkholderia cenocepacia* requires a periplasmic HtrA protease for growth under thermal and osmotic stress and for survival *in vivo*. Infect Immun **75**(4): 1679–1689. doi:10.1128/IAI.01581-06.

Flannagan, R.S., Linn, T., and Valvano, M.A. 2008. A system for the construction of targeted unmarked gene deletions in the genus *Burkholderia*. Environmental microbiology **10**(6): 1652–1660. doi:10.1111/j.1462-2920.2008.01576.x.

Flores-Juárez, C.R., González-Jasso, E., Antaramian, A., and Pless, R.C. 2016. PCR amplification of GC-rich DNA regions using the nucleotide analog N4-methyl-2′-deoxycytidine 5′-triphosphate. BioTechniques **61**(4): 175–182. Future Science. doi:10.2144/000114457.

Francis, N.R., Irikura, V.M., Yamaguchi, S., DeRosier, D.J., and Macnab, R.M. 1992. Localization of the *Salmonella typhimurium* flagellar switch protein FliG to the cytoplasmic M-ring face of the basal body. Proc Natl Acad Sci **89**(14): 6304–6308. doi:10.1073/pnas.89.14.6304.

Franco, M., D'haeseleer, P.M., Branda, S.S., Liou, M.J., Haider, Y., Segelke, B.W., and El-Etr, S.H. 2018. Proteomic Profiling of *Burkholderia thailandensis* During Host Infection Using Bio-Orthogonal Noncanonical Amino Acid Tagging (BONCAT). Frontiers in Cellular and Infection Microbiology **8**: 370. doi:10.3389/fcimb.2018.00370.

Frenken, L.G., Egmond, M.R., Batenburg, A.M., and Verrips, C.T. 1993a. *Pseudomonas glumae* lipase: increased proteolytic stability by protein engineering. Protein Eng **6**(6): 637–642. doi:10.1093/protein/6.6.637.

Frenken, L.G.J., de Groot, A., Tommassen, J., and Verrips, C.T. 1993b. Role of the lipB gene product in the folding of the secreted lipase of Pseudomonas glumae. Molecular Microbiology **9**(3): 591–599. doi:10.1111/j.1365-2958.1993.tb01719.x.

Frey, U.H., Bachmann, H.S., Peters, J., and Siffert, W. 2008. PCR-amplification of GC-rich regions: "slowdown PCR." Nat Protoc **3**(8): 1312–1317. doi:10.1038/nprot.2008.112.

Fu, J., Sharma, U., Sparling, R., Cicek, N., and Levin, D.B. 2014. Evaluation of medium-chain-length polyhydroxyalkanoate production by Pseudomonas putida LS46 using biodiesel by-product streams. Can. J. Microbiol. **60**(7): 461–468. doi:10.1139/cjm-2014-0108.

Gallagher, L.A., Ramage, E., Patrapuvich, R., Weiss, E., Brittnacher, M., and Manoil, C. 2013. Sequence-defined transposon mutant library of *Burkholderia thailandensis*. mBio **4**(6): e00604-13. doi:10.1128/mBio.00604-13; 10.1128/mBio.00604-13.

Gallagher, L.A., Shendure, J., and Manoil, C. 2011. Genome-scale identification of resistance functions in *Pseudomonas aeruginosa* using Tn-seq. MBio **2**(1): e00315-10. doi:10.1128/mBio.00315-10.

Ganesan, R., Kaltenpoth, M., and Flórez, L.V. 2021. Transposon-insertion Sequencing as a Tool to Elucidate Bacterial Colonization Factors in a *Burkholderia gladioli* Symbiont of *Lagria villosa* Beetles. JoVE (Journal of Visualized Experiments) (174): e62843. doi:10.3791/62843.

Gangoiti, J., Santos, M., Prieto, M.A., de la Mata, I., Serra, J.L., and Llama, M.J. 2012. Characterization of a Novel Subgroup of Extracellular Medium-Chain-Length Polyhydroxyalkanoate Depolymerases from Actinobacteria. Appl Environ Microbiol **78**(20): 7229–7237. doi:10.1128/AEM.01707-12.

Garcia, E.C., Anderson, M.S., Hagar, J.A., and Cotter, P.A. 2013. *Burkholderia* BcpA mediates biofilm formation independently of interbacterial contact dependent growth inhibition. Mol Microbiol **89**(6): 1213–1225. doi:10.1111/mmi.12339.

Gasteiger, E., Hoogland, C., Gattiker, A., Duvaud, S., Wilkins, M.R., Appel, R.D., and Bairoch, A. 2005. Protein Identification and Analysis Tools on the ExPASy Server. *In* The Proteomics Protocols Handbook. *Edited by* J.M. Walker. Humana Press, Totowa, NJ. pp. 571–607. doi:10.1385/1-59259-890-0:571.

Gelsinger, D.R., Vo, P.L.H., Klompe, S.E., Ronda, C., Wang, H., and Sternberg, S.H. 2023, March 21. Bacterial genome engineering using CRISPR RNA-guided transposases. bioRxiv. doi:10.1101/2023.03.18.533263.

Gilbert, L.A., Horlbeck, M.A., Adamson, B., Villalta, J.E., Chen, Y., Whitehead, E.H., Guimaraes, C., Panning, B., Ploegh, H.L., Bassik, M.C., Qi, L.S., Kampmann, M., and Weissman, J.S. 2014. Genome-Scale CRISPR-Mediated Control of Gene Repression and Activation. Cell **159**(3): 647–661. doi:10.1016/j.cell.2014.09.029.

Gislason, A.S., Turner, K., Domaratzki, M., and Cardona, S.T. 2017. Comparative analysis of the *Burkholderia cenocepacia* K56-2 essential genome reveals cell envelope functions that are uniquely required for survival in species of the genus *Burkholderia*. Microb Genom **3**(11): e000140. doi:10.1099/mgen.0.000140.

Gualdi, S., Agnoli, K., Vitale, A., Higgins, S., and Eberl, L. 2022. Identification of genes required for gold and silver tolerance in *Burkholderia cenocepacia* H111 by transposon sequencing. Environmental Microbiology **24**(2): 737–751. doi:10.1111/1462-2920.15471.

Gupta, R., Gupta, N., and Rathi, P. 2004. Bacterial lipases: an overview of production, purification and biochemical properties. Appl Microbiol Biotechnol **64**(6): 763–781. doi:10.1007/s00253-004-1568-8.

Gustafsson, C., Govindarajan, S., and Minshull, J. 2004. Codon bias and heterologous protein expression. Trends Biotechnol **22**(7): 346–353. doi:10.1016/j.tibtech.2004.04.006.

Hanuszkiewicz, A., Pittock, P., Humphries, F., Moll, H., Rosales, A.R., Molinaro, A., Moynagh, P.N., Lajoie, G.A., and Valvano, M.A. 2014. Identification of the Flagellin Glycosylation System in *Burkholderia cenocepacia* and the Contribution of Glycosylated Flagellin to Evasion of Human Innate Immune Responses *. Journal of Biological Chemistry **289**(27): 19231–19244. doi:10.1074/jbc.M114.562603.

Hassen, A.I., Khambani, L.S., and Swanevelder, Z.H. 2018. The Draft Genome Sequence of *Burkholderia* sp. Strain Nafp2/4-1b Confirms Its Ability To Produce the Plant Growth-Promoting Traits Pyoverdine Siderophores, 1-Aminocyclopropane-1-Carboxylate Deaminase, and the Phytohormone Auxin. Microbiology Resource Announcements **7**(23). doi:10.1128/MRA.01383-18.

Heacock-Kang, Y., McMillan, I.A., Zarzycki-Siek, J., Sun, Z., Bluhm, A.P., Cabanas, D., and Hoang, T.T. 2018. The heritable natural competency trait of *Burkholderia pseudomallei* in other *Burkholderia* species through comE and crp. Sci Rep **8**. doi:10.1038/s41598-018-30853-4.

Hendry, S., Steinke, S., Wittstein, K., Stadler, M., Harmrolfs, K., Adewunmi, Y., Sahukhal, G., Elasri, M., Thomashow, L., Weller, D., Mavrodi, O., Blankenfeldt, W., and Mavrodi, D. 2021. Functional Analysis of Phenazine Biosynthesis Genes in *Burkholderia* spp. Appl Environ Microbiol **87**(11): e02348-20. doi:10.1128/AEM.02348-20.

Higgins, S., Sanchez-Contreras, M., Gualdi, S., Pinto-Carbó, M., Carlier, A., and Eberl, L. 2017. The essential genome of *Burkholderia cenocepacia* H111. J. Bacteriol. **199**(22): e00260-17. doi:10.1128/JB.00260-17.

Hoang, T.T., Karkhoff-Schweizer, R.R., Kutchma, A.J., and Schweizer, H.P. 1998. A broad-host-range Flp-FRT recombination system for site-specific excision of chromosomally-

located DNA sequences: application for isolation of unmarked *Pseudomonas aeruginosa* mutants. Gene **212**(1): 77–86. doi:S0378111998001309 [pii].

Hobson, A.H., Buckley, C.M., Aamand, J.L., Jørgensen, S.T., Diderichsen, B., and McConnell, D.J. 1993. Activation of a bacterial lipase by its chaperone. Proc Natl Acad Sci U S A **90**(12): 5682–5686. doi:10.1073/pnas.90.12.5682.

Hogan, A.M., Jeffers, K.R., Palacios, A., and Cardona, S.T. 2021. Improved dynamic range of a rhamnose-inducible promoter for gene expression in *Burkholderia* spp. Appl Environ Microbiol **87**(18): e0064721. doi:10.1128/AEM.00647-21.

Hogan, A.M., Rahman, A.S.M.Z., Lightly, T.J., and Cardona, S.T. 2019. A broad-host-range CRISPRi toolkit for silencing gene expression in *Burkholderia*. ACS Synth Biol **8**(10): 2372–2384. doi:10.1021/acssynbio.9b00232.

Hogan, A.M., Scoffone, V.C., Makarov, V., Gislason, A.S., Tesfu, H., Stietz, M.S., Brassinga, A.K.C., Domaratzki, M., Li, X., Azzalin, A., Biggiogera, M., Riabova, O., Monakhova, N., Chiarelli, L.R., Riccardi, G., Buroni, S., and Cardona, S.T. 2018. Competitive fitness of essential gene knockdowns reveals a broad-spectrum antibacterial inhibitor of the cell division protein FtsZ. Antimicrob Agents Chemother **62**(12): e01231-18. doi:10.1128/AAC.01231-18.

Hong, K.-W., Tee, K.K., Yin, W.-F., Roberts, R.J., and Chan, K.-G. 2019. Methylome Characterization of *Burkholderia pseudomallei* Strain 982 at Single-Base Resolution. Microbiol Resour Announc **8**(43): e00898-19. doi:10.1128/MRA.00898-19.

Hörmann, B., Müller, M.M., Syldatk, C., and Hausmann, R. 2010. Rhamnolipid production by *Burkholderia plantarii* DSM 9509T. European Journal of Lipid Science and Technology **112**(6): 674–680. doi:10.1002/ejlt.201000030.

Howe, C., Sampath, A., and Spotnitz, M. 1971. The *pseudomallei* group: a review. J. Infect. Dis. **124**(6): 598–606.

Huber, B., Riedel, K., Hentzer, M., Heydorn, A., Gotschlich, A., Givskov, M., Molin, S., and Eberl, L. 2001. The *cep* quorum-sensing system of *Burkholderia cepacia* H111 controls biofilm formation and swarming motility. Microbiology (Reading, England) **147**(Pt 9): 2517–2528.

Hutchison, C.A., Peterson, S.N., Gill, S.R., Cline, R.T., White, O., Fraser, C.M., Smith, H.O., and Venter, J.C. 1999. Global transposon mutagenesis and a minimal *Mycoplasma* genome. Science **286**(5447): 2165–2169.

Iqbal, A., Panta, P.R., Ontoy, J., Bruno, J., Ham, J.H., and Doerrler, W.T. 2021. Chemical or Genetic Alteration of Proton Motive Force Results in Loss of Virulence of *Burkholderia glumae*, the Cause of Rice Bacterial Panicle Blight. Appl Environ Microbiol **87**(18). doi:10.1128/AEM.00915-21.

Jaeger, K.E., Steinbüchel, A., and Jendrossek, D. 1995. Substrate specificities of bacterial polyhydroxyalkanoate depolymerases and lipases: bacterial lipases hydrolyze poly(omega-hydroxyalkanoates). Appl Environ Microbiol **61**(8): 3113–3118.

Jang, M.S., Goo, E., An, J.H., Kim, J., and Hwang, I. 2014. Quorum Sensing Controls Flagellar Morphogenesis in *Burkholderia glumae*. PLoS One **9**(1): e84831. doi:10.1371/journal.pone.0084831.

Jassem, A.N. 2012. *Aminoglycoside susceptibility and acquired resistance in* Burkholderia vietnamiensis. University of British Columbia. doi:10.14288/1.0103466.

Jendrossek, D. 2009. Polyhydroxyalkanoate Granules Are Complex Subcellular Organelles (Carbonosomes). Journal of Bacteriology **191**(10): 3195–3202. doi:10.1128/jb.01723-08.

Jendrossek, D., and Handrick, R. 2002. Microbial degradation of polyhydroxyalkanoates. Annu. Rev. Microbiol. **56**: 403–432. doi:10.1146/annurev.micro.56.012302.160838.

Jia, B., Yang, J.-K., Liu, W.-S., Li, X., and Yan, Y.-J. 2010. Homologous overexpression of a lipase from *Burkholderia cepacia* using the lambda Red recombinase system. Biotechnol Lett **32**(4): 521–526. doi:10.1007/s10529-009-0189-9.

Jian, X., and Challis, G.L. 2018. Elucidation of molecular mechanisms of antibiotics biosynthesis in *Burkholderia gladioli*. University of Warwick, Coventry.

Jiang, Y., Chen, B., Duan, C., Sun, B., Yang, J., and Yang, S. 2015. Multigene editing in the *Escherichia coli* genome via the CRISPR-Cas9 system. Appl Environ Microbiol **81**(7): 2506–2514. doi:10.1128/AEM.04023-14.

Jimenez-Diaz, L., Caballero, A., and Segura, A. 2017. Pathways for the Degradation of Fatty Acids in Bacteria. *In* Aerobic Utilization of Hydrocarbons, Oils and Lipids. *Edited by* F. Rojo. Springer International Publishing, Cham. pp. 1–23. doi:10.1007/978-3-319-39782-5_42-1.

Jones, C., Webster, G., Mullins, A.J., Jenner, M., Bull, M.J., Dashti, Y., Spilker, T., Parkhill, J., Connor, T.R., LiPuma, J.J., Challis, G.L., and Mahenthiralingam, E. 2021. Kill and cure: genomic phylogeny and bioactivity of *Burkholderia gladioli* bacteria capable of pathogenic and beneficial lifestyles. Microb Genom **7**(1). doi:10.1099/mgen.0.000515.

Kang, Y., Norris, M.H., Barrett, A.R., Wilcox, B.A., and Hoang, T.T. 2009. Engineering of Tellurite-Resistant Genetic Tools for Single-Copy Chromosomal Analysis of *Burkholderia* spp. and Characterization of the *Burkholderia thailandensis* betBA Operon. Appl Environ Microbiol **75**(12): 4015–4027. doi:10.1128/AEM.02733-08.

Kang, Y., Norris, M.H., Wilcox, B.A., Tuanyok, A., Keim, P.S., and Hoang, T.T. 2011. Knock-out and pull-out recombineering protocols for naturally transformable *Burkholderia thailandensis* and *Burkholderia pseudomallei*. Nat Protoc **6**(8): 1085–1104. doi:10.1038/nprot.2011.346.

Kelley, L.A., Mezulis, S., Yates, C.M., Wass, M.N., and Sternberg, M.J.E. 2015. The Phyre2 web portal for protein modeling, prediction and analysis. Nat Protoc **10**(6): 845–858. doi:10.1038/nprot.2015.053.

Khattabi, M.E., Gelder, P.V., Bitter, W., and Tommassen, J. 2000. Role of the Lipase-specific Foldase of Burkholderia glumae as a Steric Chaperone. Journal of Biological Chemistry **275**(35): 26885–26891. Elsevier. doi:10.1016/S0021-9258(19)61457-2.

Kim, D.Y., Kim, H.C., Kim, S.Y., and Rhee, Y.H. 2005. Molecular characterization of extracellular medium-chain-length poly(3-hydroxyalkanoate) depolymerase genes from *Pseudomonas alcaligenes* strains. J. Microbiol. **43**(3): 285–294.

Klaus, J.R., Coulon, P.M.L., Koirala, P., Seyedsayamdost, M.R., Déziel, E., and Chandler, J.R. 2020. Secondary metabolites from the *Burkholderia pseudomallei* complex: structure, ecology, and evolution. J Ind Microbiol Biotechnol **47**(9–10): 877–887. doi:10.1007/s10295-020-02317-0.

Klompe, S.E., Vo, P.L.H., Halpin-Healy, T.S., and Sternberg, S.H. 2019. Transposon-encoded CRISPR–Cas systems direct RNA-guided DNA integration. Nature **571**(7764): 219–225. doi:10.1038/s41586-019-1323-z.

Knapp, A., Voget, S., Gao, R., Zaburannyi, N., Krysciak, D., Breuer, M., Hauer, B., Streit, W.R., Müller, R., Daniel, R., and Jaeger, K.-E. 2015. Mutations improving production and secretion of extracellular lipase by Burkholderia glumae PG1. Applied Microbiology and Biotechnology **100**: 1265. doi:10.1007/s00253-015-7041-z.

Kniewel, R., Revelles Lopez, O., and Prieto, M.A. 2017. Biogenesis of Medium-Chain-Length Polyhydroxyalkanoates. *In* Biogenesis of Fatty Acids, Lipids and Membranes. *Edited by* O. Geiger. Springer International Publishing, Cham. pp. 1–25. doi:10.1007/978-3-319-43676-0_29-1.

Knoll, M., Hamm, T.M., Wagner, F., Martinez, V., and Pleiss, J. 2009. The PHA Depolymerase Engineering Database: A systematic analysis tool for the diverse family of polyhydroxyalkanoate (PHA) depolymerases. BMC Bioinformatics **10**: 89. doi:10.1186/1471-2105-10-89.

Kodaka, H., Armfield, A.Y., Lombard, G.L., and Dowell, V.R. 1982. Practical procedure for demonstrating bacterial flagella. J Clin Microbiol **16**(5): 948–952.

Kolmogorov, M., Yuan, J., Lin, Y., and Pevzner, P.A. 2019. Assembly of long, error-prone reads using repeat graphs. Nat Biotechnol **37**(5): 540–546. Nature Publishing Group. doi:10.1038/s41587-019-0072-8.

Kolter, R., Inuzuka, M., and Helinski, D.R. 1978. Trans-complementation-dependent replication of a low molecular weight origin fragment from plasmid R6K. Cell **15**(4): 1199–1208. doi:10.1016/0092-8674(78)90046-6.

Kunakom, S., and Eustáquio, A.S. 2019. *Burkholderia* as a Source of Natural Products. J Nat Prod **82**(7): 2018–2037. doi:10.1021/acs.jnatprod.8b01068.

Larsen, J.C., and Johnson, N.H. 2009. Pathogenesis of *Burkholderia pseudomallei* and *Burkholderia mallei*. Mil Med **174**(6): 647–651.

Law, R.J., Hamlin, J.N.R., Sivro, A., McCorrister, S.J., Cardama, G.A., and Cardona, S.T. 2008. A functional phenylacetic acid catabolic pathway is required for full pathogenicity of *Burkholderia cenocepacia* in the *Caenorhabditis elegans* host model. J. Bacteriol. **190**(21): 7209–7218. doi:10.1128/JB.00481-08.

Lee, S.-H., and Kim, M.-N. 2010. Isolation of bacteria degrading poly(butylene succinate-*co*-butylene adipate) and their *lip A* gene. International Biodeterioration & Biodegradation **64**(3): 184–190. doi:10.1016/j.ibiod.2010.01.002.

Lefebre, M.D., and Valvano, M.A. 2002. Construction and evaluation of plasmid vectors optimized for constitutive and regulated gene expression in *Burkholderia cepacia* complex isolates. Applied and Environmental Microbiology **68**(12): 5956–5964.

Li, H., and Durbin, R. 2010. Fast and accurate long-read alignment with Burrows–Wheeler transform. Bioinformatics **26**(5): 589–595. doi:10.1093/bioinformatics/btp698.

Li, H., Handsaker, B., Wysoker, A., Fennell, T., Ruan, J., Homer, N., Marth, G., Abecasis, G., Durbin, R., and Subgroup, 1000 Genome Project Data Processing. 2009. The Sequence Alignment/Map format and SAMtools. Bioinformatics **25**(16): 2078–2079. doi:10.1093/bioinformatics/btp352.

Li, K., Fan, Y., He, Y., Zeng, L., Han, X., and Yan, Y. 2017. *Burkholderia cepacia* lipase immobilized on heterofunctional magnetic nanoparticles and its application in biodiesel synthesis. Sci Rep **7**(1): 16473. doi:10.1038/s41598-017-16626-5.

Li, R., Shi, H., Zhao, X., Liu, X., Duan, Q., Song, C., Chen, H., Zheng, W., Shen, Q., Wang, M., Wang, X., Gong, K., Yin, J., Zhang, Y., Li, A., and Fu, J. 2021. Development and application of an efficient recombineering system for *Burkholderia glumae* and *Burkholderia plantarii*. Microb Biotechnol **14**(4): 1809–1826. doi:10.1111/1751-7915.13840.

Li, Z., Yang, J., and Loh, X.J. 2016. Polyhydroxyalkanoates: opening doors for a sustainable future. NPG Asia Materials **8**(4): e265–e265. doi:10.1038/am.2016.48.

Lightly, T.J., Frejuk, K.L., Groleau, M.-C., Chiarelli, L.R., Ras, C., Buroni, S., Déziel, E., Sorensen, J.L., and Cardona, S.T. 2019. Phenylacetyl-CoA, not phenylacetic acid, attenuates CepIR-regulated virulence in *Burkholderia cenocepacia*. Appl Environ Microbiol **85**(24). doi:10.1128/AEM.01594-19.

Liu, M., Philp, J., Wang, Y., Hu, J., Wei, Y., Li, J., Ryder, M., Toh, R., Zhou, Y., Denton, M.D., Wu, Y., and Yang, H. 2022. Plant growth-promoting rhizobacteria *Burkholderia*

vietnamiensis B418 inhibits root-knot nematode on watermelon by modifying the rhizosphere microbial community. Sci Rep **12**(1): 8381. doi:10.1038/s41598-022-12472-2.

Lo, C.-F., Yu, C.-Y., Kuan, I.-C., and Lee, S.-L. 2012. Optimization of Lipase Production by Burkholderia sp. Using Response Surface Methodology. International Journal of Molecular Sciences **13**(11): 14889. doi:10.3390/ijms131114889.

Loeven, N.A., Perault, A.I., Cotter, P.A., Hodges, C.A., Schwartzman, J.D., Hampton, T.H., and Bliska, J.B. 2021. The *Burkholderia cenocepacia* Type VI Secretion System Effector TecA Is a Virulence Factor in Mouse Models of Lung Infection. mBio **12**(5): e02098-21. doi:10.1128/mBio.02098-21.

Logue, C.-A., Peak, I.R.A., and Beacham, I.R. 2009. Facile construction of unmarked deletion mutants in *Burkholderia pseudomallei* using sacB counter-selection in sucrose-resistant and sucrose-sensitive isolates. Journal of Microbiological Methods **76**(3): 320–323. doi:10.1016/j.mimet.2008.12.007.

Loong, S.K., Soh, Y.H., Mahfodz, N.H., Johari, J., and AbuBakar, S. 2016. Synovial Tissue Infection with *Burkholderia fungorum*. Emerg Infect Dis **22**(10): 1834–1835. doi:10.3201/eid2210.151114.

López, C.M., Rholl, D.A., Trunck, L.A., and Schweizer, H.P. 2009. Versatile Dual-Technology System for Markerless Allele Replacement in *Burkholderia pseudomallei*. Appl Environ Microbiol **75**(20): 6496–6503. doi:10.1128/AEM.01669-09.

de Lorenzo, V., Herrero, M., Jakubzik, U., and Timmis, K.N. 1990. Mini-Tn5 transposon derivatives for insertion mutagenesis, promoter probing, and chromosomal insertion of cloned DNA in gram-negative eubacteria. J Bacteriol **172**(11): 6568–6572. doi:10.1128/jb.172.11.6568-6572.1990.

Madeira, F., Madhusoodanan, N., Lee, J., Eusebi, A., Niewielska, A., Tivey, A.R.N., Lopez, R., and Butcher, S. 2024. The EMBL-EBI Job Dispatcher sequence analysis tools framework in 2024. Nucleic Acids Res **52**(W1): W521–W525. doi:10.1093/nar/gkae241.

Madison, L.L., and Huisman, G.W. 1999. Metabolic Engineering of Poly(3-Hydroxyalkanoates): From DNA to Plastic. Microbiol Mol Biol Rev **63**(1): 21–53.

Mahenthiralingam, E., Song, L., Sass, A., White, J., Wilmot, C., Marchbank, A., Boaisha, O., Paine, J., Knight, D., and Challis, G.L. 2011. Enacyloxins Are Products of an Unusual Hybrid Modular Polyketide Synthase Encoded by a Cryptic *Burkholderia ambifaria* Genomic Island. Chemistry & Biology **18**(5): 665–677. doi:10.1016/j.chembiol.2011.01.020.

Mahenthiralingam, E., Urban, T.A., and Goldberg, J.B. 2005. The multifarious, multireplicon *Burkholderia cepacia* complex. Nature Reviews Microbiology **3**(2): 144–156.

Mahenthiralingam, E., Vandamme, P., Campbell, M.E., Henry, D.A., Gravelle, A.M., Wong, L.T.K., Davidson, A.G.F., Wilcox, P.G., Nakielna, B., and Speert, D.P. 2001. Infection with *Burkholderia cepacia* complex genomovars in patients with cystic fibrosis: virulent transmissible strains of genomovar III can replace *Burkholderia multivorans*. Clin Infect Dis **33**(9): 1469–1475. doi:10.1086/322684.

Malott, R.J., Baldwin, A., Mahenthiralingam, E., and Sokol, P.A. 2005. Characterization of the cciIR quorum-sensing system in *Burkholderia cenocepacia*. Infect. Immun. **73**(8): 4982–4992. doi:10.1128/IAI.73.8.4982-4992.2005.

Malott, R.J., Steen-Kinnaird, B.R., Lee, T.D., and Speert, D.P. 2012. Identification of hopanoid biosynthesis genes involved in polymyxin resistance in *Burkholderia multivorans*. Antimicrob Agents Chemother **56**(1): 464–471. doi:10.1128/AAC.00602-11.

Mannaa, M., Park, I., and Seo, Y.-S. 2018. Genomic Features and Insights into the Taxonomy, Virulence, and Benevolence of Plant-Associated *Burkholderia* Species. Int J Mol Sci **20**(1). doi:10.3390/ijms20010121.

Mannweiler, O., Pinto-Carbó, M., Lardi, M., Agnoli, K., and Eberl, L. 2021. Investigation of *Burkholderia cepacia* Complex Methylomes via Single-Molecule, Real-Time Sequencing and Mutant Analysis. Journal of Bacteriology **203**: e00683-20. doi:10.1128/JB.00683-20.

Mao, D., Yoshimura, A., Wang, R., and Seyedsayamdost, M.R. 2020. Reporter-Guided Transposon Mutant Selection for Activation of Silent Gene Clusters in *Burkholderia thailandensis*. ChemBioChem **21**(13): 1826–1831. doi:10.1002/cbic.201900748.

Martin, M. 2011. Cutadapt removes adapter sequences from high-throughput sequencing reads. EMBnet.journal **17**(1): 10–12. doi:10.14806/ej.17.1.200.

Martínez, V., de la Peña, F., García-Hidalgo, J., de la Mata, I., García, J.L., and Prieto, M.A. 2012. Identification and Biochemical Evidence of a Medium-Chain-Length Polyhydroxyalkanoate Depolymerase in the *Bdellovibrio bacteriovorus* Predatory Hydrolytic Arsenal. Appl Environ Microbiol **78**(17): 6017–6026. doi:10.1128/AEM.01099-12.

Martínez, V., de Santos, P.G., García-Hidalgo, J., Hormigo, D., Prieto, M.A., Arroyo, M., and de la Mata, I. 2015. Novel extracellular medium-chain-length polyhydroxyalkanoate depolymerase from *Streptomyces exfoliatus* K10 DSMZ 41693: a promising biocatalyst for the efficient degradation of natural and functionalized mcl-PHAs. Appl Microbiol Biotechnol **99**(22): 9605–9615. doi:10.1007/s00253-015-6780-1.

Masschelein, J., Sydor, P.K., Hobson, C., Howe, R., Jones, C., Roberts, D.M., Ling Yap, Z., Parkhill, J., Mahenthiralingam, E., and Challis, G.L. 2019. A dual transacylation

mechanism for polyketide synthase chain release in enacyloxin antibiotic biosynthesis. Nat Chem **11**(10): 906–912. doi:10.1038/s41557-019-0309-7.

Matsushima, P., and Baltz, R.H.Y. 1994. Transformation of *Saccharopolyspora spinosa* protoplasts with plasmid DNA modified in vitro to avoid host restriction. Microbiology **140**(1): 139–143. doi:10.1099/13500872-140-1-139.

Mell, J.C., and Redfield, R.J. 2014. Natural Competence and the Evolution of DNA Uptake Specificity. J Bacteriol **196**(8): 1471–1483. doi:10.1128/JB.01293-13.

Mello Bueno, P.R., de Oliveira, T.F., Castiglioni, G.L., Soares Júnior, M.S., and Ulhoa, C.J. 2015. Application of lipase from *Burkholderia cepacia* in the degradation of agro-industrial effluent. Water Sci Technol **71**(7): 957–964. doi:10.2166/wst.2015.037.

Memišević, V., Zavaljevski, N., Pieper, R., Rajagopala, S.V., Kwon, K., Townsend, K., Yu, C., Yu, X., DeShazer, D., Reifman, J., and Wallqvist, A. 2013. Novel *Burkholderia mallei* Virulence Factors Linked to Specific Host-Pathogen Protein Interactions. Mol Cell Proteomics **12**(11): 3036–3051. doi:10.1074/mcp.M113.029041.

Miller, V.L., and Mekalanos, J.J. 1988. A novel suicide vector and its use in construction of insertion mutations: osmoregulation of outer membrane proteins and virulence determinants in *Vibrio cholerae* requires *toxR*. Journal of Bacteriology **170**(6): 2575–2583.

Mima, T., and Schweizer, H.P. 2010. The BpeAB-OprB Efflux Pump of *Burkholderia pseudomallei* 1026b Does Not Play a Role in Quorum Sensing, Virulence Factor Production, or Extrusion of Aminoglycosides but Is a Broad-Spectrum Drug Efflux System. Antimicrob Agents Chemother **54**(8): 3113–3120. doi:10.1128/AAC.01803-09.

Moebius, N., Ross, C., Scherlach, K., Rohm, B., Roth, M., and Hertweck, C. 2012. Biosynthesis of the respiratory toxin bongkrekic acid in the pathogenic bacterium

Burkholderia gladioli. Chem Biol **19**(9): 1164–1174. doi:10.1016/j.chembiol.2012.07.022.

Mohanan, N., Montazer, Z., Sharma, P.K., and Levin, D.B. 2020. Microbial and Enzymatic Degradation of Synthetic Plastics. Front Microbiol **11**: 580709. doi:10.3389/fmicb.2020.580709.

Mohanan, N., Wong, C.H., Budisa, N., and Levin, D.B. 2022. Characterization of Polymer Degrading Lipases, LIP1 and LIP2 From Pseudomonas chlororaphis PA23. Front Bioeng Biotechnol **10**: 854298. doi:10.3389/fbioe.2022.854298.

Morya, R., Salvachúa, D., and Thakur, I.S. 2020. *Burkholderia*: An Untapped but Promising Bacterial Genus for the Conversion of Aromatic Compounds. Trends Biotechnol **38**(9): 963–975. doi:10.1016/j.tibtech.2020.02.008.

Moule, M.G., Hemsley, C.M., Seet, Q., Guerra-Assunção, J.A., Lim, J., Sarkar-Tyson, M., Clark, T.G., Tan, P.B.O., Titball, R.W., Cuccui, J., and Wren, B.W. 2014. Genome-wide saturation mutagenesis of *Burkholderia pseudomallei* K96243 predicts essential genes and novel targets for antimicrobial development. MBio **5**(1): e00926-00913. doi:10.1128/mBio.00926-13.

Mullins, A.J., Murray, J.A.H., Bull, M.J., Jenner, M., Jones, C., Webster, G., Green, A.E., Neill, D.R., Connor, T.R., Parkhill, J., Challis, G.L., and Mahenthiralingam, E. 2019. Genome mining identifies cepacin as a plant-protective metabolite of the biopesticidal bacterium *Burkholderia ambifaria*. Nat Microbiol **4**(6): 996–1005. doi:10.1038/s41564-019-0383-z.

Muneer, F., Rasul, I., Azeem, F., Siddique, M.H., Zubair, M., and Nadeem, H. 2020. Microbial Polyhydroxyalkanoates (PHAs): Efficient Replacement of Synthetic Polymers. J Polym Environ **28**: 2301–2323. doi:10.1007/s10924-020-01772-1.

Musso, M., Bocciardi, R., Parodi, S., Ravazzolo, R., and Ceccherini, I. 2006. Betaine, Dimethyl Sulfoxide, and 7-Deaza-dGTP, a Powerful Mixture for Amplification of GC-Rich DNA Sequences. J Mol Diagn **8**(5): 544–550. doi:10.2353/jmoldx.2006.060058.

Myers-Morales, T., Oates, A.E., Byrd, M.S., and Garcia, E.C. 2019. *Burkholderia cepacia* Complex Contact-Dependent Growth Inhibition Systems Mediate Interbacterial Competition. J Bacteriol **201**(12): e00012-19. doi:10.1128/JB.00012-19.

Nam, Y., Goo, E., Kang, Y., and Hwang, I. 2021. Membrane Depolarization and Apoptosis-Like Cell Death in an Alkaline Environment in the Rice Pathogen *Burkholderia glumae*. Front Microbiol **12**: 755596. doi:10.3389/fmicb.2021.755596.

Narancic, T., and O'Connor, K.E. 2019. Plastic waste as a global challenge: are biodegradable plastics the answer to the plastic waste problem? Microbiology **165**(2): 129–137. doi:10.1099/mic.0.000749.

Narancic, T., Verstichel, S., Reddy Chaganti, S., Morales-Gamez, L., Kenny, S.T., De Wilde, B., Babu Padamati, R., and O'Connor, K.E. 2018. Biodegradable Plastic Blends Create New Possibilities for End-of-Life Management of Plastics but They Are Not a Panacea for Plastic Pollution. Environ. Sci. Technol. **52**(18): 10441–10452. doi:10.1021/acs.est.8b02963.

Nor Azura Azam et al. 2018. Enhanced degradation of polyhydroxyalkanoates (PHAs) by newly isolated *Burkholderia cepacia* DP1 with high depolymerase activity. 3 biotech **75**(7): 11. doi:10.1007/s13205-017-0716-7.

Norris, M.H., Heacock-Kang, Y., Zarzycki-Siek, J., Bluhm, A.P., McMillan, I.A., Schweizer, H.P., and Hoang, T.T. 2017. *Burkholderia pseudomallei* natural competency and DNA catabolism: Identification and characterization of relevant genes from a constructed fosmid library. PLoS One **12**(12): e0189018. doi:10.1371/journal.pone.0189018.

Norris, M.H., Kang, Y., Lu, D., Wilcox, B.A., and Hoang, T.T. 2009. Glyphosate Resistance as a Novel Select-Agent-Compliant, Non-Antibiotic-Selectable Marker in Chromosomal Mutagenesis of the Essential Genes asd and dapB of *Burkholderia pseudomallei*. Appl Environ Microbiol **75**(19): 6062–6075. doi:10.1128/AEM.00820-09.

Norris, M.H., Kang, Y., Wilcox, B., and Hoang, T.T. 2010. Stable, Site-Specific Fluorescent Tagging Constructs Optimized for *Burkholderia* Species. Appl Environ Microbiol **76**(22): 7635–7640. doi:10.1128/AEM.01188-10.

Oliveira, B.H., Santos, R.É., Loiola, L.E.A., and Nascimento, V.M.G. 2015. Overproduction and properties of lipase by a wild strain of Burkholderia lata LBBIO-BL02 using chicken fat. Ann Microbiol **65**(2): 865–877. BioMed Central. doi:10.1007/s13213-014-0928-6.

Orpana, A.K., Ho, T.H., and Stenman, J. 2012. Multiple Heat Pulses during PCR Extension Enabling Amplification of GC-Rich Sequences and Reducing Amplification Bias. Anal. Chem. **84**(4): 2081–2087. American Chemical Society. doi:10.1021/ac300040j.

O'Sullivan, L.A., Weightman, A.J., Jones, T.H., Marchbank, A.M., Tiedje, J.M., and Mahenthiralingam, E. 2007. Identifying the genetic basis of ecologically and biotechnologically useful functions of the bacterium *Burkholderia vietnamiensis*. Environmental Microbiology **9**(4): 1017–1034. doi:10.1111/j.1462-2920.2006.01228.x.

Paloyan, A., Tadevosyan, M., Ghevondyan, D., Khoyetsyan, L., Karapetyan, M., Margaryan, A., Antranikian, G., and Panosyan, H. 2025. Biodegradation of polyhydroxyalkanoates: current state and future prospects. Front. Microbiol. **16**: 1542468. Frontiers. doi:10.3389/fmicb.2025.1542468.

Papaneophytou, C.P., Velali, E.E., and Pantazaki, A.A. 2011. Purification and characterization of an extracellular medium-chain length polyhydroxyalkanoate depolymerase from

Thermus thermophilus HB8. Polymer Degradation and Stability **96**(4): 670–678. doi:10.1016/j.polymdegradstab.2010.12.015.

Park, J.-D., Moon, K., Miller, C., Rose, J., Xu, F., Ebmeier, C.C., Jacobsen, J.R., Mao, D., Old, W.M., DeShazer, D., and Seyedsayamdost, M.R. 2020. Thailandenes, Cryptic Polyene Natural Products Isolated from *Burkholderia thailandensis* Using Phenotype-Guided Transposon Mutagenesis. ACS Chem. Biol. **15**(5): 1195–1203. doi:10.1021/acschembio.9b00883.

Park, J.-U., Tsai, A.W.-L., Chen, T.H., Peters, J.E., and Kellogg, E.H. 2022. Mechanistic details of CRISPR-associated transposon recruitment and integration revealed by cryo-EM. Proc Natl Acad Sci **119**(32): e2202590119. doi:10.1073/pnas.2202590119.

Park, O.-J., and Lee, S.-H. 2005. Stereoselective lipases from *Burkholderia* sp., cloning and their application to preparation of methyl (*R*)-*N*-(2,6-dimethylphenyl)alaninate, a key intermediate for (*R*)-Metalaxyl. Journal of Biotechnology **120**(2): 174–182. doi:10.1016/j.jbiotec.2005.06.026.

Parke, J.L., and Gurian-Sherman, D. 2001. Diversity of the *Burkholderia cepacia* complex and implications for risk assessment of biological control strains. Annu Rev Phytopathol **39**: 225–258. doi:10.1146/annurev.phyto.39.1.225.

Perault, A.I., and Cotter, P.A. 2018. Three Distinct Contact-Dependent Growth Inhibition Systems Mediate Interbacterial Competition by the Cystic Fibrosis Pathogen *Burkholderia dolosa*. J Bacteriol **200**(22): e00428-18. doi:10.1128/JB.00428-18.

Plastics – the Facts 2018 An analysis of European plastics production, demand and waste data. 2018. PlasticsEurope. Available from https://www.plasticseurope.org/application/files/6315/4510/9658/Plastics_the_facts_2018_AF_web.pdf.

Prentki, P., and Krisch, H.M. 1984. In vitro insertional mutagenesis with a selectable DNA fragment. Gene **29**(3): 303–313. doi:10.1016/0378-1119(84)90059-3.

Prior, J.E., Lynch, M.D., and Gill, R.T. 2010. Broad-host-range vectors for protein expression across gram negative hosts. Biotechnol Bioeng **106**(2): 326–332. doi:10.1002/bit.22695.

Qi, L.S., Larson, M.H., Gilbert, L.A., Doudna, J.A., Weissman, J.S., Arkin, A.P., and Lim, W.A. 2013. Repurposing CRISPR as an RNA-guided platform for sequence-specific control of gene expression. Cell **152**(5): 1173–1183. doi:10.1016/j.cell.2013.02.022.

Qiu, D., Damron, F.H., Mima, T., Schweizer, H.P., and Yu, H.D. 2008. PBAD-Based Shuttle Vectors for Functional Analysis of Toxic and Highly Regulated Genes in *Pseudomonas* and *Burkholderia* spp. and Other Bacteria. Appl Environ Microbiol **74**(23): 7422–7426. doi:10.1128/AEM.01369-08.

Rathi, P., Saxena, R.K., and Gupta, R. 2001. A novel alkaline lipase from *Burkholderia cepacia* for detergent formulation. Process Biochemistry **37**(2): 187–192. doi:10.1016/S0032-9592(01)00200-X.

Rhee, Y.H., Kim, Y.H., and Shin, K.-S. 2006. Characterization of an extracellular poly (3-hydroxyoctanoate) depolymerase from the marine isolate, *Pseudomonas luteola* M13-4. Enzyme and microbial technology **38**(3–4): 529–535.

Rhodes, K.A., and Schweizer, H.P. 2016. Antibiotic resistance in *Burkholderia* species. Drug Resist Updat **28**: 82–90. doi:10.1016/j.drup.2016.07.003.

Rice, P.A., Craig, N.L., and Dyda, F. 2020. Comment on "RNA-guided DNA insertion with CRISPR-associated transposases." Science **368**(6495): eabb2022. American Association for the Advancement of Science. doi:10.1126/science.abb2022.

Riley, L.A., and Guss, A.M. 2021. Approaches to genetic tool development for rapid domestication of non-model microorganisms. Biotechnology for Biofuels **14**(1): 30. doi:10.1186/s13068-020-01872-z.

Roberts, R.J., Vincze, T., Posfai, J., and Macelis, D. 2015. REBASE—a database for DNA restriction and modification: enzymes, genes and genomes. Nucleic Acids Research **43**(D1): D298–D299. doi:10.1093/nar/gku1046.

Ronda, C., Pedersen, L.E., Sommer, M.O.A., and Nielsen, A.T. 2016. CRMAGE: CRISPR Optimized MAGE Recombineering. Sci Rep **6**: 19452. doi:10.1038/srep19452.

Rosenau, F., and Jaeger, K. 2000. Bacterial lipases from *Pseudomonas*: regulation of gene expression and mechanisms of secretion. Biochimie **82**(11): 1023–1032. doi:10.1016/s0300-9084(00)01182-2.

Roux, D., Schaefers, M., Clark, B.S., Weatherholt, M., Renaud, D., Scott, D., LiPuma, J.J., Priebe, G., Gerard, C., and Yoder-Himes, D.R. 2018. A putative lateral flagella of the cystic fibrosis pathogen *Burkholderia dolosa* regulates swimming motility and host cytokine production. PLoS One **13**(1): e0189810. doi:10.1371/journal.pone.0189810.

Sánchez, D.A., Tonetto, G.M., and Ferreira, M.L. 2018. Burkholderia cepacia lipase: A versatile catalyst in synthesis reactions. Biotechnology and Bioengineering **115**(1): 6–24. doi:10.1002/bit.26458.

Santos, M., Gangoiti, J., Keul, H., Möller, M., Serra, J.L., and Llama, M.J. 2013. Polyester hydrolytic and synthetic activity catalyzed by the medium-chain-length poly(3-hydroxyalkanoate) depolymerase from *Streptomyces venezuelae* SO1. Appl Microbiol Biotechnol **97**(1): 211–222. doi:10.1007/s00253-012-4210-1.

Santos, P.E.-D.L., Bustillos-Cristales, R., and Caballero-Mellado, J. 2001. *Burkholderia*, a Genus Rich in Plant-Associated Nitrogen Fixers with Wide Environmental and Geographic Distribution. Appl Environ Microbiol **67**(6): 2790–2798. doi:10.1128/AEM.67.6.2790-2798.2001.

Sato, T., Nonoyama, S., Kimura, A., Nagata, Y., Ohtsubo, Y., and Tsuda, M. 2017. The Small Protein HemP Is a Transcriptional Activator for the Hemin Uptake Operon in

Burkholderia multivorans ATCC 17616. Appl Environ Microbiol **83**(16): e00479-17. doi:10.1128/AEM.00479-17.

Sawana, A., Adeolu, M., and Gupta, R.S. 2014. Molecular signatures and phylogenomic analysis of the genus *Burkholderia*: proposal for division of this genus into the emended genus *Burkholderia* containing pathogenic organisms and a new genus *Paraburkholderia* gen. nov. harboring environmental species. Front. Genet. **5**. doi:10.3389/fgene.2014.00429.

Schaefers, M.M., Liao, T.L., Boisvert, N.M., Roux, D., Yoder-Himes, D., and Priebe, G.P. 2017. An Oxygen-Sensing Two-Component System in the *Burkholderia cepacia* Complex Regulates Biofilm, Intracellular Invasion, and Pathogenicity. PLoS Pathog. **13**(1): e1006116. doi:10.1371/journal.ppat.1006116.

Schirmer, A., and Jendrossek, D. 1994. Molecular characterization of the extracellular poly(3-hydroxyoctanoic acid) [P(3HO)] depolymerase gene of *Pseudomonas fluorescens* GK13 and of its gene product. J Bacteriol **176**(22): 7065–7073.

Schmerk, C.L., and Valvano, M.A. 2013. *Burkholderia multivorans* survival and trafficking within macrophages. J Med Microbiol **62**(Pt 2): 173–184. doi:10.1099/jmm.0.051243-0.

Schuster, L.A., and Reisch, C.R. 2021. A plasmid toolbox for controlled gene expression across the Proteobacteria. Nucleic Acids Research **49**(12): 7189–7202. doi:10.1093/nar/gkab496.

Schweizer, H.P., and Peacock, S.J. 2008. Antimicrobial Drug–Selection Markers for *Burkholderia pseudomallei* and *B. mallei*. Emerg Infect Dis **14**(11): 1689–1692. doi:10.3201/eid1411.080431.

Schwengers, O., Jelonek, L., Dieckmann, M.A., Beyvers, S., Blom, J., and Goesmann, A. 2021. Bakta: rapid and standardized annotation of bacterial genomes via alignment-free

sequence identification. Microbial Genomics **7**(11): 000685. Microbiology Society,. doi:10.1099/mgen.0.000685.

Scoffone, V.C., Chiarelli, L.R., Trespidi, G., Mentasti, M., Riccardi, G., and Buroni, S. 2017. *Burkholderia cenocepacia* infections in cystic fibrosis patients: drug resistance and therapeutic approaches. Front Microbiol **8**: 1592. doi:10.3389/fmicb.2017.01592.

Scoffone, V.C., Trespidi, G., Barbieri, G., Irudal, S., Israyilova, A., and Buroni, S. 2021. Methodological tools to study species of the genus *Burkholderia*. Appl Microbiol Biotechnol **105**(24): 9019–9034. doi:10.1007/s00253-021-11667-3.

Shalem, A., Yehezkeli, O., and Fishman, A. 2024. Enzymatic degradation of polylactic acid (PLA). Appl Microbiol Biotechnol **108**(1): 413. doi:10.1007/s00253-024-13212-4.

Sharma, P.K., Mohanan, N., Sidhu, R., and Levin, D.B. 2019. Colonization and degradation of polyhydroxyalkanoates by lipase-producing bacteria. Can J Microbiol. **65**(6): 461–475. doi:10.1139/cjm-2019-0042.

Shastri, S., Spiewak, H.L., Sofoluwe, A., Eidsvaag, V.A., Asghar, A.H., Pereira, T., Bull, E.H., Butt, A.T., and Thomas, M.S. 2017. An efficient system for the generation of marked genetic mutants in members of the genus *Burkholderia*. Plasmid **89**: 49–56. doi:10.1016/j.plasmid.2016.11.002.

Shu, Z., Wu, J., Chen, D., Cheng, L., Zheng, Y., Chen, J., and Huang, J. 2012. Optimization of Burkholderia sp. ZYB002 lipase production for pitch control in thermomechanical pulping (TMP) processes. Holzforschung **66**(3): 341–348. De Gruyter. doi:10.1515/hf.2011.152.

Smith, M.J., and Jeddeloh, J.A. 2005. DNA Methylation in Lysogens of Pathogenic *Burkholderia* spp. Requires Prophage Induction and Is Restricted to Excised Phage DNA. J Bacteriol **187**(3): 1196–1200. doi:10.1128/JB.187.3.1196-1200.2005.

Somprasong, N., Hall, C.M., Webb, J.R., Sahl, J.W., Wagner, D.M., Keim, P., Currie, B.J., and Schweizer, H.P. 2020. *Burkholderia ubonensis* Meropenem Resistance: Insights into Distinct Properties of Class A β-Lactamases in *Burkholderia cepacia* Complex and *Burkholderia pseudomallei* Complex Bacteria. mBio **11**(2): e00592-20. doi:10.1128/mBio.00592-20.

Somprasong, N., McMillan, I., Karkhoff-Schweizer, R.R., Mongkolsuk, S., and Schweizer, H.P. 2010. Methods for genetic manipulation of *Burkholderia gladioli* pathovar cocovenenans. BMC Research Notes **3**(1): 308. doi:10.1186/1756-0500-3-308.

Sood, S., Sharma, A., Sharma, N., and Kanwar, S. 2016. Carboxylesterases: Sources, Characterization and Broader Applications. Enzyme research **1**(1): 1–11. doi:10.21767/2573-4466.100002.

Srinon, V., Withatanung, P., Chaiwattanarungruengpaisan, S., Thongdee, M., Meethai, C., Stevens, J.M., Titball, R.W., and Korbsrisate, S. 2020. Functional redundancy of *Burkholderia pseudomallei* phospholipase C enzymes and their role in virulence. Sci Rep **10**: 19242. doi:10.1038/s41598-020-76186-z.

Strecker, J., Ladha, A., Gardner, Z., Schmid-Burgk, J.L., Makarova, K.S., Koonin, E.V., and Zhang, F. 2019. RNA-guided DNA insertion with CRISPR-associated transposases. Science **365**(6448): 48–53. doi:10.1126/science.aax9181.

Strecker, J., Ladha, A., Makarova, K.S., Koonin, E.V., and Zhang, F. 2020. Response to Comment on "RNA-guided DNA insertion with CRISPR-associated transposases." Science **368**(6495): eabb2920. doi:10.1126/science.abb2920.

Su, S., Bangar, H., Saldanha, R., Pemberton, A., Aronow, B., Dean, G.E., Lamkin, T.J., and Hassett, D.J. 2014. Construction and characterization of stable, constitutively expressed, chromosomal green and red fluorescent transcriptional fusions in the select agents,

Bacillus anthracis, *Yersinia pestis*, *Burkholderia mallei*, and *Burkholderia pseudomallei*. Microbiologyopen **3**(5): 610–629. doi:10.1002/mbo3.192.

Suárez-Moreno, Z.R., Caballero-Mellado, J., Coutinho, B.G., Mendonça-Previato, L., James, E.K., and Venturi, V. 2012. Common Features of Environmental and Potentially Beneficial Plant-Associated *Burkholderia*. Microb Ecol **63**(2): 249–266. doi:10.1007/s00248-011-9929-1.

Suzuki, M., Tachibana, Y., and Kasuya, K. 2020. Biodegradability of poly(3-hydroxyalkanoate) and poly(ε -caprolactone) via biological carbon cycles in marine environments. Polymer Journal **53**(1): 47–66. doi:10.1038/s41428-020-00396-5.

Tasnádi, G., Forró, E., and Fülöp, F. 2009. *Burkholderia cepacia* lipase is an excellent enzyme for the enantioselective hydrolysis of β-heteroaryl-β-amino esters. Tetrahedron: Asymmetry **20**(15): 1771–1777. doi:10.1016/j.tetasy.2009.06.019.

Teufel, R., Mascaraque, V., Ismail, W., Voss, M., Perera, J., Eisenreich, W., Haehnel, W., and Fuchs, G. 2010. Bacterial phenylalanine and phenylacetate catabolic pathway revealed. Proc Natl Acad Sci **107**(32): 14390–14395. doi:10.1073/pnas.1005399107.

Thongdee, M., Gallagher, L.A., Schell, M., Dharakul, T., Songsivilai, S., and Manoil, C. 2008. Targeted Mutagenesis of *Burkholderia thailandensis* and *Burkholderia pseudomallei* through Natural Transformation of PCR Fragments. Appl Environ Microbiol **74**(10): 2985–2989. doi:10.1128/AEM.00030-08.

Trujillo Rodríguez, L., Ellington, A.J., Reisch, C.R., and Chevrette, M.G. 2023. CRISPR-Associated Transposase for Targeted Mutagenesis in Diverse Proteobacteria. ACS Synth. Biol. **12**(7): 1989–2003. doi:10.1021/acssynbio.3c00065.

Tung, T.T., Quoc Thang, N., Cao Huy, N., Bao Phuong, P., Ngoc Minh, D., Hai Nam, N., and Nielsen, J. 2024. Identification of novel phenylalanine derivatives bearing a

hydroxamic acid moiety as potent quorum sensing inhibitors. RSC Med Chem **15**(4): 1320–1328. doi:10.1039/d3md00670k.

Vandamme, P., Holmes, B., Vancanneyt, M., Coenye, T., Hoste, B., Coopman, R., Revets, H., Lauwers, S., Gillis, M., Kersters, K., and Govan, J.R. 1997. Occurrence *Burkholderia cepacia* in cystic fibrosis patients and proposal of *Burkholderia multivorans* sp. nov. Int. J. Syst. Bacteriol. **47**(4): 1188–1200. doi:10.1099/00207713-47-4-1188.

Vandenbussche, I., Sass, A., Pinto-Carbó, M., Mannweiler, O., Eberl, L., and Coenye, T. 2020. DNA Methylation Epigenetically Regulates Gene Expression in *Burkholderia cenocepacia* and Controls Biofilm Formation, Cell Aggregation, and Motility. mSphere **5**(4): e00455-20. doi:10.1128/mSphere.00455-20.

Vial, L., Groleau, M.-C., Dekimpe, V., and Deziel, E. 2007. *Burkholderia* Diversity and Versatility: An Inventory of the Extracellular Products. Journal of Microbiology and Biotechnology **17**(9): 1407–1429.

Viljakainen, V.R., and Hug, L.A. 2021. The phylogenetic and global distribution of bacterial polyhydroxyalkanoate bioplastic-degrading genes. Environmental Microbiology **23**(3): 1717–1731. doi:https://doi.org/10.1111/1462-2920.15409.

Vo, P.L.H., Acree, C., Smith, M.L., and Sternberg, S.H. 2021. Unbiased profiling of CRISPR RNA-guided transposition products by long-read sequencing. Mobile DNA **12**(1): 13. doi:10.1186/s13100-021-00242-2.

Vo, P.L.H., Ronda, C., Klompe, S.E., Chen, E.E., Acree, C., Wang, H.H., and Sternberg, S.H. 2020. CRISPR RNA-guided integrases for high-efficiency, multiplexed bacterial genome engineering. Nat Biotechnol **39**(4): 480–489. doi:10.1038/s41587-020-00745-y.

Wallner, A., Moulin, L., Busset, N., Rimbault, I., and Béna, G. 2021. Genetic Diversity of Type 3 Secretion System in *Burkholderia s.l.* and Links With Plant Host Adaptation. Front Microbiol **12**: 761215. doi:10.3389/fmicb.2021.761215.

Wang, X., Yu, X., and Xu, Y. 2009. Homologous expression, purification and characterization of a novel high-alkaline and thermal stable lipase from *Burkholderia cepacia* ATCC 25416. Enzyme and Microbial Technology **45**(2): 94–102. doi:10.1016/j.enzmictec.2009.05.004.

W. Meereboer, K., Misra, M., and K. Mohanty, A. 2020. Review of recent advances in the biodegradability of polyhydroxyalkanoate (PHA) bioplastics and their composites. Green Chemistry **22**(17): 5519–5558. doi:10.1039/D0GC01647K.

Wong, Y.C., Ghany, M.A.E., Naeem, R., Lee, K.W., Tan, Y.G., Pain, A., and Nathan, S. 2016. Candidate essential genes in *Burkholderia cenocepacia* J2315 identified by genome-wide TraDIS. Frontiers in Microbiology **7**: 1288. doi:10.3389/fmicb.2016.01288.

Yabuuchi, E., Kosako, Y., Oyaizu, H., Yano, I., Hotta, H., Hashimoto, Y., Ezaki, T., and Arakawa, M. 1992. Proposal of *Burkholderia* gen. nov. and transfer of seven species of the genus *Pseudomonas* homology group II to the new genus, with the type species *Burkholderia cepacia* (Palleroni and Holmes 1981) comb. nov. Microbiology and Immunology **36**(12): 1251–1275. doi:10.1111/j.1348-0421.1992.tb02129.x.

Yang, P., Zhang, M., and Elsas, J.D. van. 2017. Role of flagella and type four pili in the co-migration of *Burkholderia terrae* BS001 with fungal hyphae through soil. Scientific Reports **7**(1): 2997. doi:10.1038/s41598-017-02959-8.

Yap, Z.L., Motnenko, A., and Cardona, S. 2023. Complete Genome Sequence of Burkholderia vietnamiensis LMG16232. Microbiol Resour Announc **12**(8): e0032823. doi:10.1128/mra.00328-23.

Yap, Z.L., Rahman, A.S.M.Z., Hogan, A.M., Levin, D.B., and Cardona, S.T. 2024. A CRISPR-Cas-associated transposon system for genome editing in Burkholderia cepacia complex species. Appl Environ Microbiol **90**(7): e0069924. doi:10.1128/aem.00699-24.

Yoshimura, A., Covington, B.C., Gallant, É., Zhang, C., Li, A., and Seyedsayamdost, M.R. 2020. Unlocking Cryptic Metabolites with Mass Spectrometry-Guided Transposon Mutant Selection. ACS Chem. Biol. **15**(10): 2766–2774. doi:10.1021/acschembio.0c00558.

Yudistira, H., McClarty, L., Bloodworth, R.A., Hammond, S.A., Butcher, H., Mark, B.L., and Cardona, S.T. 2011. Phenylalanine induces *Burkholderia cenocepacia* phenylacetic acid catabolism through degradation to phenylacetyl-CoA in synthetic cystic fibrosis sputum medium. Microb Pathog **51**: 183–196. doi:10.1016/j.micpath.2011.04.002.

Zeng, T., Yin, J., Liu, Z., Li, Z., Zhang, Y., Lv, Y., Lu, M.-L., Luo, M., Chen, M., and Xiao, Y. 2023. Mechanistic insights into transposon cleavage and integration by TnsB of ShCAST system. Cell Reports **42**(7): 112698. doi:10.1016/j.celrep.2023.112698.

CHAPTER 6: APPENDIX

6.1 Related to Chapter 2

6.1.1 Supplemental Figures

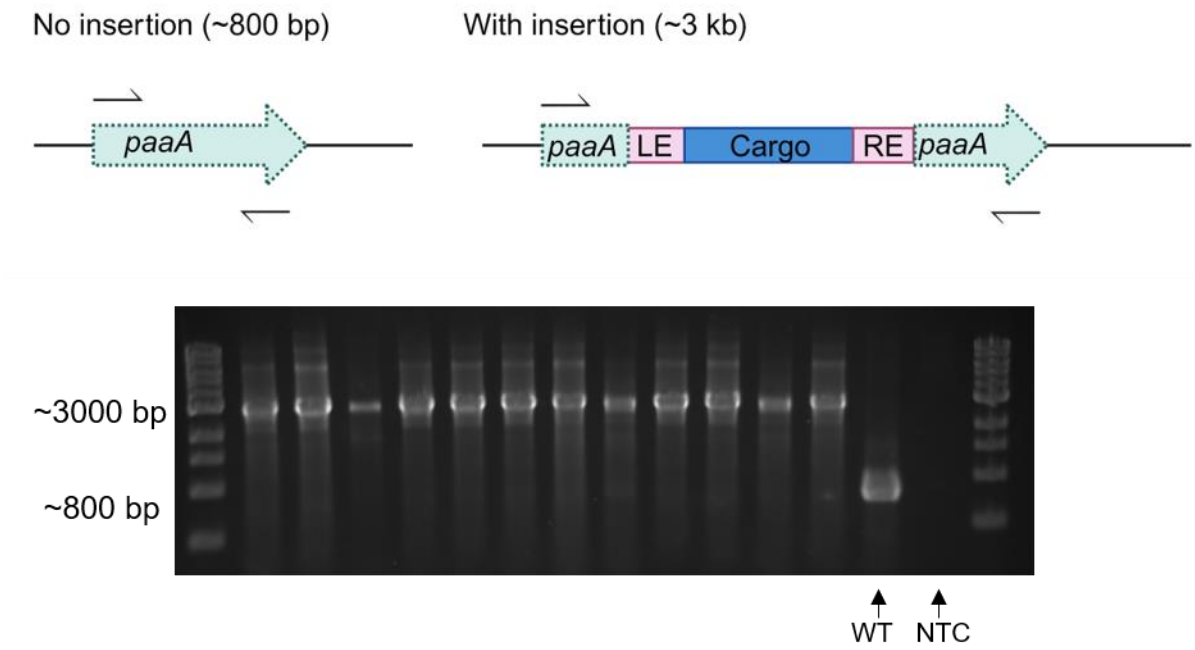


Figure S2. 1 PCR targeting *paaA* in *B. cenocepacia* K56-2 after RhaCAST conjugation. Schematics indicate the location of the primers and the expected product size. Twelve representative trimethoprim-resistant colonies were selected after conjugation, and the presence of insertion was assessed using colony PCR. WT: Wild-type, NTC: Non-template control.

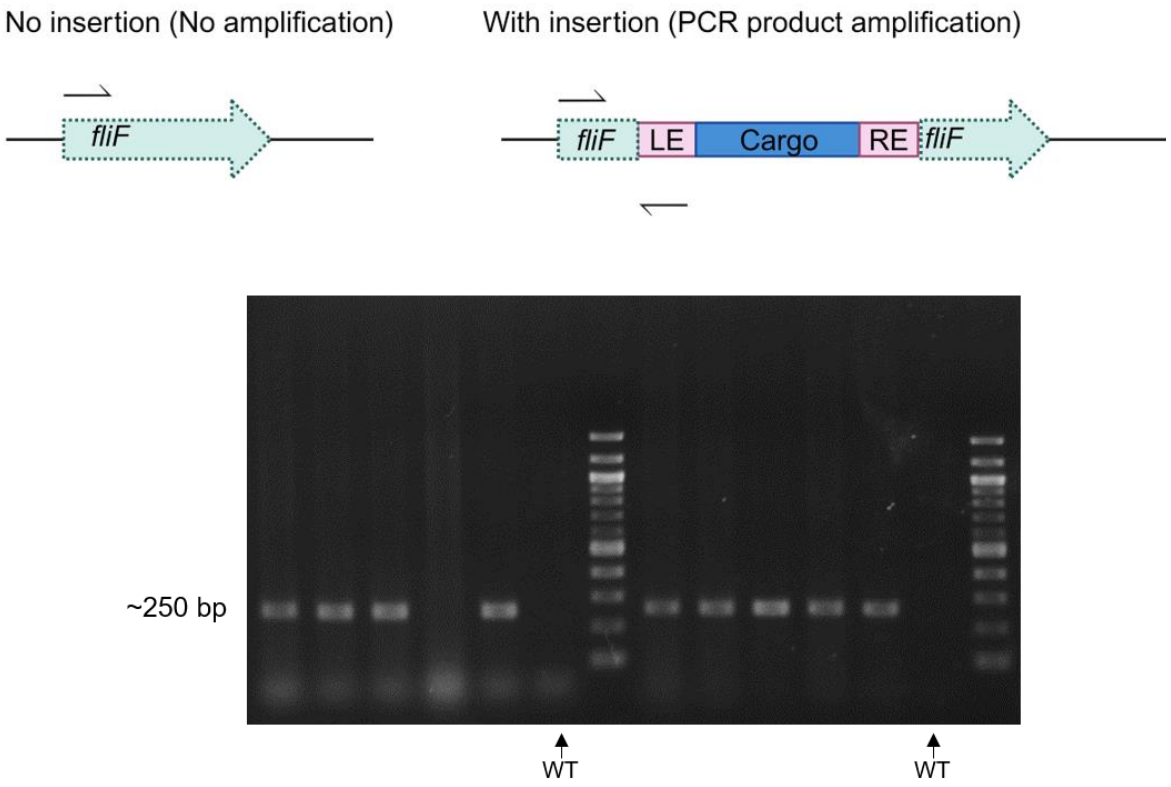


Figure S2. 2 PCR targeting *fliF* of *B. cenocepacia* K56-2 after RhaCAST conjugation.

The mutants were targeted with two different crRNA. Schematics indicate the location of the primers and the expected product size. WT: Wild-type.

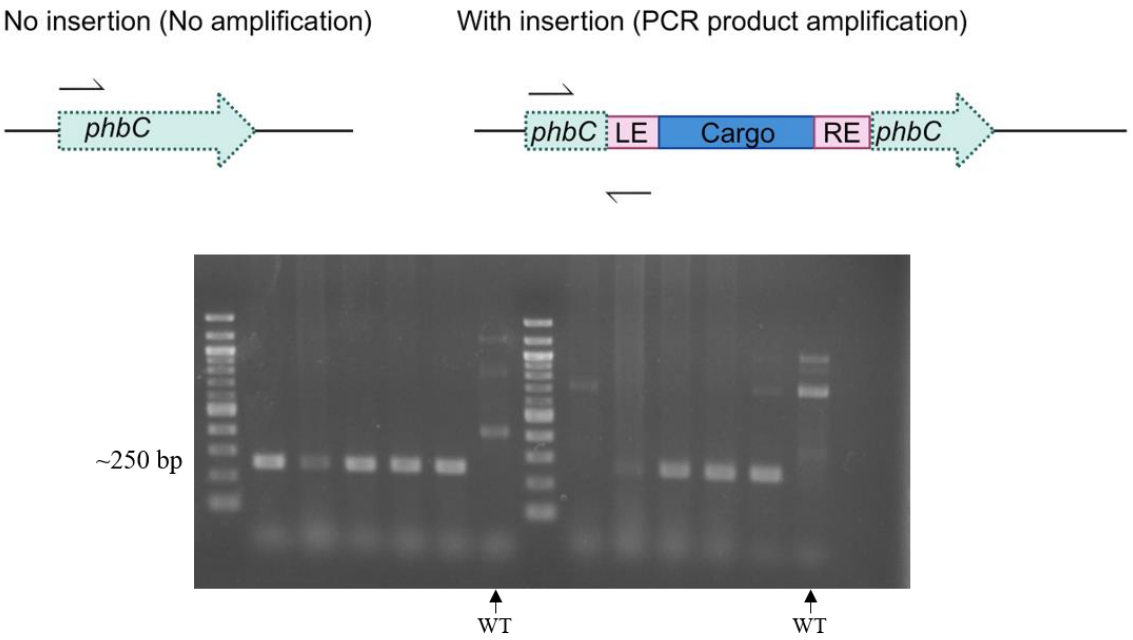


Figure S2. 3 PCR targeting *phbC* of *B. cenocepacia* K56-2 after RhaCAST conjugation.

The mutants were targeted with two different crRNA. Schematics indicate the location of the primers and the expected product size. WT: Wild-type.

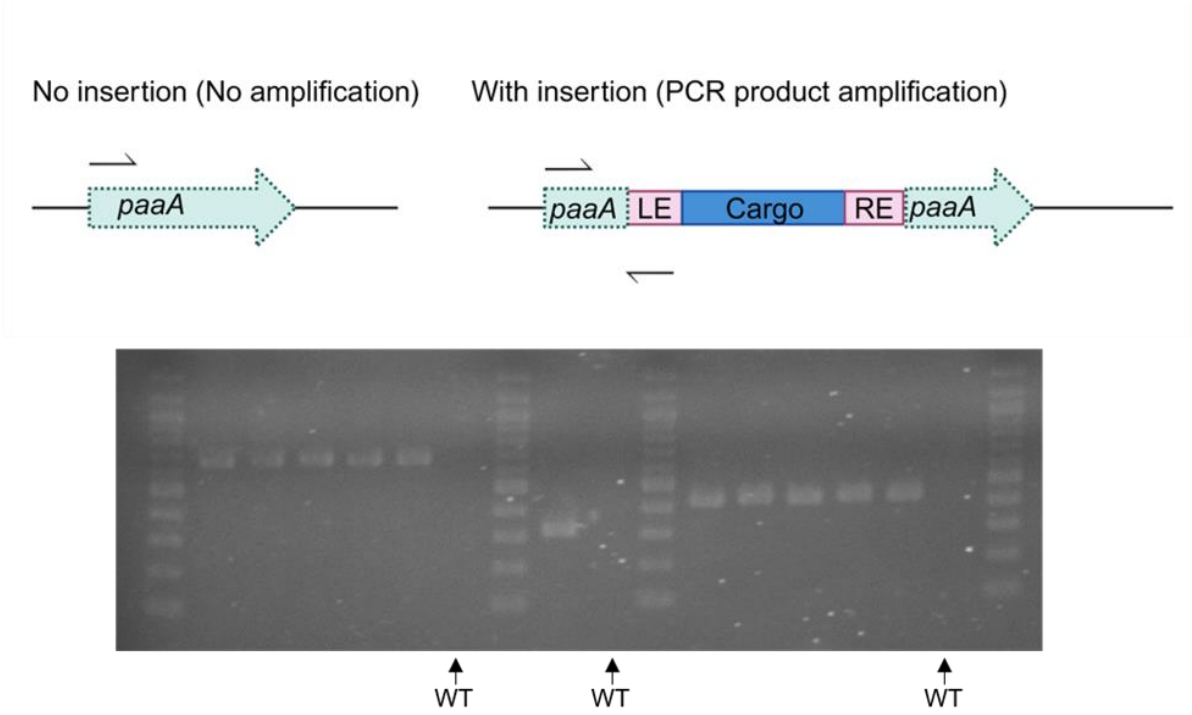


Figure S2. 4 PCR targeting *paaA* and the left end (LE) of the cargo insertion in *B. multivorans* ATCC17616 after RhaCAST conjugation.

The mutants were targeted with three different crRNA. Schematics indicate the location of the primers and the expected presence or absence of PCR product. Eleven representative trimethoprim resistant colonies were selected after conjugation and the presence of the insertion was assessed with colony PCR. WT: Wild-type.

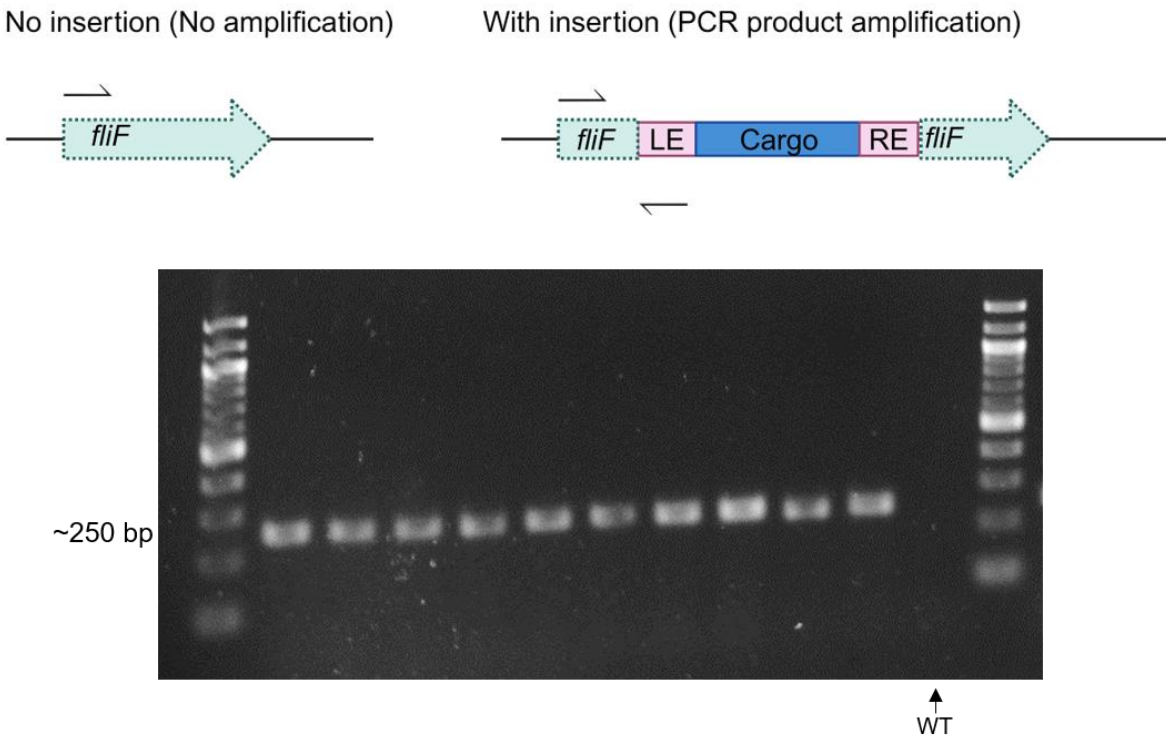


Figure S2. 5 PCR targeting *fliF* of *B. multivorans* ATCC17616 after RhaCAST conjugation.

Schematics indicate the location of the primers and the expected product size. WT: Wild-type.

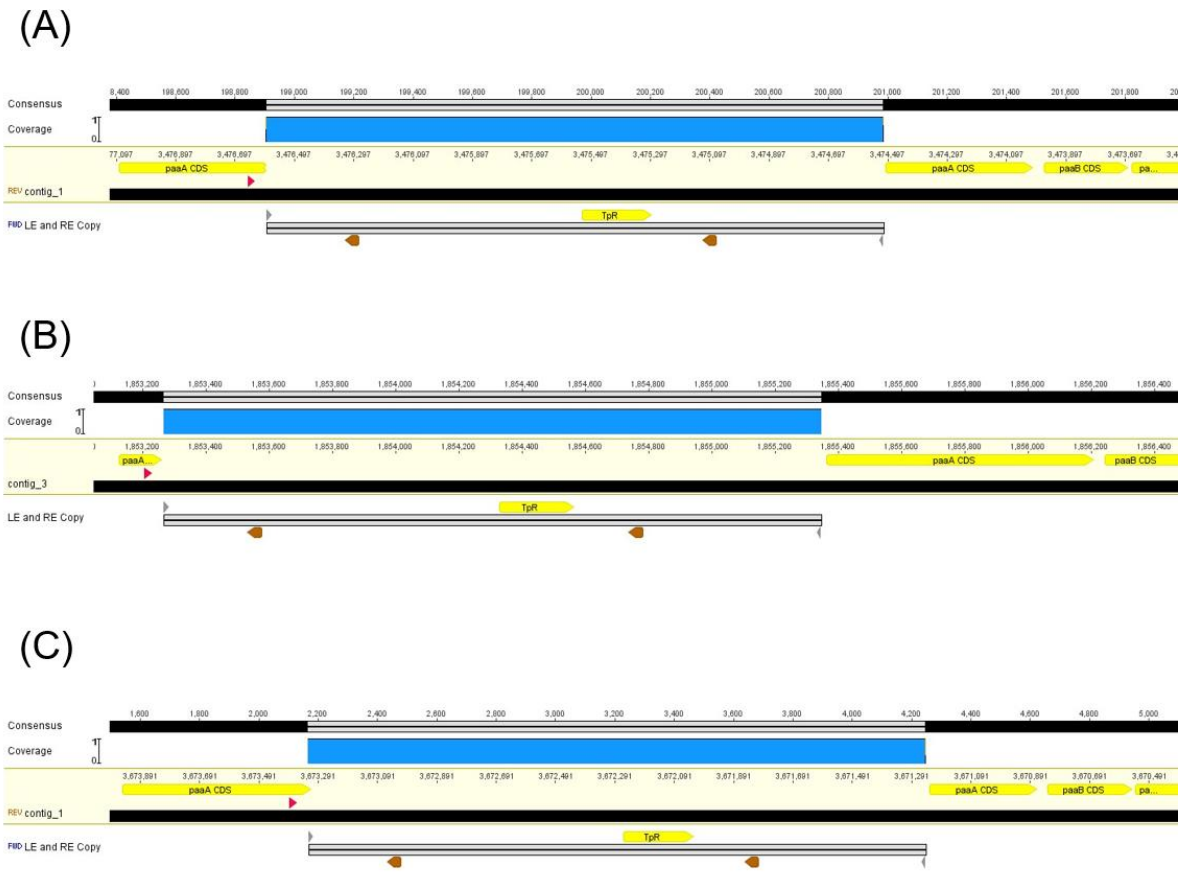


Figure S2. 6 Alignment of nanopore sequencing of *B. cenocepacia* K56-2 transconjugants with genomic integration in *paaA* created using the RhaCAST system. The cargo region flanking the left end (LE) and right end (RE) of the plasmid pDonorTp was mapped and aligned to the sequenced genome. The pink arrows indicate the position of crRNA used to target different regions of paaA. Transposon's left end (LE) and right end (RE) elements are represented in a grey arrow. Trimethoprim resistance cassette (TpR) was situated between FRT recognition sites (brown arrow). (a) Mutant created with crRNA 3390, distance from PAM: 63 (b) Mutant created with crRNA 3422, distance from PAM: 61 (c) Mutant created with crRNA 3423, distance from PAM: 63



Figure S2. 7 Alignment of nanopore sequencing of *B. cenocepacia* K56-2 transconjugants with genomic integration in *fliF* created using the RhaCAST system. The cargo region flanking the left end (LE) and right end (RE) of the plasmid pDonorTp was mapped and aligned to the sequenced genome. The pink arrows indicate the position of crRNA used to target different regions of *fliF*. Transposon's left end (LE) and right end (RE) elements are represented in a grey arrow. Trimethoprim resistance cassette (TpR) was situated between FRT recognition sites (brown arrow). (a) Mutant created with crRNA 3463, distance from PAM: 67 (b) Mutant created with crRNA 3466, distance from PAM: 64



Figure S2. 8 Alignment of nanopore sequencing of *B. cenocepacia* K56-2 transconjugants with genomic integration of transposon in *phbC* created using the RhaCAST system.

The cargo region flanking the left end (LE) and right end (RE) of the plasmid pDonorTp was mapped and aligned to the sequenced genome. The pink arrows indicate the position of crRNA used to target different regions of *phbC*. Transposon's left end (LE) and right end (RE) elements are represented in a grey arrow. Trimethoprim resistance cassette (TpR) was situated between FRT recognition sites (brown arrow). (a) Mutant created with crRNA 3469, distance from PAM: 64 (b) Mutant created with crRNA 3472, distance from PAM: 64



Figure S2. 9 Alignment of nanopore sequencing of *B. cenocepacia* K56-2 transconjugants with genomic integration of *fugfp* in genetically neutral locus created using RhaCAST system.

The cargo region flanking the left end (LE) and right end (RE) of the plasmid pDonorTp-fugfp was mapped and aligned to the sequenced genome. The pink arrows indicate the position of crRNA used to target different regions of paaA. Transposon's left end (LE) and right end (RE) elements are represented in a grey arrow. Trimethoprim resistance cassette (TpR) was situated between FRT recognition sites (brown arrow). (a) Mutant created with crRNA 3475, distance from PAM: 63 (b) Mutant created with crRNA 3478, distance from PAM: 64

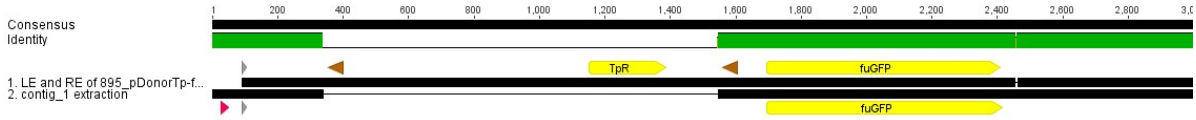


Figure S2. 10 Sequence alignment of *B. cenocepacia* K56-2::CAST-*fugfp* genome showing the removal of TpR via FLP-FRT mediated recombination.

The cargo region flanking the left end (LE) and right end (RE) of the plasmid pDonorTp-fugfp was mapped and aligned to the sequenced genome. The pink arrows indicate the position of crRNA used to direct the insertion site. Transposon's left end (LE) and right end (RE) elements are represented in a grey arrow. Trimethoprim resistance cassette (TpR) was situated between FRT recognition sites (brown arrow) found in the cargo region that found in pDonorTp-fugfp was absent in the genome of *B. cenocepacia* K56-2::CAST-*fugfp*.



Figure S2. 11 Alignment of nanopore sequencing of *B. cenocepacia* K56-2::CAST-fugfp *fliF*::CAST-Tp created with RhaCAST system using *B. cenocepacia* K56-2::CAST-fugfp-Tp as background by targeting *fliF*.

The pDonorTp consists of a cargo region flanking the left end (LE), and the right end (RE) consists of a Trimethoprim resistance cassette (TpR). LE and RE elements are represented in a grey arrow. TpR was situated between FRT recognition sites (brown arrow). (a) This mutant has the integration of the cargo element of pDonorTp only. (b) This mutant has co-integration of the whole pDonorTp plasmid.

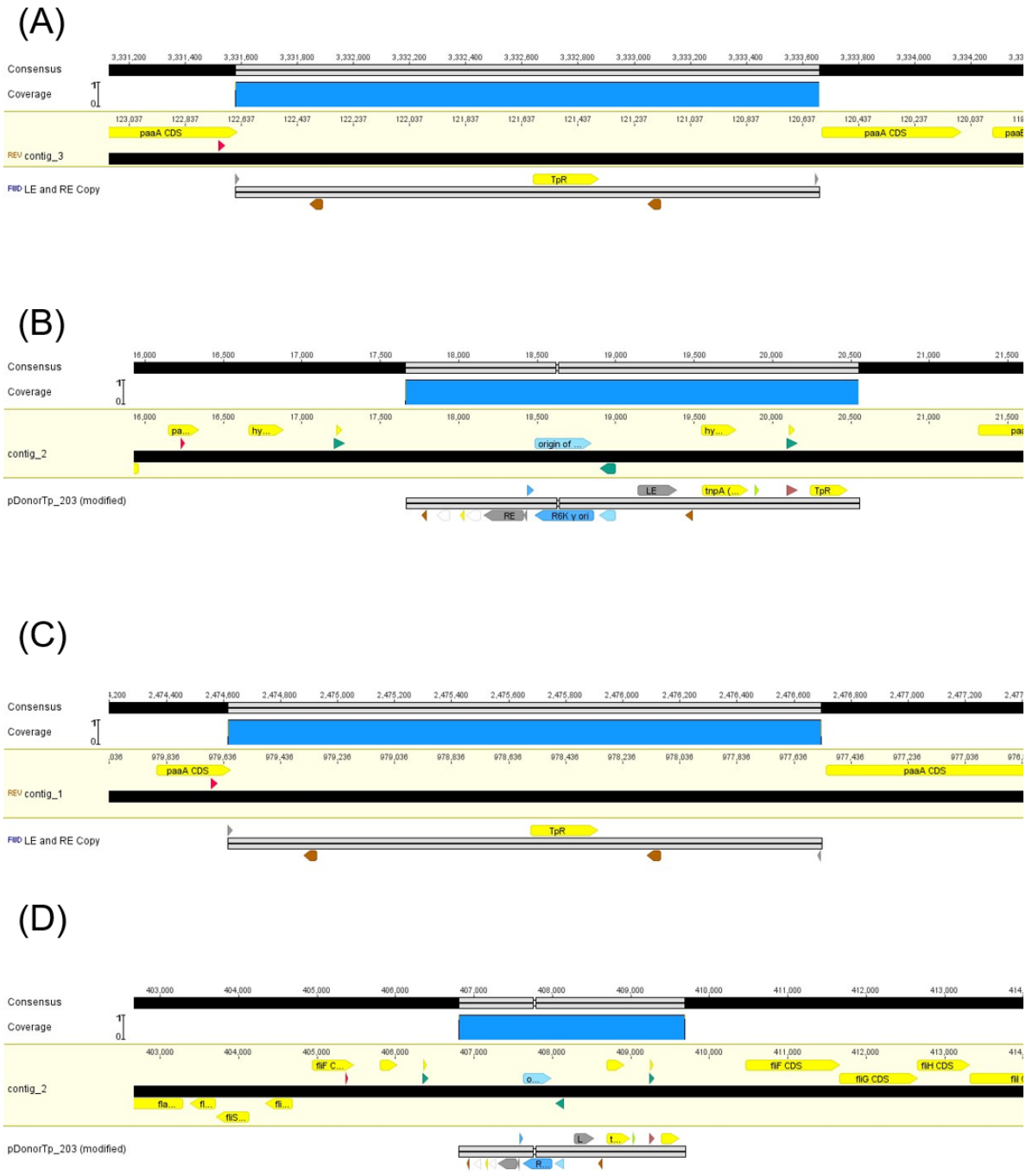


Figure S2. 12 The alignment of nanopore sequencing of *B. multivorans* ATCC17616 transconjugants with genomic integration of transposon in *paaA* and *fliF* created using the RhaCAST system.

The cargo region flanking the left end (LE) and right end (RE) of the plasmid pDonorTp and the entire pDonorTp were mapped and aligned to the sequenced genome. The pink arrows indicate the position of crRNA used to target the selected region of the gene. Transposon's left end (LE) and right end (RE) elements are represented in a grey arrow. Trimethoprim resistance cassette (TpR) was situated between FRT recognition sites (brown arrow). (a) *paaA* mutant possesses cargo integration, created with crRNA 3390, distance from PAM: 59 (b) *paaA* mutant created with crRNA 3422, co-integration with whole plasmid, distance from PAM: 65 (c) *paaA* mutant created with crRNA 3423, possess cargo integration only, distance from PAM: 59 (d) *fliF* mutant created with crRNA 3463, co-integration with whole plasmid integration, distance from PAM: 60

6.2 Related to Chapter 3

6.2.1 Supplemental Figures

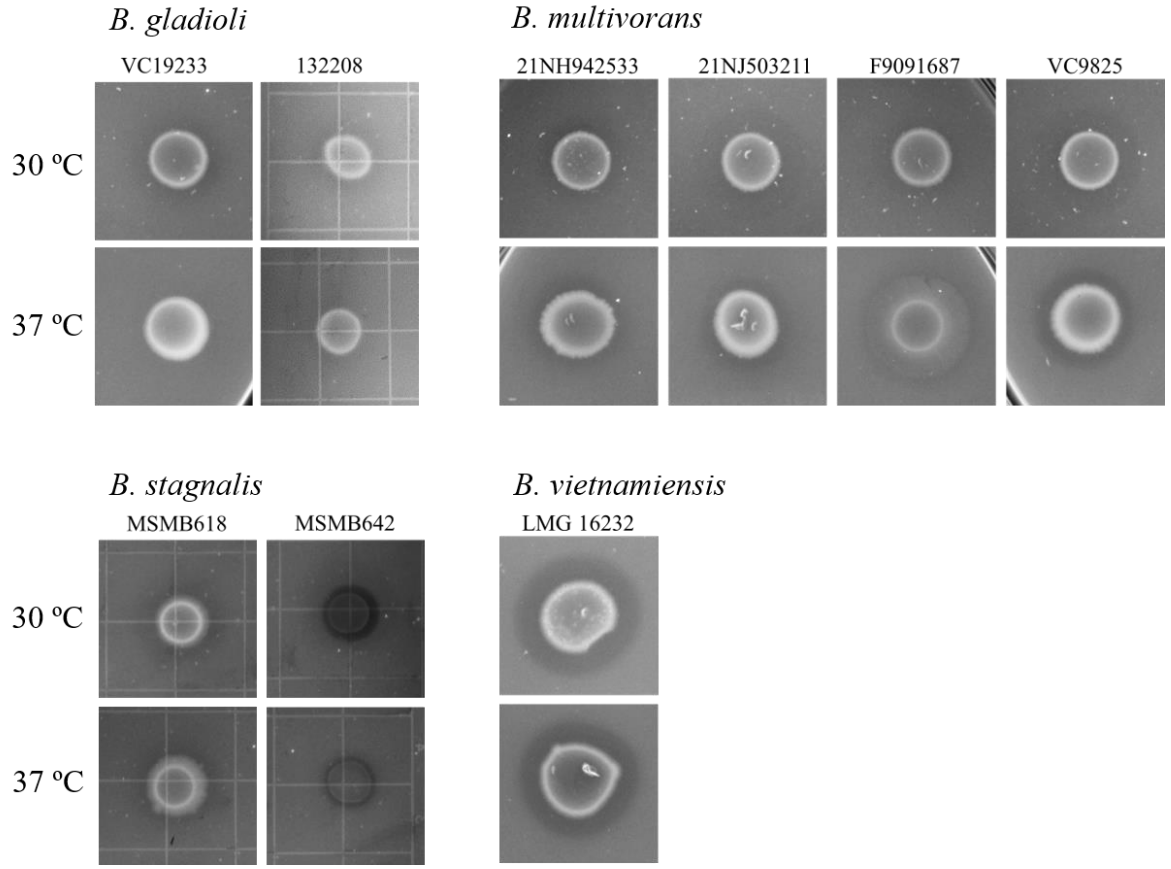


Figure S3. 1 The mcl-PHA degradation activity of *Burkholderia* strains.

The strains were grown on agar plates containing Nile red and PHO for 20 days at 30°C and 37°C. The phenotypes were visualized under UV irradiation, and the mcl-PHA degradation activity was ranked based on the following scale: (–) no clearing, (+) weak clearing, (++) moderate clearing. The phenotypes observed for each strain were as follows: *B. gladioli* VC19233 showed a rating of (+) at both temperatures, while *B. gladioli* 132208 exhibited (+) at 30°C and (-) at 37°C. Both *B. multivorans* strains, 21NH942533 and VC9825 displayed a rating of (+) at both temperatures, while *B. multivorans* 21NJ503211 and showed (+) at 30°C and (-) at 37°C. Finally, *B. stagnalis* MSMB618, *B. stagnalis* MSMB642, and *B. vietnamiensis* LMG 16232 were rated (++) at both temperatures.



Figure S3. 2 Alignment of nanopore sequencing of *B. vietnamiensis* LMG 16232 transconjugants with genomic integration in triacylglycerol lipase CDS (locus tag: P4G95_16805) created using the RhaCAST system.

The cargo region flanking the left end (LE) and right end (RE) of the plasmid pDonorTp was mapped and aligned to the sequenced genome. The pink arrows indicate the position of crRNA. Transposon's left end (LE) and right end (RE) elements are represented in a grey arrow. Trimethoprim resistance cassette (TpR) was situated between FRT recognition sites (brown arrow). Mutant created with crRNA 3668, distance from PAM: 63.

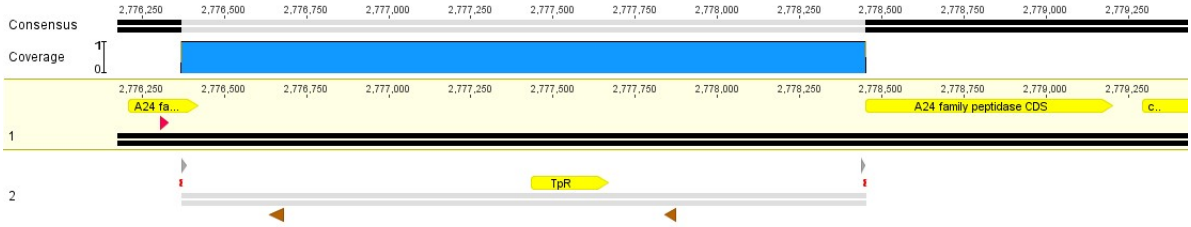


Figure S3. 3 Alignment of nanopore sequencing of *B. vietnamiensis* LMG 16232 transconjugants with genomic integration in A24 family peptidase CDS (locus tag: P4G95_07805) created using the RhaCAST system.

The cargo region flanking the left end (LE) and right end (RE) of the plasmid pDonorTp was mapped and aligned to the sequenced genome. The pink arrows indicate the position of crRNA. Transposon's left end (LE) and right end (RE) elements are represented in a grey arrow. Trimethoprim resistance cassette (TpR) was situated between FRT recognition sites (brown arrow). Mutant created with crRNA 3952, distance from PAM: 64.

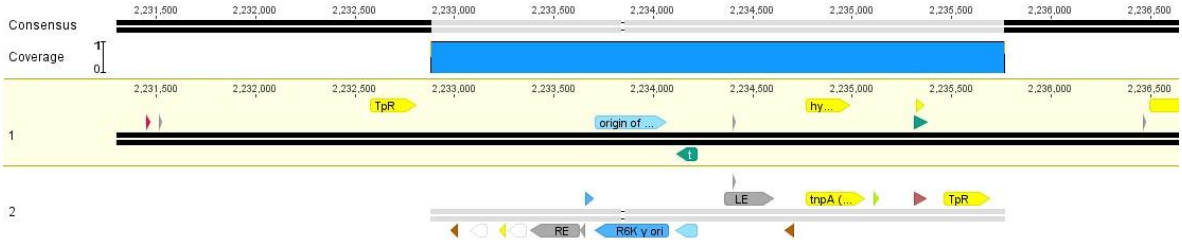


Figure S3. 4 Alignment of nanopore sequencing of *B. vietnamiensis* LMG 16232 transconjugants with genomic integration in *otsB* (locus tag: P4G95_10885) created using the RhaCAST system.

The pink arrows indicate the position of crRNA. Transposon's left end (LE) and right end (RE) elements are represented in a grey arrow. Trimethoprim resistance cassette (TpR) was situated between FRT recognition sites (brown arrow). This mutant has co-integration of the whole pDonorTp plasmid. Mutant created with crRNA 3956 distance from PAM: 65.

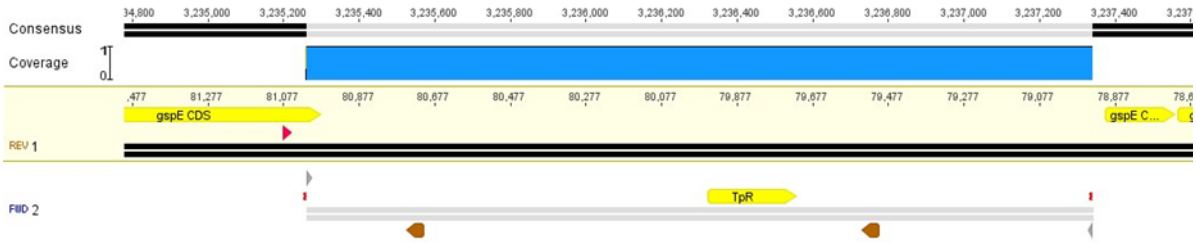


Figure S3. 5 Alignment of nanopore sequencing of *B. vietnamiensis* LMG 16232 transconjugants with genomic integration in *gspE* (locus tag: P4G95_05530) created using the RhaCAST system.

The cargo region flanking the left end (LE) and right end (RE) of the plasmid pDonorTp was mapped and aligned to the sequenced genome. The pink arrows indicate the position of crRNA. Transposon's left end (LE) and right end (RE) elements are represented in a grey arrow. Trimethoprim resistance cassette (TpR) was situated between FRT recognition sites (brown arrow). Mutant created with crRNA 3996, distance from PAM: 63.

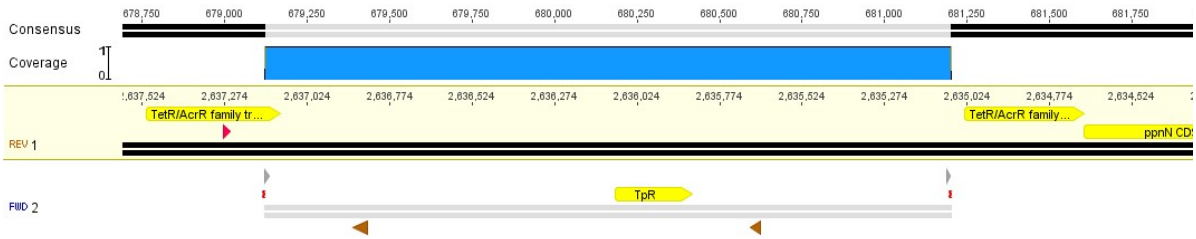


Figure S3. 6 Alignment of nanopore sequencing of *B. vietnamiensis* LMG 16232 transconjugants with genomic integration in TetR/AcrR family transcriptional regulator CDS (locus tag: P4G95_00865) created using the RhaCAST system.

The cargo region flanking the left end (LE) and right end (RE) of the plasmid pDonorTp was mapped and aligned to the sequenced genome. The pink arrows indicate the position of crRNA. Transposon's left end (LE) and right end (RE) elements are represented in a grey arrow. Trimethoprim resistance cassette (TpR) was situated between FRT recognition sites (brown arrow). Mutant created with crRNA 4000, distance from PAM: 126.

6.3 Complete Genome Sequence of *Burkholderia vietnamiensis* LMG16232

6.3.1 Abstract

We report here the complete annotated closed genome sequence of *Burkholderia vietnamiensis* LMG16232. There were three contigs, with a combined size of 6,739,172 bp and a GC composition of 67%.

6.3.2 Announcement

Burkholderia vietnamiensis LMG16232, (CCUG 31370) was obtained in 1993 from the sputum of a 20-year-old cystic fibrosis patient in Göteborg, Sweden and belongs to the *Burkholderia cepacia* complex strain panel, which was created for diagnostic purposes (Mahenthiralingam et al. 2000b, 2000a). The strain is deposited at the Belgium Coordinated Collection of Microorganisms (BCCM) (https://bccm.belspo.be/catalogues/lmg-strain-details?NUM=16232).

The strain was obtained from the BCCM in 1999 and stored at -80°C in LB medium containing 20% glycerol. Since the original acquisition, the strain was passaged three times by collecting bacterial lawns and isolated colonies from LB agar petri dishes, prior to storage. To extract the DNA, a test tube containing 5 ml of LB medium was inoculated with a loopful of the last stored stock, and the culture was incubated for 16 h at 30°C. The DNA was extracted using the PureLink microbiome DNA purification kit (Invitrogen) according to the manufacturer's instruction. Nanopore and Illumina libraries were prepared from the same DNA preparation at the Microbial Genome Sequencing Center MiGS (Pittsburgh, PA) using the workflow described elsewhere (Baym et al. 2015). Briefly, the libraries for Illumina sequencing and Nanopore sequencing were prepared using the Illumina Nextera kit and the SQK-LSK109 kit, respectively, as per the manufacturer’s specifications. The libraries were sequenced on an Illumina NextSeq 550 platform (pair-end sequencing), and on an Oxford Nanopore Technologies (ONT) MinION R9 flow cell, respectively. All reads were provided as FASTQ

files (Illumina: 2,654,441 reads, 698,867,643 bases, 106X coverage; ONT: 99,965 reads, 1,304,948,489 bases, 193X coverage, N_{50} value of 13,049 bp. Genome assembly was performed using the Galaxy bioinformatics platform (https://usegalaxy.org/) using both Illumina and Nanopore reads. Quality control and adapter trimming were performed using FastQC (Galaxy Version 0.73+galaxy0) and Trimmomatic (Galaxy Version 0.38.1) (Bolger et al. 2014) for Illumina pair-end reads. The Nanopore scaffold was assembled using Flye (Galaxy Version 2.9+galaxy0) (Lin et al. 2016). The trimmed Illumina paired-end data were mapped to the Nanopore genome assembly using BWA-MEM (Galaxy Version 0.7.17.2) (Li 2013), and the resulting BAM file was used to polish the Nanopore assembly using Pilon (Galaxy Version 1.20.1) (Walker et al. 2014). Genome annotation was performed using Prokka (Galaxy Version 1.14.6+galaxy1) (Seemann 2014). Default parameters were used for all software unless otherwise specified.

The *B. vietnamiensis* LMG16232 genome was assembled into three circular replicons of 3,314,184 bp (GC, 67.0%), 2,219,983 bp (GC, 67.6%), and 1,205,005 (GC, 67.0%). The total size is 6,739,172 bp and the average GC composition is 67%. Coverages for Illumina and ONT are 106X and 193X, respectively. Replicon one consists of 3,003 coding genes, 12 rRNA, 65 tRNA, and one tmRNA; replicon two consists of 1,874 coding genes, 3 rRNA, and 11 tRNA; replicon three consists of 1,014 coding genes, 3 rRNA, and 4 tRNA. In total, the LMG15232 genome is predicted to have 5891 coding genes, 18 rRNA, 80 tRNA, and one tmRNA. Compared to the previously sequenced draft genome performed with Illumina (ENA accession: ERS785077), this closed genome has additional 67835 bp.

6.3.3 Data availability statement

The genome sequence of *B. vietnamiensis* LMG16232 is available in GenBank under accession no. CP120730 to CP120732. The raw sequence reads are accessible under Sequence Read Archive accession no. SRR24175964 (Illumina) and SRR24175963 (ONT).

6.3.4 References for appendix

Baym, M., Kryazhimskiy, S., Lieberman, T.D., Chung, H., Desai, M.M., and Kishony, R. 2015. Inexpensive multiplexed library preparation for megabase-sized genomes. PLoS One **10**(5): e0128036. doi:10.1371/journal.pone.0128036.

Bolger, A.M., Lohse, M., and Usadel, B. 2014. Trimmomatic: a flexible trimmer for Illumina sequence data. Bioinformatics **30**(15): 2114–2120. doi:10.1093/bioinformatics/btu170.

Li, H. 2013. Aligning sequence reads, clone sequences and assembly contigs with BWA-MEM. arXiv:1303.3997 [q-bio]. Available from http://arxiv.org/abs/1303.3997 [accessed 12 May 2022].

Lin, Y., Yuan, J., Kolmogorov, M., Shen, M.W., Chaisson, M., and Pevzner, P.A. 2016. Assembly of long error-prone reads using de Bruijn graphs. Proc Natl Acad Sci U S A **113**(52): E8396–E8405. doi:10.1073/pnas.1604560113.

Mahenthiralingam, E., Bischof, J., Byrne, S.K., Radomski, C., Davies, J.E., Av-Gay, Y., and Vandamme, P. 2000a. DNA-Based diagnostic approaches for identification of *Burkholderia cepacia* complex, *Burkholderia vietnamiensis*, *Burkholderia multivorans*, *Burkholderia stabilis*, and *Burkholderia cepacia* genomovars I and III. Journal of clinical microbiology **38**(9): 3165–3173.

Mahenthiralingam, E., Coenye, T., Chung, J.W., Speert, D.P., Govan, J.R., Taylor, P., and Vandamme, P. 2000b. Diagnostically and experimentally useful panel of strains from the *Burkholderia cepacia* complex. Journal of clinical microbiology **38**(2): 910–913.

Seemann, T. 2014. Prokka: rapid prokaryotic genome annotation. Bioinformatics **30**(14): 2068–2069. doi:10.1093/bioinformatics/btu153.

Walker, B.J., Abeel, T., Shea, T., Priest, M., Abouelliel, A., Sakthikumar, S., Cuomo, C.A., Zeng, Q., Wortman, J., Young, S.K., and Earl, A.M. 2014. Pilon: An Integrated Tool for Comprehensive Microbial Variant Detection and Genome Assembly Improvement. PLOS ONE **9**(11): e112963. Public Library of Science. doi:10.1371/journal.pone.0112963.